eCAM Evidence-Based Complementary and Alternative Medicine

Potential of Terpenoids and Flavonoids from Asteraceae as Anti-Inflammatory, Antitumor, and Antiparasitic Agents

Lead Guest Editor: Valeria Sulsen
Guest Editors: Emilio Lizarraga, Nilufar Mamadalieva, and João H. G. Lago

Potential of Terpenoids and Flavonoids from Asteraceae as Anti-Inflammatory, Antitumor, and Antiparasitic Agents

Evidence-Based Complementary and Alternative Medicine

Potential of Terpenoids and Flavonoids from Asteraceae as Anti-Inflammatory, Antitumor, and Antiparasitic Agents

Lead Guest Editor: Valeria Sulsen
Guest Editors: Emilio Lizarraga, Nilufar Mamadalieva, and João H. G. Lago

Editorial Board

Contents

Hindawi
Evidence-Based Complementary and Alternative Medicine
Volume 2017, Article ID 6196198, 2 pages
https://doi.org/10.1155/2017/6196198

Editorial

Potential of Terpenoids and Flavonoids from Asteraceae as Anti-Inflammatory, Antitumor, and Antiparasitic Agents

Valeria P. Sülsen,[1,2] Emilio Lizarraga,[3] Nilufar Z. Mamadalieva,[4] and João Henrique G. Lago[5]

[1]*Departamento de Farmacología, Cátedra de Farmacognosia, Facultad de Farmacia y Bioquímica, Universidad de Buenos Aires, Buenos Aires, Argentina*
[2]*Universidad de Buenos Aires, CONICET, Instituto de Química y Metabolismo del Fármaco (IQUIMEFA), Buenos Aires, Argentina*
[3]*Instituto de Fisiología Animal, Fundación Miguel Lillo y Facultad de Ciencias Naturales e Instituto Miguel Lillo, Universidad Nacional de Tucumán, Tucumán, Argentina*
[4]*Institute of the Chemistry of Plant Substances, Academy of Sciences of Uzbekistan, 100170 Tashkent, Uzbekistan*
[5]*Federal University of ABC, Center of Natural Sciences and Humanities (CCNH-UFABC), Santo André, SP, Brazil*

Correspondence should be addressed to Valeria P. Sülsen; vsulsen@ffyb.uba.ar

Received 7 June 2017; Accepted 7 June 2017; Published 12 July 2017

Asteraceae (formerly known as Compositae) is one of the largest families of higher plants, with more than 1700 genera and approximately 24000 species, which grow in varied environments [1]. The economic importance of the Asteraceae family has been described and, for centuries, several species of this family have been used for medicinal and food purposes [2].

Over the last decades, different species from this family have been studied due to the great variety and amount of bioactive compounds they synthesize. Among them, terpenoids and flavonoids stand out because of their biological activities and potential health benefits.

Terpenoids constitute the largest class of natural products derived from isoprene (C5) units joined head-to-tail or tail-to-head, among other possibilities. They are classified as hemiterpenes (C5), monoterpenes (C10), sesquiterpenes (C15), diterpenes (C20), sesterpenes (C25), triterpenes (C30), tetraterpenes (C40), and polyterpenes (>C40). They can be found in numerous living organisms, especially plants, fungi, and marine animals. Terpenoids are of great interest due to the broad range of biological activities reported such as cancer preventive effects and analgesic, anti-inflammatory, antimicrobial, antifungal, antiviral, and antiparasitic activities [3].

Flavonoids are hydroxylated phenolic compounds that are present in plants and occupy a special place among secondary metabolites. They are classified into different classes, with flavones, flavonols, flavanones, catechins, isoflavones, and anthocyanidins being the most common. Similar to terpenoids, they also present a wide range of biological activities. These compounds have been demonstrated to have protective effects against many infectious and degenerative diseases such as cancer, among other important pharmacological activities such as antioxidant and anti-inflammatory activities [4, 5].

Many of these bioactive compounds and their derivatives either are already being used to treat diseases or are under study in preclinical and clinical trials. The sesquiterpene lactones artemisinin and arglabin, isolated both from *Artemisia* species, are approved drugs for the treatment of human malaria and cancer, respectively. The anticancer drug paclitaxel is also a terpenoid compound used nowadays against several types of cancer [6]. Among flavonoids, the flavone quercetin is currently being assessed in clinical trials on prostate cancer and its primary prevention [7].

This special issue offers original research contributions related to the evaluation of antiparasitic and cytotoxic extracts by means of screening processes, the evaluation of

the effect of extracts on inflammation and the detection of their bioactive compounds, and the assessment of the anti-inflammatory and cytotoxic activities of terpenoids and flavonoids as well as those formulae containing such compounds, together with attempts to gain an insight into the possible mechanism of action of these groups of substances.

Considering the biological and pharmacological activities of terpenoids and flavonoids and the importance of these metabolites as potential lead compounds, we decided to include in this special issue some research articles describing the activity of these groups of compounds isolated from species belonging to families other than Asteraceae.

Acknowledgments

We are grateful to the authors for their valuable contributions to this special issue. We are also thankful to all the reviewers for their opinions and suggestions. We also want to thank Evidence Based Complementary and Alternative Medicine for inviting us to edit this special issue.

Valeria P. Sülsen
Emilio Lizarraga
Nilufar Z. Mamadalieva
João Henrique G. Lago

References

[1] M. C. Telleria, "Asteraceae visited by honeybees in Argentina: a record from entomopalynological studies," *Boletin de la Sociedad Argentina de Botánica*, vol. 44, pp. 65–74, 2009.

[2] G. E. Barboza, J. J. Cantero, C. Núñez, A. Pacciaroni, and L. Ariza Espinar, "Medicinal plants: A general review and a phytochemical and ethnopharmacological screening of the native Argentine Flora," *Kurtziana*, vol. 34, p. 365, 2009.

[3] B. Singh and R. A. Sharma, "Plant terpenes: defense responses, phylogenetic analysis, regulation and clinical applications," *3 Biotech*, vol. 5, no. 2, pp. 129–151, 2015.

[4] S. Kumar and A. K. Pandey, "Chemistry and biological activities of flavonoids: an overview," *The Scientific World Journal*, vol. 2013, Article ID 162750, 16 pages, 2013.

[5] N. Z. Mamadalieva, F. Herrmann, M. Z. El-Readi et al., "Flavonoids in Scutellaria immaculata and S. ramosissima (Lamiaceae) and their biological activity," *Journal of Pharmacy and Pharmacology*, vol. 63, no. 10, pp. 1346–1357, 2011.

[6] A. G. Atanasov, B. Waltenberger, and E. M. Pferschy-Wenzig et al., "Discovery and resupply of pharmacologically active plant-derived natural products: a review," *Biotechnology Advances*, vol. 33, pp. 1582–1614, 2015.

[7] ClinicalTrials.gov, "A service of the U.S. National Institutes of Health," 2017. https://clinicaltrials.gov/ct2/results?term=quercetin+and+cancer&Search=Search.

Hindawi
Evidence-Based Complementary and Alternative Medicine
Volume 2017, Article ID 8248142, 9 pages
https://doi.org/10.1155/2017/8248142

Research Article

Andrographolide Inhibits Inflammatory Cytokines Secretion in LPS-Stimulated RAW264.7 Cells through Suppression of NF-κB/MAPK Signaling Pathway

Yu Li,[1] Shengnan He,[1] Jishun Tang,[2] Nana Ding,[1] Xiaoyan Chu,[1] Lianping Cheng,[1] Xuedong Ding,[1] Ting Liang,[1] Shibin Feng,[1] Sajid Ur Rahman,[1] Xichun Wang,[1] and Jinjie Wu[1]

[1]*College of Animal Science and Technology, Anhui Agricultural University, 130 West Changjiang Road, Hefei 230036, China*
[2]*Institute of Animal Husbandry and Veterinary Medicine, Anhui Academy of Agriculture Sciences, Nongkenan Road, Hefei 230031, China*

Correspondence should be addressed to Jinjie Wu; wjj@ahau.edu.cn

Received 24 January 2017; Revised 16 March 2017; Accepted 11 April 2017; Published 5 June 2017

Academic Editor: Emilio Lizarraga

Andrographolide, the main active component extracted from *Andrographis paniculata* (Burm.f.) Wall. ex Nees, exerts anti-inflammatory effects; however, the principal molecular mechanisms remain unclear. The objective of this study was to investigate the molecular mechanisms of Andrographolide in modifying lipopolysaccharide- (LPS-) induced signaling pathway in RAW264.7 cells. An in vitro model of inflammation was induced by LPS in mouse RAW264.7 cells in the presence of Andrographolide. The concentration and expression levels of proinflammatory cytokines were determined by an enzyme-linked immunosorbent assay (ELISA) and quantitative real-time polymerase chain reaction (qRT-PCR), respectively. The nuclear level of NF-κB was measured by an electrophoretic mobility shift assay (EMSA). The expression levels of NF-κB, p38, ERK, and JNK were determined by western blot. Andrographolide dose-dependently inhibited the release and mRNA expression of TNF-α, IL-6, and IL-1β in LPS-stimulated RAW264.7 cells. The nuclear level of p65 protein was decreased in Andrographolide treatment group. Western blot analysis showed that Andrographolide suppressed LPS-induced NF-κB activation and the phosphorylation of IkBa, ERK1/2, JNK, and p38. These results suggest that Andrographolide exerts an anti-inflammatory effect by inhibiting the activation of NF-κB/MAPK signaling pathway and the induction of proinflammatory cytokines.

1. Introduction

Inflammation is a complex reaction that occurs within local or systemic animal organs in response to multiple endogenous or exogenous injuries, which mainly result in redness, swelling, fever, pain of organs, and tissue damage [1]. The *Andrographis paniculata* plant has been widely used for long periods in Asian traditional medicinal [2]. Common *Andrographis* herb is derived from *Andrographis paniculata* (Burm.f.) Wall. ex Nees. The whole plant or aerial parts of plant are employed for the purposes like cooling properties and a bitter taste that can reduce heat, detoxify, cool the blood, and reduce swellings [3]. Andrographolide ($C_{20}H_{30}O_5$, Figure 1), a labdane diterpenoid that is produced by *Andrographis paniculata* plant, has been reported to have several pharmacological properties, including antibacterial, antiviral, and antiplatelet properties, stimulation of cell differentiation, protection of the liver, being a cholagogue, antitumor properties, and immunoregulation [4]. Previous studies reported that Andrographolide can inhibit the increase in capillary permeability caused by xylene and acetic acid in mice. Moreover, Andrographolide has exhibited obvious anti-inflammatory properties in response to the rat model of hind paw edema induced by egg white protein and carrageenan [5]. Andrographolide can inhibit the expression of inducible nitric oxide synthase (iNOS) by LPS-activated macrophages and the production of prostaglandin E2 [6]. However, the potential pharmacodynamic function and mechanisms by

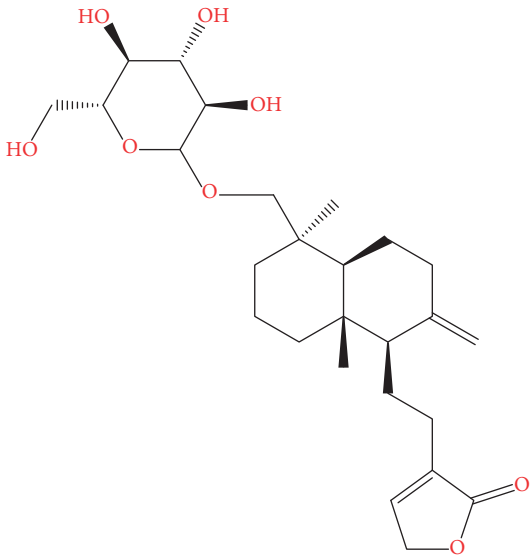

Figure 1: The chemical structure of Andrographolide.

which Andrographolide exerts such anti-inflammatory properties remains unclear [7].

LPS is considered as one of the most potent inducers of proinflammatory factors [8], and bacterial infections often cause a strong inflammatory reaction. Macrophages are important immune activating cells and play a critical role in the induction of the inflammatory response in response to pathogen invasion [9]. Mouse macrophage RAW264.7 cells stimulated by LPS can produce inflammatory mediators and inflammatory factor, such as TNF-α, IL-1β, and IL-6 [10, 11]. Therefore, an excessive production of these proinflammatory cytokines can cause severe damage to surrounding tissues.

Studies have confirmed that LPS induces inflammation primarily by stimulating NF-κB and the MAPK signaling pathway [12]. Therefore, inhibition of the inflammatory response by targeting signal transduction pathways has become a novel avenue for the treatment of inflammation.

In the present study, LPS was used to activate the NF-κB and MAPK signaling pathways as the theoretical basis to investigate mechanisms of the anti-inflammatory effects of Andrographolide in LPS-induced inflammation of RAW264.7 cells. The aim of current investigation was to provide a theoretical basis for the further development of anti-inflammatory drugs.

2. Materials and Methods

2.1. Reagents. Andrographolide (Control of Pharmaceutical and Biological Product, Beijing, China), dimethyl sulfoxide (DMSO), fetal bovine serum, and 0.25% trypsin were purchased from HyClone (Logan, UT, USA); LPS (*Escherichia coli* 055:B5) was purchased from Sigma Chemical CO. (St. Louis, MO, USA); Mouse TNF-α, IL-1β, and IL-6 ELISA kits were purchased from Sbjbio company (Nanjing, China); primary antibodies of rabbit mAb p65, rabbit mAb ERK, and rabbit mAb JNK; secondary antibodies of goat anti-rabbit IgG antibody; and goat anti-mouse IgG antibody were purchased from Wuhan Boster Biological Engineering Co. (Wuhan, China); primary antibodies of rabbit mAb IκBα, mouse mAb phospho-IκBα, mouse mAb phospho-p65, mouse mAb phospho-p38, mouse mAb phospho-specific p42-p44 ERK, and mouse mAb phospho-specific p46-p54 JNK were purchased from Beyotime Biotechnology Co. (Nanjing, China).

2.2. Culture of RAW264.7 Cells. RAW264.7 mouse monocyte-macrophage cells were received as a gift from Jilin University (Changchun, China). RAW264.7 cells were inoculated in cell culture bottles, and then the cells were placed in an incubator at 37°C and 5% CO_2. The culture medium (DMEM medium with 10% fetal bovine serum, 1% Gln, and 100 U/ml penicillin-streptomycin) were changed according to the cell growth conditions and color of the media, respectively. When the cells reached 80% confluence, the cells were subcultured by replacing the culture medium and the adherent cells were aspirated with a pipette, washed, and then seeded into new cell culture bottles to be incubated.

2.3. Microscopic Observation and Cell Counting Kit-8 (CCK-8) Assay for Cell Viability. Briefly, RAW264.7 cells in the logarithmic phase were plated at a density of 1×10^5 cells/ml into 96-well plates in a 37°C, 5% CO_2 incubator for 24 h. Subsequently, 100 μL cells were added to each well, and the cells were treated with indicated concentrations of Andrographolide for 1 h in the incubator. When the cell morphology observed by microscope was adequate, the same concentration was being performed in triplicate, followed by stimulating with 1 μg/ml LPS in a 37°C, 5% CO_2 incubator for 18 h. A volume of 10 μL CCK-8 (Dojindo, Kumamoto, Japan) was added to each well, and the cells were further incubated for additional 1–4 h. The optical density (OD) was measured at 450 nm using a Bio-Rad Model 550 Microplate Reader (Bio-Rad, Hercules, CA, USA), and the cell viability was calculated.

2.4. ELISA Assay for the Contents of Proinflammatory Cytokines. The RAW264.7 cells (2×10^6 cells/ml, with 2 ml in each well) were seeded into six-well plates and incubated in the presence of different concentrations (6.25, 12.5, and 25 μg/ml) of Andrographolide for 1 h, followed by stimulating with LPS (l μg/ml) for 18 h [13]. The cell-free supernatants were subsequently employed to quantify the contents of proinflammatory cytokines (TNF-α, IL-1β, and IL-6) using a mouse ELISA kit, according to the manufacturer's instructions (Sbjbio company, Nanjing, China).

2.5. Total RNA Isolation and qRT-PCR. The RAW264.7 cells (2×10^6 cells/ml, with 2 ml in each well) were seeded into six-well plates and incubated in the presence of different concentrations (6.25, 12.5, and 25 μg/ml) of Andrographolide for 1 h, followed by stimulation with LPS (l μg/ml) for 18 h. The supernatant was removed, and the sediments were washed with PBS twice. The total RNA was extracted using Trizol reagent following the manufacturer's instructions (TaKaRa, Dalian, China), and the RNA was reverse-transcribed into cDNA according to the Reverse Transcription System's

Table 1: The TNF-α, IL-1β, and IL-6 primers.

Genes	Primer	Sequence $5' \rightarrow 3'$	Product size (bp)
TNF-α	Sense	GTCTCAGCCTCTTCTCATTC	128
	Antisense	CATAGAACTGATGAGAGGGA	
IL-1β	Sense	AAATACCTGTGGCCTTGGGC	101
	Antisense	CTTGGGATCCACACTCTCCAG	
IL-6	Sense	GAGTCCTTCAGAGAGATACAG	125
	Antisense	CTGTGACTCCAGCTTATCTG	
β-Actin	Sense	CTTCATTGACCTCAACTACATGG	134
	Antisense	CTCGCTCCTGGAAGATGGTGAT	

instructions (TaKaRa, Dalian, China). According to the GenBank sequence, the primer sequence of the target genes (i.e., TNF-α, IL-1β, and IL-6) and the *β-actin* gene were designed using the software Primer Premier 5.0 (Table 1). The amplification products were analyzed by 1.5% agarose gel electrophoresis and a gel imaging and analysis system (UVItec, Cambridge, UK).

2.6. EMSA Assay for Protein Transportation to the Nucleus. RAW264.7 cells (2×10^6 cells/ml, with 1 ml in each well) were seeded into six-well plates; 2 ml was added to each plate and incubated in the presence of different concentrations (6.25, 12.5, and 25 μg/ml) of Andrographolide for 1 h when the cells reached 5×10^6~1×10^7 cells/ml. Following this incubation, the cells were stimulated with LPS (1 μg/ml) for 18 h; after that cells were collected and washed twice with ice-cold PBS, centrifuged at 500g and 4°C for 3 min, the supernatant was removed, and packed cell volume was estimated. The nucleoprotein was extracted with nuclear protein extraction reagent (Sagon, Shanghai, China) and the total protein was determined using the Bradford method (Biosharp, China). A 6.5% polyacrylamide gel was produced and made into a gel slab, an EMSA binding reaction was performed, and the samples were produced and dispensed.

Electrophoresis was initiated with a 0.5x TBE as the running buffer at 10 V/cm. When the bromophenol blue in the EMSA/Gel-Shift loading buffer ran to the lower edge of the gel, the electrophoresis was stopped. The required gel was cut, and the protein and probe (5′-AGTTGAGGG-GACTTTCCCAGGC-3′) complexes were transferred into a nylon membrane (GE Healthcare, USA) with a transfer buffer at 254 nm, 120 mJ/cm^2 in the cross-linking machine. After 45–60 s, cross-linking was completed, the sealing and washing liquid was dissolved at 37–50°C in a water bath, the nylon membrane was blocked with 15 ml sealing liquid for 15 min on a horizontal rotator, and the sealing liquid was removed. The new sealing liquid containing streptavidin-HRP conjugate (1 : 2000 dilution) was introduced; the membrane was shaken for 15 minutes on the horizontal rotator, followed by washing (4 × 5 min) with the washing liquid. The nylon membrane was then placed in a container with 20–25 ml of a determined equilibrium liquid and shook for 5 min. Then the nylon membrane was removed and the extra liquid was absorbed with absorbent paper. The chemiluminescent nucleic acid detection module working solution was added until the membrane was covered completely and then left at room temperature for 2-3 min. The nylon membrane was removed and the extra liquid was placed into the middle of two pieces of plastic wrap and tested using the G:BOX chemiXR5 Gel Imaging System. The results were analyzed using the Gel-Pro32 software (Syngene, Cambridge, UK).

2.7. Western Blot Analysis. RAW264.7 cells at 4×10^5 cells/ml were seeded into six-well plates (2 ml per plate) and incubated for 24 h and then pretreated with different concentrations (6.25, 12.5, and 25 μg/ml) of Andrographolide for 1 h. The cells were stimulated with LPS (1 μg/ml) for 18 h and then collected and washed twice with ice-cold PBS. The total protein from the cells was extracted using a RIPA lysis buffer solution (Wuhan Boster Biological Engineering Co., Wuhan, China), and the total protein concentration was determined using a BCA Protein Assay Kit (Beyotime Inst. Biotech, Peking, China). The protein was split and the SDS-PAGE loading buffer (Beyotime Biotechnology Co., Shanghai, China) was added and placed into a 100°C water bath for 10 min and preserved at 4°C for later use.

The gel board was installed; a 12% separating gel and 15% stacking gel were produced; then five samples of proteins were added. Electrophoresis was initiated at 80 V and changed to 120 V after 25 min and continued until the samples run to the bottom of the gel. The required gel was cut and transferred into a PVDF membrane (Shanghai Jinsheng Biological Engineering Co) with electrophoresis buffer. The resulting membrane was blocked with 5% BSA for 4 h on a horizontal rotator at room temperature and then incubated with the primary antibodies at 4°C overnight. Subsequently, the membrane was washed with TBST three times followed by an incubation on the horizontal rotator for 5 min and incubated with the secondary antibody at room temperature for 45 min on the horizontal rotator. The blots were washed again with TBST three times for 5 min and then tested by the Gel Imaging System (Bio-Rad, Hercules, CA, USA). The results were analyzed using quantity one software (Bio-Rad, Hercules, CA, USA).

2.8. Statistical Analysis. Date were presented as mean ± SEM. Differences between the mean values of the normally distributed data were analyzed using one-way ANOVA (Dunnett's t-test) and a two-tailed Student's t-test. The criterion for the differences was considered significant at $P < 0.05$ or $P < 0.01$ in all studies.

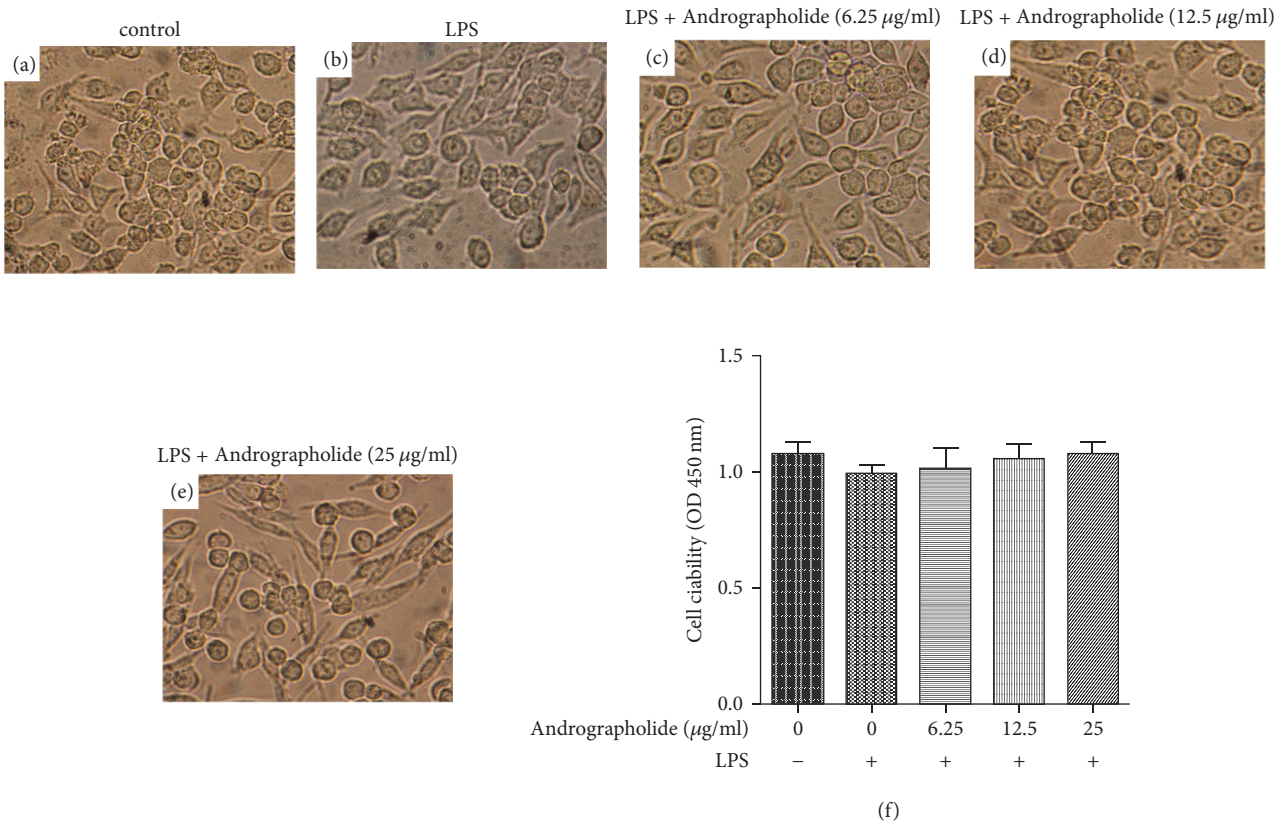

Figure 2: Effect of Andrographolide on morphologic changes and viability of RAW264.7 cells. (a) represents cells in control group; (b) represents cells treated by LPS; (c)–(e) represent cells treated with different concentration Andrographolide (6.25, 12.5, and 25 μg/ml) for 1 h and LPS for another 18 h, respectively; (f) represents the effect of Andrographolide on the cell viability of RAW264.7 cells in control, LPS, and Andrographolide treated groups. Results are representative of three (f) independent experiments.

3. Results

3.1. Effect of Andrographolide on Cell Viability. To evaluate the effects of Andrographolide (6.25, 12.5, and 25 g/ml) on RAW264.7 cells morphologic changes and viability, we performed inverted light microscopy (Nikon, Tokyo, Japan) and CCK-8 assay. As shown in Figures 2(a)–2(f), the cell morphology and viability of RAW264.7 cells have no recognizable changes with the increasing of Andrographolide concentrations. Cell viability in experimental groups with different doses of Andrographolide did not show any significant difference compared with the control group. These results indicated that the Andrographolide used in this study has no toxic effect.

3.2. Effect of Andrographolide on the Secretion of Proinflammatory Cytokines in LPS-Stimulated RAW264.7 Cells. To evaluate the effects of Andrographolide on the secretion of the proinflammatory cytokines in LPS-stimulated RAW264.7 cells, we measured the level of each cytokine using an ELISA. As presented in Figures 3(a)–3(c), the levels of proinflammatory cytokine in the LPS group were significantly higher than that in the control group ($P < 0.05$). Moreover, the proinflammatory cytokine levels of the Andrographolide groups (doses of 6.25, 12.5, and 25 g/ml) were significantly lower than that in the LPS group ($P < 0.05$ or $P < 0.01$) and gradually decreased with the increasing doses of Andrographolide.

3.3. Effect of Andrographolide on the Expression Level of the Proinflammatory Cytokines in LPS-Stimulated RAW264.7 Cells. Next, we sought to evaluate the effects of Andrographolide on the expression level of the proinflammatory cytokines in LPS-stimulated RAW264.7 cells by qRT-PCR. As shown in Figures 4(a)–4(c), the mRNA expression levels of the proinflammatory cytokines in the LPS group were significantly higher than that in the control group ($P < 0.05$). Moreover, the mRNA expression levels of the proinflammatory cytokines in the Andrographolide groups (doses of 6.25, 12.5, and 25 g/ml) were significantly lower than that in the LPS group ($P < 0.01$) and decreased in a dose-dependent manner.

3.4. Effect of Andrographolide on the Nuclear Level of NF-kB Probe Binding Activity. We evaluated the effect of Andrographolide on the NF-κB probe binding activity in NF-κB pathway. Figure 5 showed that the nuclear level of NF-kB probe binding activity in LPS group was significantly higher than that in the control group ($P < 0.01$). However, the nuclear level of NF-kB probe binding activity is significantly decreased in the nuclear extract obtained from

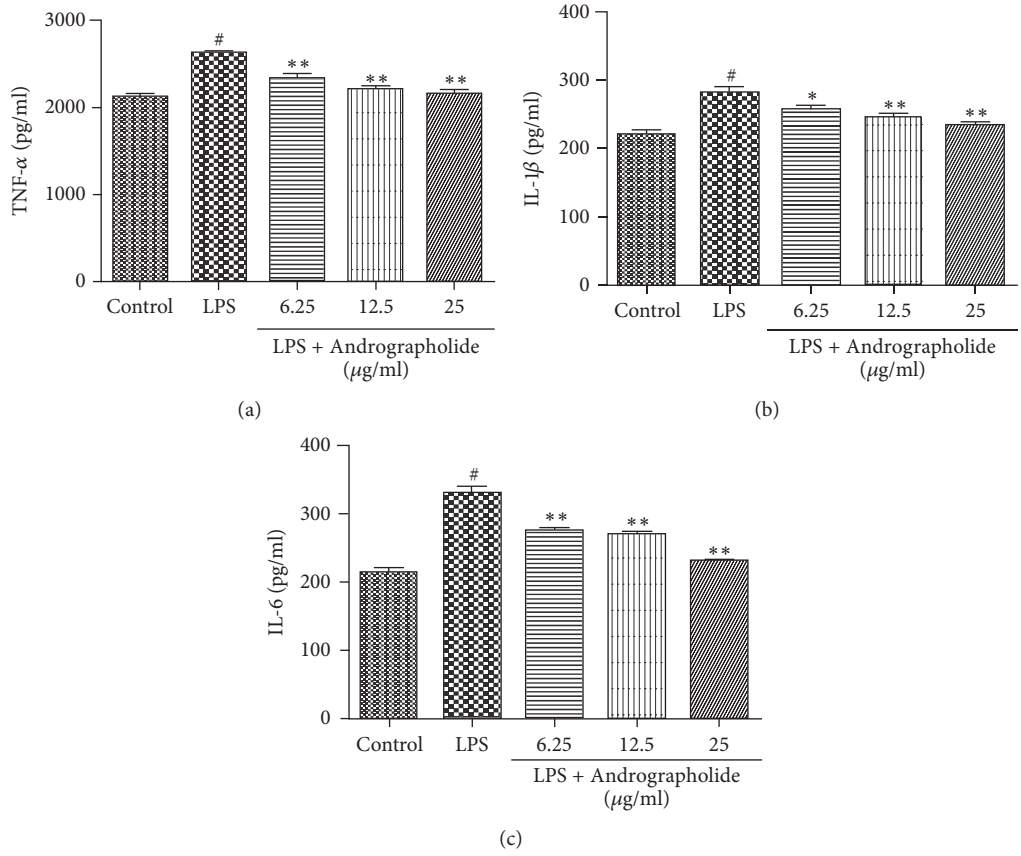

Figure 3: Effect of Andrographolide on the secretion of TNF-α, IL-1β, and IL-6 induced by LPS. # indicates the control group compared with the LPS group ($P < 0.05$); $*$ and $**$ indicate the Andrographolide group compared with the LPS group ($P < 0.05$) and ($P < 0.01$). Results of TNFα (a), IL-1β (b), and IL-6 (c) secretion are representative of three (a–c) independent experiments.

Andrographolide treated cells and was significantly lower than that of the LPS group ($P < 0.01$).

3.5. Effect of Andrographolide on the Suppression of LPS-Induced NF-κB/MAPK Pathway. Since IkBa is phosphorylated after stimulation by LPS, followed by the release of the NF-κB-p65 protein into the nucleus, and promotes the production of proinflammatory cytokines, we next evaluated the effect of Andrographolide on the inhibition of LPS-induced NF-κB and MAPK pathways by a western blot. As shown in Figure 6, the levels of phosphorylated p65 and phosphorylated IkBa in the NF-κB signaling pathway were significantly increased, while the levels of total IkBa in the NF-κB signaling pathway were significantly reduced in LPS group. However, the levels of p65 and IkBa phosphorylation in the NF-κB signaling pathway were significantly reduced in the Andrographolide groups (doses of 6.25, 12.5, and 25 g/ml) compared with the LPS group in a dose-dependent manner. In contrast, the level of total IkBa increased significantly with the increasing doses of Andrographolide. The above results indicate that the Andrographolide can suppress the LPS-induced NF-κB pathway.

As shown in Figure 7, the phosphorylation of JNK, ERK1/2, and p38 in the MAPK signaling pathway was significantly increased in LPS-stimulated samples, but the levels of p-JNK, p-ERK1/2, and p-p38 significantly decreased in the Andrographolide group (doses of 6.25, 12.5, and 25 g/ml) in a dose-dependent manner compared with the LPS group. These results suggest that Andrographolide can also suppress the LPS-induced MAPK pathway.

4. Discussion

Andrographis has many active components that have anti-inflammatory properties. Current research has shown that various active ingredients of *Andrographis* affect immune function, interacting with the platelet activating factor receptor, improving the nitric oxide levels in the body, scavenging oxygen free radicals, and inhibiting various proinflammatory cytokines, thus exhibiting a potent anti-inflammatory effect [14].

Andrographolide, the major active constituent extracted from *Andrographis*, occupies 70% of the *Andrographis* extract and has been reported to have many pharmacological properties, (e.g., it has antibacterial, antiviral, and antiplatelet properties, stimulates cellular differentiation, protects the liver, is a cholagogue, has antitumor properties, and is immunoregulatory). In addition, previous studies have shown that Andrographolide can inhibit increases in capillary permeability caused by xylene and acetic acid in mice [15]. Moreover, it has obvious anti-inflammatory effect, such as in laryngitis,

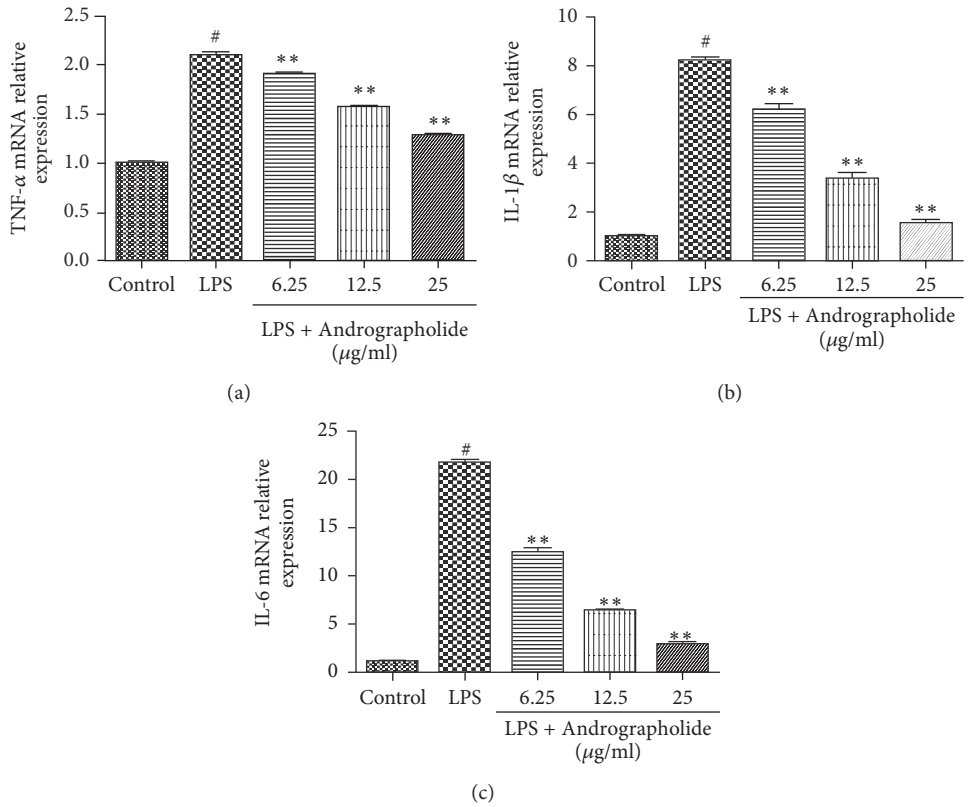

Figure 4: Effect of Andrographolide on the mRNA expression of TNF-α, IL-1β, and IL-6 induced by LPS. # indicates the control group compared with the LPS group ($P < 0.05$) and ** indicates the Andrographolide group compared with the LPS group ($P < 0.01$). Results of TNFα (a), IL-1β (b), and IL-6 (c) mRNA expression are representative of six (a–c) independent experiments.

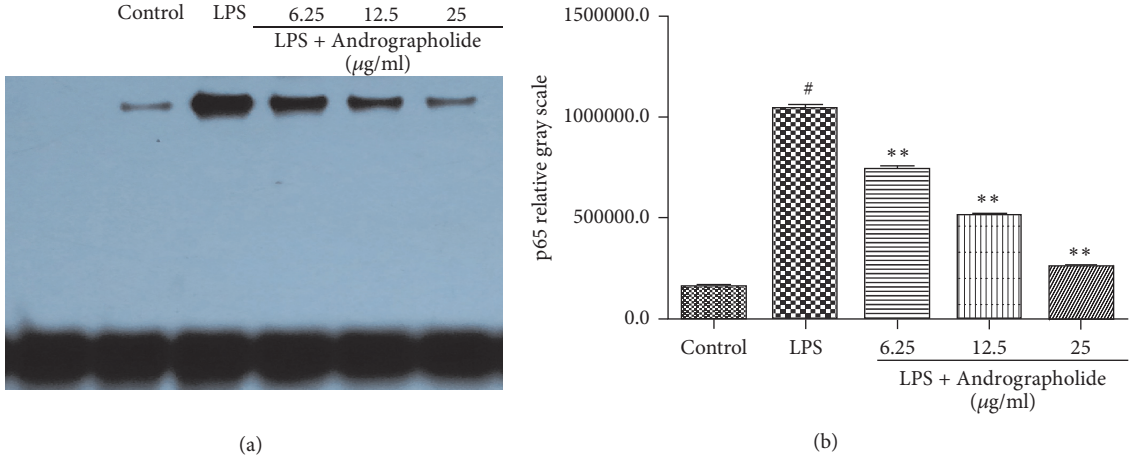

Figure 5: Effect of Andrographolide on nuclear level of transcription factor NF-kB. # indicates the control group compared with the LPS group ($P < 0.05$); ** indicates the Andrographolide group compared with the LPS group ($P < 0.01$). Results of the nuclear level of NF-kB probe binding activity (a) and gray scale (b) are representative of three (a-b) independent experiments.

upper respiratory tract infection, and rheumatoid arthritis [16–22].

Inflammation is a complex process involving the interaction between an organism and pathogens, with the results of these complex interactions to induce macrophage activation [23]. In addition, activated macrophages can eliminate invading infectious microbes and trigger the release of inflammatory cytokines, such as TNF-α, IL-1β, and IL-6, and then complete a variety of immune function in response to these cytokines [24]. Existing research shows that LPS is a potent inducer of inflammation and can stimulate macrophages to produce TNF-α, IL-1β, and IL-6. Thus, the

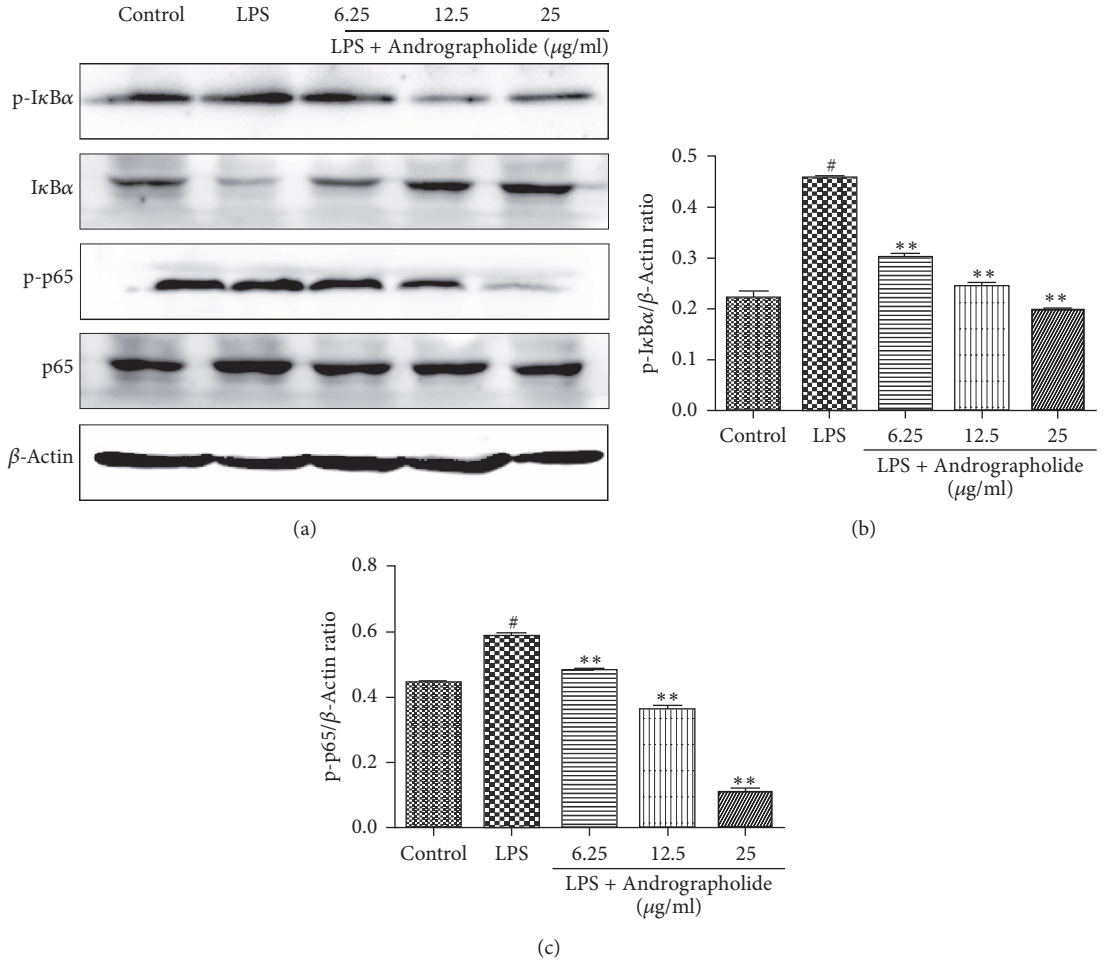

Figure 6: Effect of Andrographolide on the activation of NF-κB pathways of RAW264.7 cells induced by LPS. # indicates the control group compared with the LPS group ($P < 0.05$); ** indicates the Andrographolide group compared with the LPS group ($P < 0.01$). Results of western blot (a), gray scale (b) and (c) are representative of three (a–c) independent experiments.

organic damage caused by inflammation can be reduced by inhibiting the excessive production of inflammatory cytokines [25].

In the present study, an in vitro model of inflammation was induced by LPS in mouse RAW264.7 cells, followed by treatment with different concentrations of Andrographolide. Our results demonstrated that Andrographolide significantly inhibits the expression of TNF-α, IL-6, and IL-1β in LPS-stimulated RAW264.7 cells. Furthermore, we also found that Andrographolide has in vitro anti-inflammatory effects.

Andrographolide can inhibit the expression of TNF-α, IL-1β, and IL-6 in LPS-stimulated macrophages. Thus, the exploration of the anti-inflammatory mechanism of Andrographolide is significance [26]. The NF-κB and MAPK signaling pathways are two extremely classical activation pathways in the process of LPS-induced signal transduction [27]. Under normal resting conditions, NF-κB and IkBa aggregate into a trimer within the cytoplasm. In response to LPS, IkBa is predominately phosphorylated and subsequently degraded, which frees NF-κB-p65 into the nucleus, and gene transcription of various proinflammatory factors is initiated [28, 29].

MAPK can also adjust the synthesis and release of the proinflammatory factors, p38, JNK, and ERK, which are three important pathways primarily involved in the inflammatory responses. When activated by external stimuli, p38, JNK, and ERK phosphorylation is increased and related proinflammatory cytokines will begin to be expressed [30]. Furthermore, the present study explores the anti-inflammatory mechanism of Andrographolide regarding the NF-κB and MAPKs pathways. Our results demonstrated that LPS could induce the phosphorylation of IkBa, NF-κB-p65, p38, JNK, and ERK, but the phosphorylation of IkBa, NF-κB-p65, p38, JNK, and ERK was significantly inhibited when the cells were treated with Andrographolide. Consequently, the inhibition of the NF-κB and MAPK pathways and the production of proinflammatory cytokines were inhibited, thus indicating that its anti-inflammatory effect was exerted via these pathways.

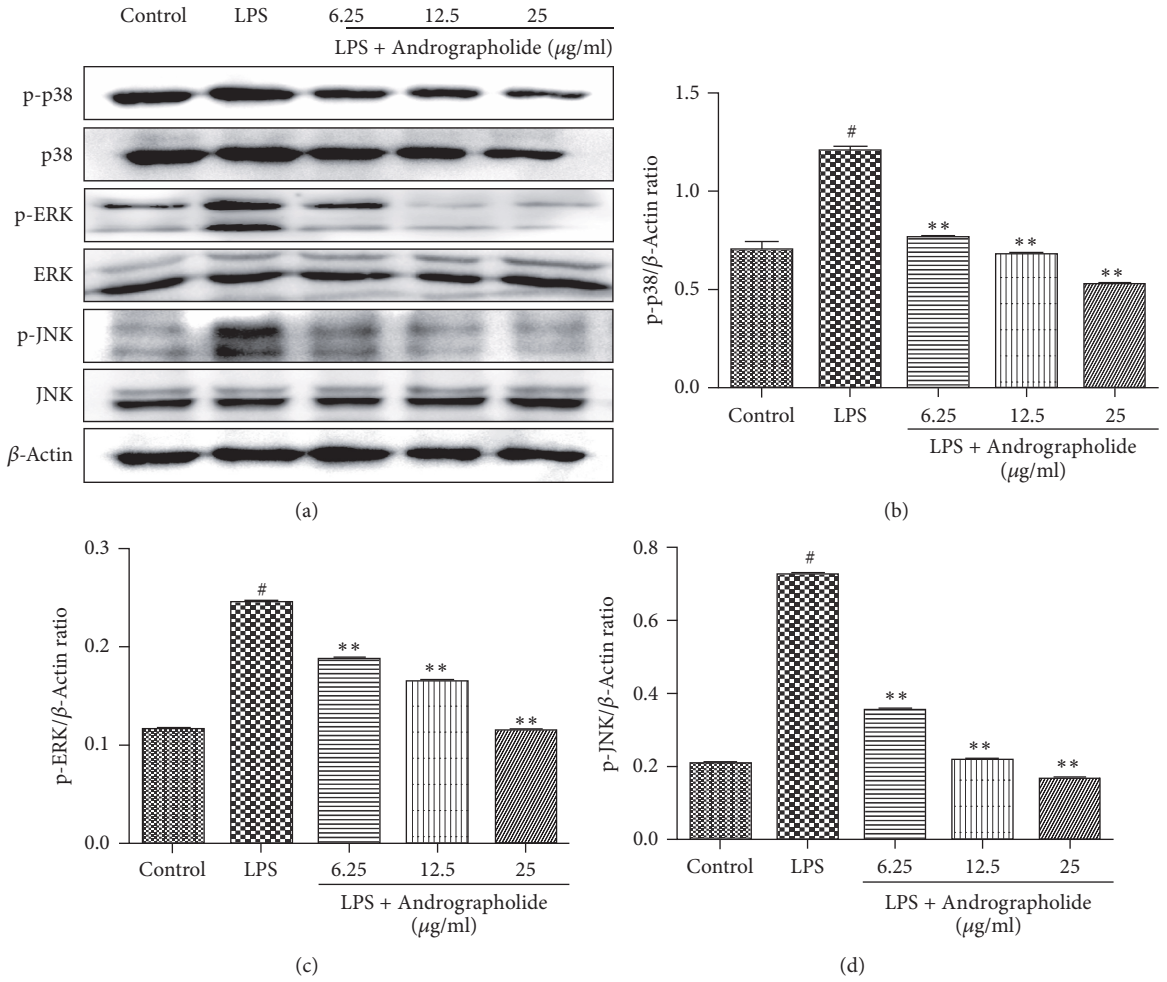

Figure 7: Effect of Andrographolide on the activation of MAPK pathways of RAW264.7 cells induced by LPS. # indicates the control group compared with the LPS group ($P < 0.05$); ** indicates the Andrographolide group compared with the LPS group ($P < 0.01$). Results of western blot (a), gray scale (b), (c) and (d) are representative of four (a–d) independent experiments.

5. Conclusions

Andrographolide has anti-inflammatory effect and significantly inhibits the expression of TNF-α, IL-6, and IL-1β in LPS-stimulated RAW264.7 cells. Its anti-inflammatory mechanism may be through the inhibition of NF-κB and MAPKs signaling pathway.

Conflicts of Interest

The authors declare that they have no conflicts of interest regarding the publication of this paper.

Authors' Contributions

Yu Li, Shengnan He, and Jishun Tang contributed equally to this work.

Acknowledgments

This work was supported by grants from the National Key Research and Development Program of China (2016YFD0501009) and the Project of Modern Agricultural Industry and Technology System of Anhui Province (2016–2020).

References

[1] B. Levine, N. Mizushima, and H. W. Virgin, "Autophagy in immunity and inflammation," *Nature*, vol. 469, no. 7330, pp. 323–335, 2011.

[2] F. Li, D. Liang, Z. Yang et al., "Astragalin suppresses inflammatory responses via down-regulation of NF-κB signaling pathway in lipopolysaccharide-induced mastitis in a murine model," *International Immunopharmacology*, vol. 17, no. 2, pp. 478–482, 2013.

[3] X. P. Li, C. L. Zhang, P. Gao, J. Gao, and D. Liu, "Effects of andrographolide on the pharmacokinetics of aminophylline and doxofylline in rats," *Drug Research*, vol. 63, no. 5, pp. 258–262, 2013.

[4] A. Varma, H. Padh, and N. Shrivastava, "Andrographolide: a new plant-derived antineoplastic entity on horizon," *Evidence-Based Complementary and Alternative Medicine*, vol. 2011, Article ID 815390, 9 pages, 2011.

[5] T. Zhu, D. X. Wang, W. Zhang et al., "Andrographolide protects against LPS-induced acute lung injury by inactivation of NF-κB," *PLoS ONE*, vol. 8, no. 2, Article ID e56407, 2013.

[6] C. V. Chandrasekaran, P. Thiyagarajan, H. B. Deepak, and A. Agarwal, "In vitro modulation of LPS/calcimycin induced inflammatory and allergic mediators by pure compounds of Andrographis paniculata (King of bitters) extract," *International Immunopharmacology*, vol. 11, no. 1, pp. 79–84, 2011.

[7] J.-M. Zhang and J. An, "Cytokines, inflammation, and pain," *International Anesthesiology Clinics*, vol. 45, no. 2, pp. 27–37, 2007.

[8] X. Jin, S. N. Shi, and D. F. Zhang, "Study on composition of andrographolide," *Chinese Herbal Medicines*, vol. 43, pp. 47–50, 2014.

[9] M. Rossol, H. Heine, U. Meusch et al., "LPS-induced cytokine production in human monocytes and macrophages," *Critical Reviews in Immunology*, vol. 31, pp. 379–446, 2011.

[10] A. A. Abu-Ghefreh, H. Canatan, and C. I. Ezeamuzie, "*In vitro* and *in vivo* anti-inflammatory effects of andrographolide," *International Immunopharmacology*, vol. 9, no. 3, pp. 313–318, 2009.

[11] S. H. Diks, D. J. Richel, and M. P. Peppelenbosch, "LPS signal transduction: the picture is becoming more complex," *Current Topics in Medicinal Chemistry*, vol. 4, no. 11, pp. 1115–1126, 2004.

[12] Z. Meng, C. Yan, Q. Deng, D.-F. Gao, and X.-L. Niu, "Curcumin inhibits LPS-induced inflammation in rat vascular smooth muscle cells in vitro via ROS-relative TLR4-MAPK/NF-κB pathways," *Acta Pharmacologica Sinica*, vol. 34, no. 7, pp. 901–911, 2013.

[13] L.-H. Qin, Z.-W. Zheng, L. Kong, J. Lü, Y.-X. Shi, and Y.-P. Li, "Andrographolide inhibits expression of TNF-α and IL-12 in activated macrophages," *Academic Journal of Second Military Medical University*, vol. 32, no. 7, pp. 717–720, 2011.

[14] D. Talei, A. Valdiani, M. Maziah, S. R. Sagineedu, and R. Abiri, "Salt stress-induced protein pattern associated with photosynthetic parameters and andrographolide content in Andrographis paniculata Nees," *Bioscience, Biotechnology and Biochemistry*, vol. 79, no. 1, pp. 51–58, 2015.

[15] H. Du, X. Niu, and H. Y. Li, "Andrographolide microemulsion anti-inflammatory effects," *Chinese Journal of Traditional Medicine*, pp. 94–96, 2012.

[16] Y. F. Xia, B. Q. Ye, Y. D. Li et al., "Andrographolide attenuates inflammation by inhibition of NF-kB activation through covalent modification of reduced cysteine," *Journal of Immunology*, vol. 173, no. 6, pp. 4207–4217, 2004.

[17] J. Batkhuu, K. Hattori, F. Takano et al., "Suppression of NO production in activated macrophages in vitro and ex vivo by neoandrographolide isolated from Andrographis paniculata," *Biological & Pharmaceutical Bulletin*, vol. 25, pp. 1169–1174, 2002.

[18] E. Amroyan, E. Gabrielian, A. Panossian, G. Wikman, and H. Wagner, "Inhibitory effect of andrographolide from *Andrographis paniculata* on PAF-induced platelet aggregation," *Phytomedicine*, vol. 6, no. 1, pp. 27–31, 1999.

[19] A. Puri, R. Saxena, R. P. Saxena, K. C. Saxena, V. Srivastava, and J. S. Tandon, "Immunostimulant agents from *Andrographis paniculata*," *Journal of Natural Products*, vol. 56, no. 7, pp. 995–999, 1993.

[20] Y. C. Shen, C. F. Chen, and W. F. Chiou, "Andrographolide prevents oxygen radical production by human neutrophils: possible mechanism(s) involved in its anti-inflammatory effect," *British Journal of Pharmacology*, vol. 135, no. 2, pp. 399–406, 2002.

[21] Y.-C. Shen, C.-F. Chen, and W.-F. Chiou, "Suppression of rat neutrophil reactive oxygen species production and adhesion by the diterpenoid lactone andrographolide," *Planta Medica*, vol. 66, no. 4, pp. 314–317, 2000.

[22] A. Kapil, I. B. Koul, S. K. Banerjee, and B. D. Gupta, "Antihepatotoxic effects of major diterpenoid constituents of *Andrographis paniculata*," *Biochemical Pharmacology*, vol. 46, no. 1, pp. 182–185, 1993.

[23] X. Zeng, H. C. Bi, and M. Huang, "Research progress of drug control in the process of inflammatory reaction," *Acta Pharmacologica Sinica*, vol. 7, pp. 773–779, 2011.

[24] P. Rainard and C. Riollet, "Innate immunity of the bovine mammary gland," *Veterinary Research*, vol. 37, no. 3, pp. 369–400, 2006.

[25] K. Takeda and S. Akira, "TLR signaling pathways," *Seminars in Immunology*, vol. 16, no. 1, pp. 3–9, 2004.

[26] Q.-Q. Zhang, Y. Ding, Y. Lei et al., "Andrographolide suppress tumor growth by inhibiting TLR4/NF-kB signaling activation in insulinoma," *International Journal of Biological Sciences*, vol. 10, no. 4, pp. 404–414, 2014.

[27] M. Yamamoto, S. Sato, H. Hemmi et al., "Essential role for TIRAP in activation of the signalling cascade shared by TLR2 and TLR4," *Nature*, vol. 420, no. 6913, pp. 324–329, 2002.

[28] J. C. Rosa, F. S. Lira, R. Eguchi et al., "Exhaustive exercise increases inflammatory response via toll like receptor-4 and NF-κBp65 pathway in rat adipose tissue," *Journal of Cellular Physiology*, vol. 226, no. 6, pp. 1604–1607, 2011.

[29] H.-Y. Kim, K. W. Hwang, and S.-Y. Park, "Extracts of Actinidia arguta stems inhibited LPS-induced inflammatory responses through nuclear factor-κB pathway in Raw 264.7 cells," *Nutrition Research*, vol. 34, no. 11, pp. 1008–1016, 2014.

[30] L. Koch, D. Frommhold, K. Buschmann, N. Kuss, J. Poeschl, and P. Ruef, "LPS- and LTA-induced expression of IL-6 and TNF-α in neonatal and adult blood: role of MAPKs and NF-κB," *Mediators of Inflammation*, vol. 2014, Article ID 283126, 8 pages, 2014.

Hindawi
Evidence-Based Complementary and Alternative Medicine
Volume 2017, Article ID 7187168, 12 pages
https://doi.org/10.1155/2017/7187168

Research Article

Targeting Tumor Microenvironment: Effects of Chinese Herbal Formulae on Macrophage-Mediated Lung Cancer in Mice

Fei Xu,[1,2] Wenqiang Cui,[2,3] Zhengxiao Zhao,[1,2] Weiyi Gong,[1,2] Ying Wei,[1,2] Jiaqi Liu,[1,2] Mihui Li,[1,2] Qiuping Li,[1,2] Chen Yan,[1,2] Jian Qiu,[1,2] Baojun Liu,[1,2] and Jingcheng Dong[1,2]

[1]*Department of Integrative Medicine, Huashan Hospital, Fudan University, Shanghai, China*
[2]*Institutes of Integrative Medicine, Fudan University, Shanghai, China*
[3]*Department of Integrative Medicine and Neurobiology, State Key Laboratory of Medical Neurobiology, Institute of Acupuncture Research, School of Basic Medical Science, Fudan University, Shanghai, China*

Correspondence should be addressed to Baojun Liu; lbj825@163.com and Jingcheng Dong; jcdong2004@126.com

Received 11 January 2017; Revised 11 April 2017; Accepted 4 May 2017; Published 28 May 2017

Academic Editor: Valeria Sulsen

Our previous studies have shown that Qing-Re-Huo-Xue (QRHX) formulae had significant anti-inflammatory effects in chronic airway diseases such as asthma and chronic obstructive lung disease. Here, we examined the effects of QRHX on lung cancer cell invasion and the potential associated mechanism(s), mainly polarization of macrophages in the tumor microenvironment. In vivo, QRHX both inhibited tumor growth and decreased the number of tumor-associated macrophages (TAMs) in mice with lung cancer. Further study indicated that QRHX inhibited cancer-related inflammation in tumor by decreasing infiltration of TAMs and IL-6 and TNF-α production and meanwhile decreased arginase 1 (Arg-1) expression and increased inducible NO synthase (iNOS) expression. QRHX could markedly inhibit CD31 and VEGF protein expression. Additionally, CXCL12/CXCR4 expression and JAK2/STAT3 phosphorylation were reduced in QRHX treatment group. Thus, we draw that QRHX played a more important role in inhibiting tumor growth by regulating TAMs in mice, which was found to be associated with the inhibition of inflammation and the CXCL12/CXCR4/JAK2/STAT3 signaling pathway.

1. Introduction

Lung cancer is the most common cause of cancer-related deaths in men and women globally and with the highest rate of morbidity and mortality [1]. In 2014, about 1.5 million new patients were diagnosed worldwide and approximately 1.6 million die of this disease every year [2]. Non-small-cell lung cancer (NSCLC), accounting for 80% of lung cancer, has a dismal five-year survival at 15% and even worse, patients with advanced NSCLC, if left untreated, have a median survival of 4-5 months after diagnosis [2, 3]. During the past decades, new treatments, such as minimally invasive, surgery, targeted therapy, adjuvant chemotherapy, and individualized therapy, have been applied but have a less important effect in improving the overall 5-year survival, especially in the advanced stage [4]. Nonetheless, all above therapies have focused on tumor cells.

However, uncontrolled growth in tumors, invasion, and metastasis cannot be elucidated solely by aberrations in cancer cells themselves. Over the past few decades, a major paradigm shift happens to cancer therapy and a great deal of effort has been put forth to develop therapies that target the tumor microenvironment. Accumulating evidences suggest that the alterations that occur in the stroma around a tumor prove useful in antiangiogenesis, antitumor metastasis, and prognosis [5]. Nontumoral cells, including stromal cells (fibroblasts, endothelium cells, etc.) and leukocytes, are a prominent component of solid tumors [6]. Tumor-associated macrophages (TAMs), an important component, acquire a distinct, tissue-specific phenotype in different microenvironments and have both anti- and protumor effect due to two distinctly different polarization, respectively, referred to as "classical" (or M1) and "alternative" (or M2) activation [7]. In tumor microenvironment, TAMs are primarily polarized

toward a M2-like phenotype, which have the ability to promote the growth and vascularization of tumors. Collective evidences demonstrate that the dual roles of TAMs have been demonstrated both in vitro and in vivo in different tumor models [8]. Moreover, clinical studies make strong cases that TAMs, characterized by M2 phenotypes, are poor predictors of prognosis and progression in numerous malignancies [9].

TAMs also profoundly influence the effects of conventional treatment modalities (chemotherapy and radiotherapy), targeted drugs, antiangiogenic agents, and immunotherapy, including checkpoint blockade [10]. Therefore, TAMs are essential for effective therapy and M2-like TAMs are considered to be potential target for adjuvant anticancer therapies. In addition, extensive studies have been carried out to declare that approaches targeting M2-like TAMs have gained encouraging results. Thus there is a growing appreciation that skewing TAM polarization away from the M2- to M1-like phenotype is of great importance.

Accumulated data indicates that traditional Chinese medicine (TCM) plays a pivotal role in regulating tumor microenvironment, including remodeling immunosuppressive microenvironment, hypoxia microenvironment, angiogenesis/lymphangiogenesis, and extracellular matrix [11]. Qing-Re-Huo-Xue (QRHX) formulae consist of a 1 : 1 mixture (w/w) of Radix Paeoniae Rubra and *Scutellaria baicalensis*. The above formula is frequently used in treatment of chronic inflammatory diseases in the respiratory system and immunocompromised diseases in TCM. Increasing evidence revealed that QRHX and its components, extracts, and derivative have the ability of anticancer and anti-inflammation [12–14]. Nevertheless, there are no reports which concerned the alleviated effects of QRHX on macrophage-mediated lung cancer. In the present study, we aimed to investigate the relevance between macrophage polarization and the antitumor effect of QRHX in mice.

2. Methods

2.1. Animal. Male C57BL/6J mice (5 weeks old) were purchased from Shanghai SLAC Co. (Shanghai, China) and housed in separate stainless steel cages (six mice per cage) at constant temperature (23°C) with a 12 h light/dark cycle had free access to water and food. All procedures of this study were approved by the Fudan University Animal Care and Use Committee (number 2015000518547).

2.2. Reagents. The following antibodies were used: VEGF, abcam46160 and abcam1613; CXCR4, abcam124824; CXCL12, abcam25117; p-JAK, CST3717; CD31, abcam28364; inducible NO synthase (iNOS), abcam15323; arginase 1 (Arg-1), CST385; CD11b, abcam1211; CD206, abcam64693 and abcam8918; Alexa Fluor 488, ALEXA21202 and 594 and ALEXA21207.

2.3. QRHX Preparation Chemical Constituents Identification. QRHX, a two-herb Chinese medicinal formula, is comprised of Radix Paeoniae Rubra and *Scutellaria baicalensis*. QRHX granules (batch number: 1211301) were prepared and supplied by Jiangyin Tianjiang Pharmaceutical Co. Ltd. Briefly, their component herbs were admixed in the prescribed proportion, which were soaked in distilled water (1 : 10 w/v) for 2 h and extracted at 100°C for twice (1 h each time). Then the decoction was filtered and concentrated to the extract with a relative density 1.13 at 60°C. After spray drying, the drying powder was blended thoroughly and made into 18–40 mesh particles. The granules were stored at 4°C and dissolved in distilled water of double volume before use. To ensure standardization and maintain interbatch reliability of QRHX, chemical ingredients of QRHX were separated and identified by high-performance liquid chromatography quadrupole time-off light mass spectrometry ultraviolet (HPLUNG CANCER-Q/TOF MS-UV). Briefly, 8 chemical components were, respectively, identified as major material basis in QRHX (Supplementary Figure 1 and Table 1 in Supplementary Material available online at https://doi.org/10.1155/2017/7187168).

2.4. Cell Culture. Lewis lung cancer (LLC) cells lines were cultured in DMEM supplemented with 10% Hyclone Fetal Bovine Serum (FBS; ThermoFisher Scientific, Fremont, CA, USA) in an atmosphere of 95% oxygen and 5% CO_2 at 37°C. The cells were grown in 75 cm^2 culture flasks and harvested in a solution of trypsin-EDTA at the logarithmic growth phase.

2.5. Subcutaneous Models and Drugs Administration. LLC cells were harvested by a brief treatment with trypsin/EDTA and then resuspended in DMEM with 10% FBS. Then cells were washed with cold PBS by centrifugation and resuspended in PBS to the concentration of 1×10^7/mL and kept on ice before used. The male mice were randomly divided into two groups ($n = 12$, each group), including NS and QRHX groups. Tumor cells (2×10^6 cells in 0.2 mL PBS) were injected subcutaneously into the right of the back. After 10 days, tumor size was measured twice weekly by a digital caliper and was estimated as $(D^2 \times d)/2$, where D is the large diameter and d is the small diameter of the tumor. Twenty-four hours after establishing model, mice were administered by intragastric (i.g.) in 0.2 mL volume for 24 consecutive days to different groups with QRHX and normal saline (NS) respectively and then sacrificed at day 24 after injection.

2.6. Enzyme-Linked Immunosorbent Assay (ELISA). Concentrations of serum IL-6 and TNF-a were measured using an ELISA. The blood sample was stored at room temperature for 2 h, centrifuged (5000 rpm) for 30 min, and then cryopreserved at −80°C. The concentrations of IL-6 and TNF-a were measured using a sandwich ELISA kit (Multisciences, China).

2.7. Flow Cytometric Analysis. Tumor tissue was smeared, pushed through 200 mesh screen twice, and then resuspended by PBS. The suspension was treated with erythrocytolysin and then wash by PBS twice and finally suspended by PBS. Cells were then fixed and stained with PerCP-Cyanine 5.5-labeled anti-mouse CDD45, FITC labeled anti-mouse CD11b, Antigen PE labeled anti-mouse F4/80, and Alexa Fluor 647 labeled anti-mouse CD206 antibodies according

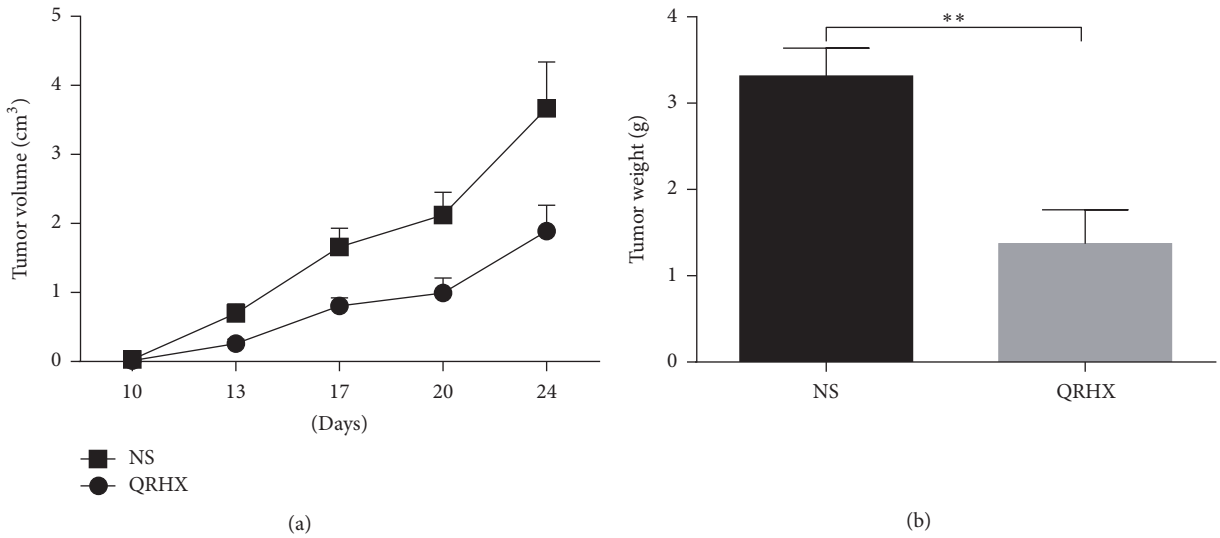

Figure 1: *QRHX inhibits growth of tumor in a subcutaneous mouse model.* C57/BL6 mice were subcutaneously injected with LLC. QRHX reduced tumor volume (a) and weight (b). The data represent means ± SEM ($n \geq 10$). Compared with NS group, $^{**}P < 0.01$.

to the manufacturer's instructions followed by detection by a FACSCalibur instrument (BD Bioscience).

2.8. Western Blot Analysis. Total protein was extracted from the cells using a RIPA kit (Beyotime, China). Cell debris was removed by microcentrifugation, and supernatants were quickly frozen. The protein concentration was determined by BSA method. And then the protein was electrophoresed on a polyacrylamide gel and transferred to a PVDF membrane. Next, the membranes was incubated 1 h–1.5 h with 5% milk at room temperature and then incubated overnight at 4°C with a 1 : 1000 or 1 : 500 dilution of corresponding primary antibodies. Blots were again washed three times with Tris-buffered saline/Tween 20 (TBST) and then incubated with a 1 : 5000 dilution of HRP-conjugated secondary antibody for 1 h at room temperature. Blots were again washed three times with TBST and then developed by enhanced chemiluminescence. Band intensities were quantified using UN-SCAN-IT gel analysis software (version 6).

2.9. QT-PCR. Total RNA was extracted with Trizol reagent (Ambion, Thermo), and reverse transcriptionwas performed to obtain the cDNA using the PrimeScript RT Reagent Kit (Takara, Japan), according to the manufacturer's protocol. The primers used were synthesized by (Sangon Biotech, China). These queues were as follows: iNOS: 5′-GTT-CTCAGCCCAACA ATACAAGA-3′ (forward) and 5′-GTG-GACGGGTCGATGTCAC-3′ (reverse); IL-6: 5′-GATACC-ACTCCCAAC AGAC-3′ (forward) and 5′-CTTTTCTCA-TTTCCACGAT-3′ (reverse); CCL22: 5′-AGGAAGGC TTG-GCTTTTAGG-3′ (forward) and 5′-TGGTACCTTGCA-GGCTCTCT-3′ (reverse); TNF-α: 5′-ACGGCATGGATC-TCAAAGAC-3′ (forward) and 5′-GTGGGTGAGGAGCAC-GTAGT-3′ (reverse); GAPDH: 5′-AAATGGTGAAGGTCG-GTGTG-3′ (forward) and 5′-AGGTCAATG AAGGGGTCG-TT-3′ (reverse). Quantitative real-time PCR (QT-PCR) was performed using SYBR green reaction mixture in the ViiA™ 7 Real Time PCR System (Bio-Rad, MiniOpticon). The relative expression levels were calculated using 2−ΔΔCt methods.

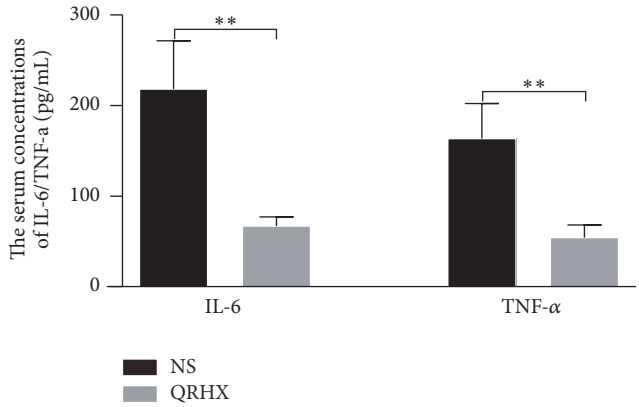

Figure 2: *QRHX suppresses cancer-related inflammation in lung cancer.* A subcutaneous mouse model was established and treated with QRHX or NS as described above. Blood was collected from each mouse, and the serum concentrations of the proinflammatory cytokines IL-6 and TNF-a were detected by ELISA. Student's t-test was used to determine the statistical significance, $^{**}P < 0.01$.

2.10. Immunofluorescence (IF). Cryostat sections were fixed and permeated. CD11b and CD206 antibodies for mice tumor tissue were used, followed by Alexa Fluor 488 (ALEXA) or 594 (ALEXA).

2.11. Immunohistochemical Analysis. IHC stain was performed using a two-step EnVision/HRP technique according to the manufacture's instruction. For three slides, cytoplasm stained with brown was scored as positive. The expression of CD206, CD31, and VEGF was quantitatively evaluated using

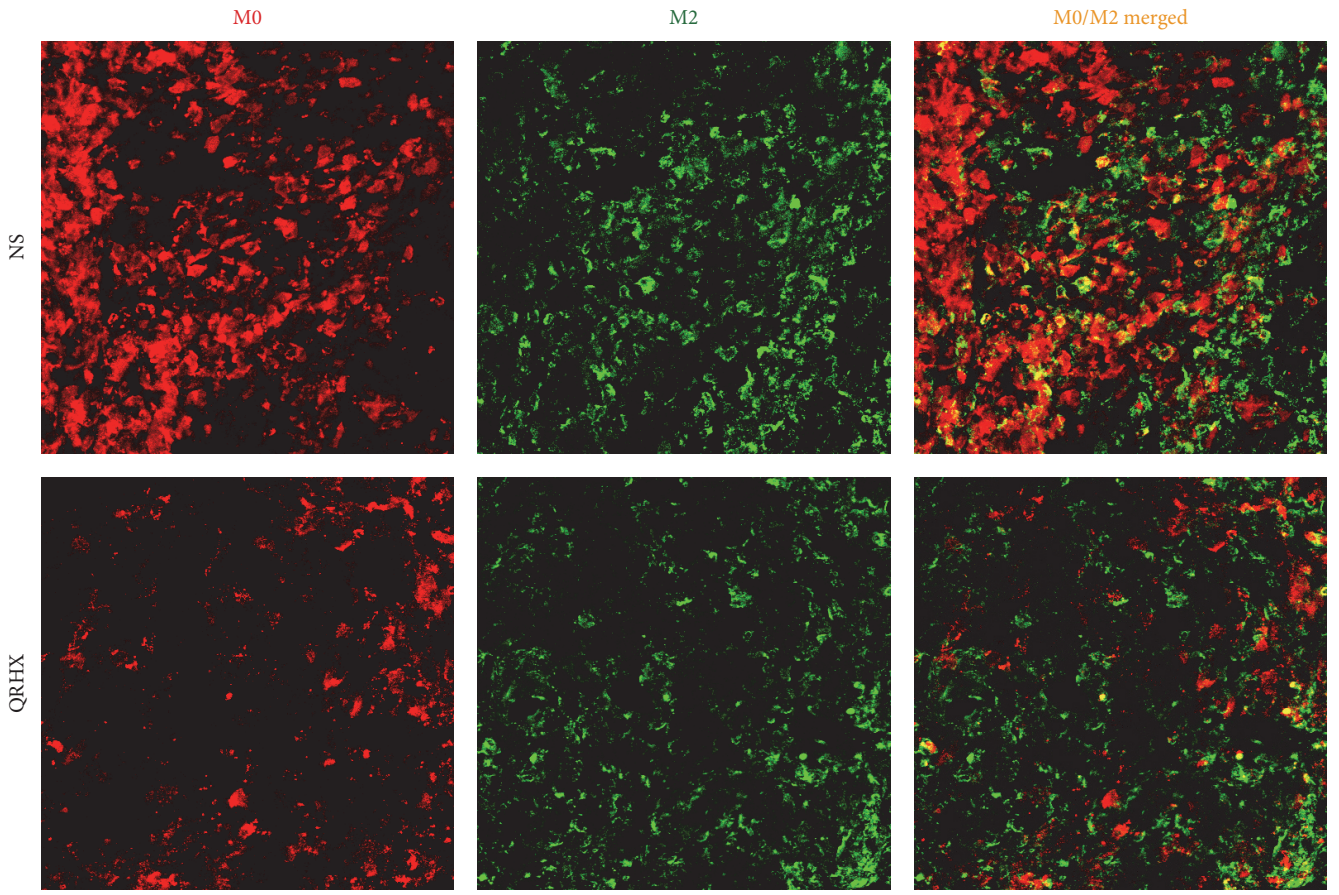

Figure 3: *Immunofluorescence staining for CD11b and CD206 of tumor tissues in subcutaneous tumor*. Mice with subcutaneous tumor were dealt with NS and QRHX. Images are at magnification of 200x. The expression of M0 and TAMs (M2-like macrophage) was, respectively, analyzed using an Alexa Fluor-549- and Alexa Fluor-488-conjugated secondary antibody.

Olympus Cx31 microscope with Image-Pro Plus medical image analysis system. The digital images were captured using a digital camera (Canon A640). The positive area and OD of CD206 and VEGF positive cells were evaluated by Image-J software and determined by measuring three randomly selected microscopic fields for each slide. The IHC index was defined as average integral optical density (AIOD) (AIOD = positive area × OD/total area).

CD31, a marker factor in vascular endothelial cell, was positively correlated with microvascular density (MVD). Then we counted the MVD by detecting the expression of CD31 antibody in tumor tissues by immunohistochemistry method. Firstly, at low power field (×40), three most intense tissue sections were selected each slice and then at high power field (×100), MVD counts of these areas were evaluated. Finally, the mean microvessel counts of the three most vascular areas were regarded as MVD.

2.12. Statistical Analyses. Data were from three independent experiments and expressed as mean ± SEM. Statistical analyses were performed by the one-way analysis of variance (ANOVA) for differences among different groups. About comparison of two groups, Student's t-test was used. All analyses were undertaken using GraphPad Prism6. $P < 0.05$ was considered statistically significant.

3. Results

3.1. QRHX Inhibits Tumor Growth in a Subcutaneous Mouse Model. In order to explore the role of QRHX in tumor growth in vivo, subcutaneous mouse model was established by subcutaneous injection of LLC in left extremity auxiliary. Mice were sacrificed at the end of treatment. As shown in Figure 1, the tumor volumes were performed on days 10, 13, 17, 20, and 24. In NS group, the tumor volume gradually increased in a time-dependent manner (Figure 1(a)). However, treatment with QRHX significantly suppressed the tumor volume (Figure 1(a)). The final tumor weight on day 24 after the start of treatment showed a significant decrease in the QRHX group compared with NS control (Figure 1(b), $P < 0.01$). These data suggested that QRHX could dramatically inhibit tumor growth in vivo.

3.2. QRHX Suppresses Cancer-Related Inflammation in Lung Cancer. Numerous studies have indicated that cancer-related inflammation promotes the development of tumor [15, 16].

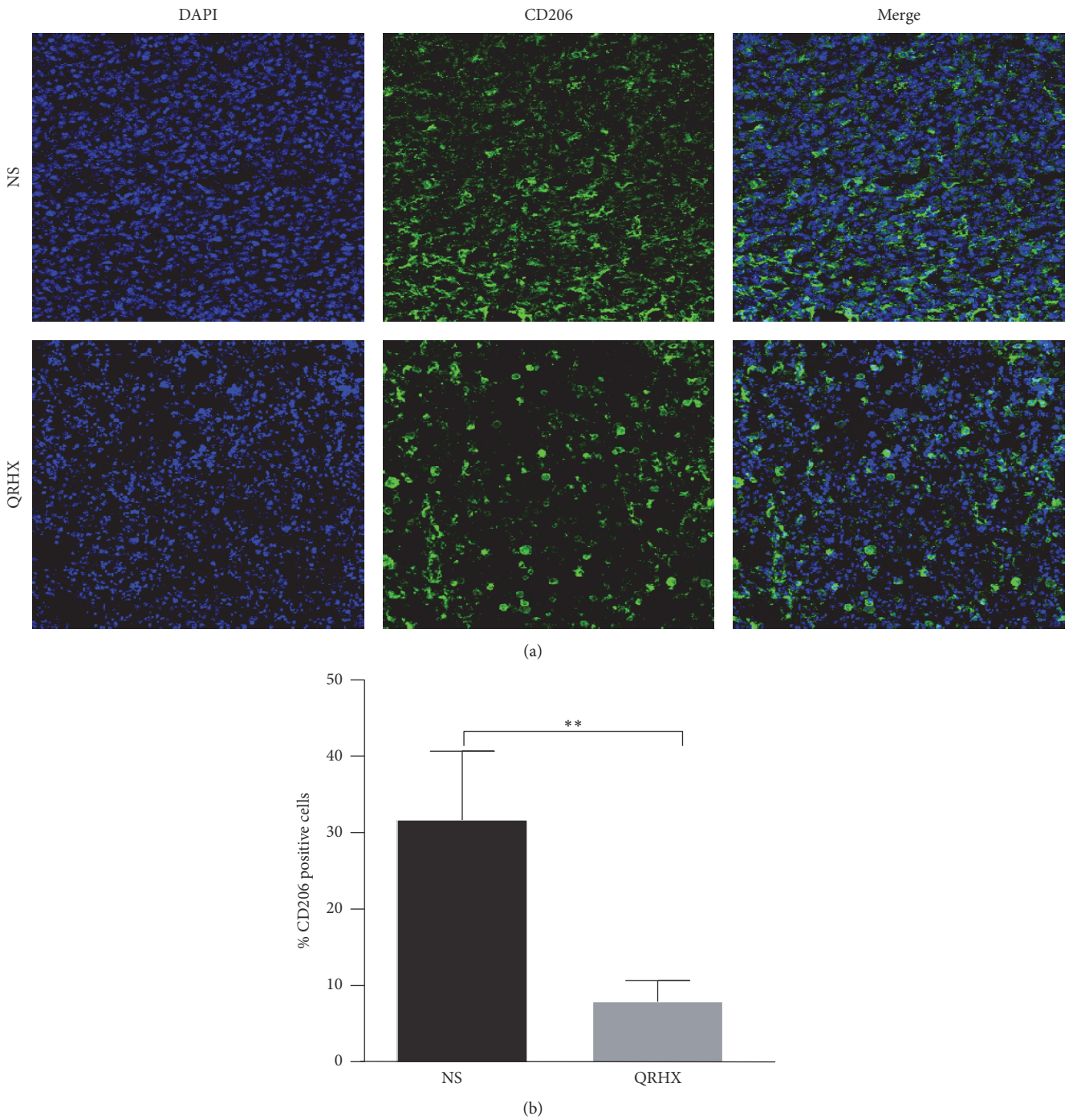

Figure 4: *Immunofluorescence staining for CD206 of tumor tissues in subcutaneous tumor*. Mice with subcutaneous tumor were dealt with the group of NS and QRHX. Images are at magnification of 200x. The expression of TAMs was, respectively, analyzed using an Alexa Fluor-488-conjugated secondary antibody. The nuclei were stained with DAPI. Compared with NS group, $^{**}P < 0.01$.

In addition, some proinflammatory cytokines, such as IL-8, IL-6, and TNF-a, have been shown to ultimately facilitate cell invasion and metastasis [15]. Therefore, we used an ELISA assay to examine serum levels of the two proinflammatory cytokines IL-6 and TNF-α in peripheral blood. Serum IL-6 and TNF-α levels were lower in mice treated with QRHX compared with those receiving NS treatment (Figure 2, both $P < 0.01$). These data demonstrated that QRHX decreased the production of proinflammatory cytokines.

3.3. QRHX Reduces the Accumulation of TAMs in Lung Cancer. In order to ascertain the effects of the QRHX on TAMs, M2-like macrophage phenotype, we used flow cytometry, IF, and IHC assay to examine CD206 expression. As shown

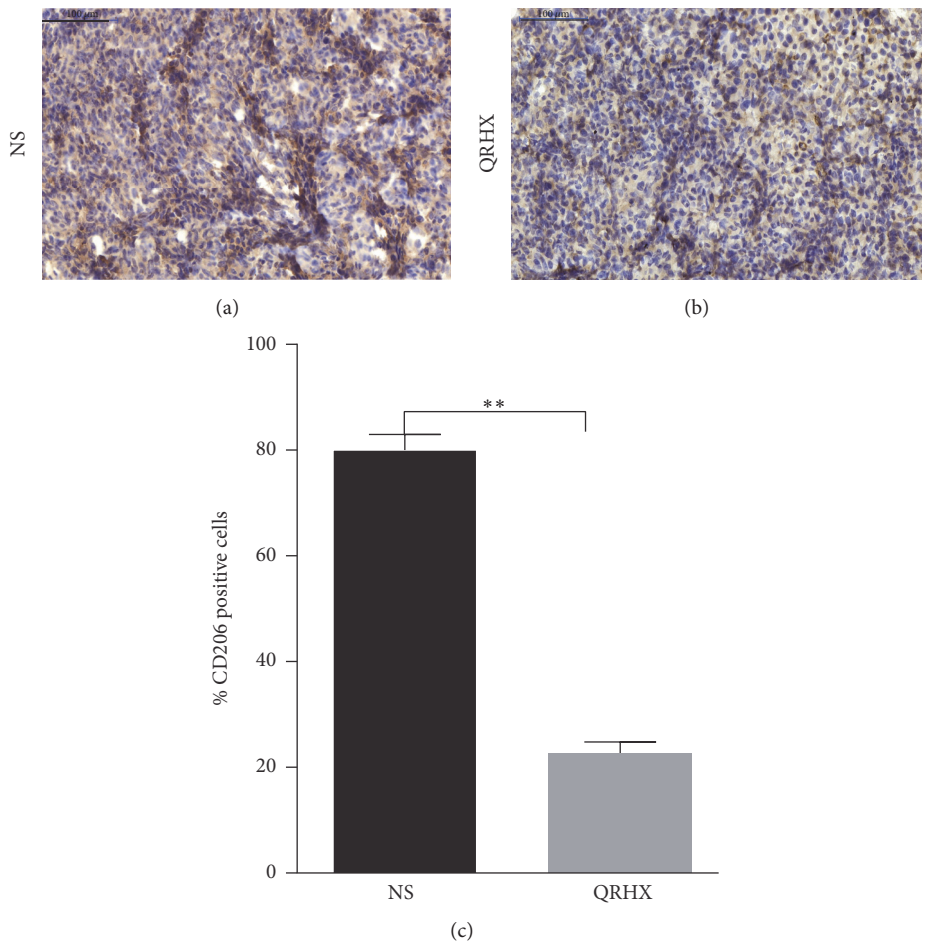

Figure 5: *Comparison of CD206+ macrophages infiltration between NS and QRHX groups*. Immunohistochemical staining of CD206+ macrophages in lung cancer tissues. Images are at magnification of 200x. Data represent mean ± SEM; $n = 4$. Compared with NS group, $^{**}P < 0.01$.

in Figures 3–6, our results revealed that CD206 expression was dramatically expressed in tumor tissue. Compared to NS group, oral administration with QRHX led to a prominent inhibition in TAMs (Figures 3–6, $P < 0.01$). These data demonstrated that QRHX had a more significant role in impeding accumulating and reducing the number of TAMs in lung cancer.

3.4. QRHX Alters Hallmarkers of M1 and M2 Macrophage in Lung Cancer. To further confirm the role of QRHX in TAMs, we analyzed the level of Arg-1 protein, M2 marker, and the mRNA expression of M1 marker iNOS. After QRHX treatment, Arg-1 level decreased (Figure 7(a), $P < 0.01$) and iNOS level increased (Figure 7(b), $P < 0.05$). Accordingly, these results strongly supported the inhibitory effect of QRHX on suppressing TAMs infiltration and regulating M2-like macrophage polarization.

3.5. QRHX Inhibits Angiogenesis in Lung Cancer. CD31, endothelial cell surface antigen, is a vascular endothelial marker for MVD and TAMs have a positive effect on blood vessels by inducing the production of various proangiogenic genes [17]. Therefore, CD31 was evaluated in implanted tumors using IHC and WB. MVD stained by anti-CD31 was measured by counting tissue sections of central areas of the tumor. As shown in Figure 8, QRHX treatment induced a remarkable reduction in MVD and CD31 protein ($P < 0.01$). Furthermore, IHC and WB demonstrated reduced vascular endothelial growth factor (VEGF) expression in the QRHX treated groups, relative to NS controls (Figure 8, $P < 0.01$). Taken together, these data clearly showed that QRHX reduced angiogenesis in lung cancer.

3.6. QRHX Blocks CXCL 12/CXCR4/JNK2/STAT3 Signaling Pathways. To investigate the molecular mechanism underlying the formulae decreasing M2 macrophages, we tested the effects of inhibitors of signaling molecules. CXCL12/CXCR4 and JNK2/STAT3 are known to be important molecules involved in M2 polarization [18, 19]. Compared to NS group, oral administration of QRHX dramatically attenuated the increased expressions of CXCL12 and CXCR4 in tumor tissue (Figure 9(a), $P < 0.01$). As shown in Figure 9(b), JAK2 and STAT3 activation was significantly suppressed by QRHX treatment (both, $P < 0.01$) compared to NS group.

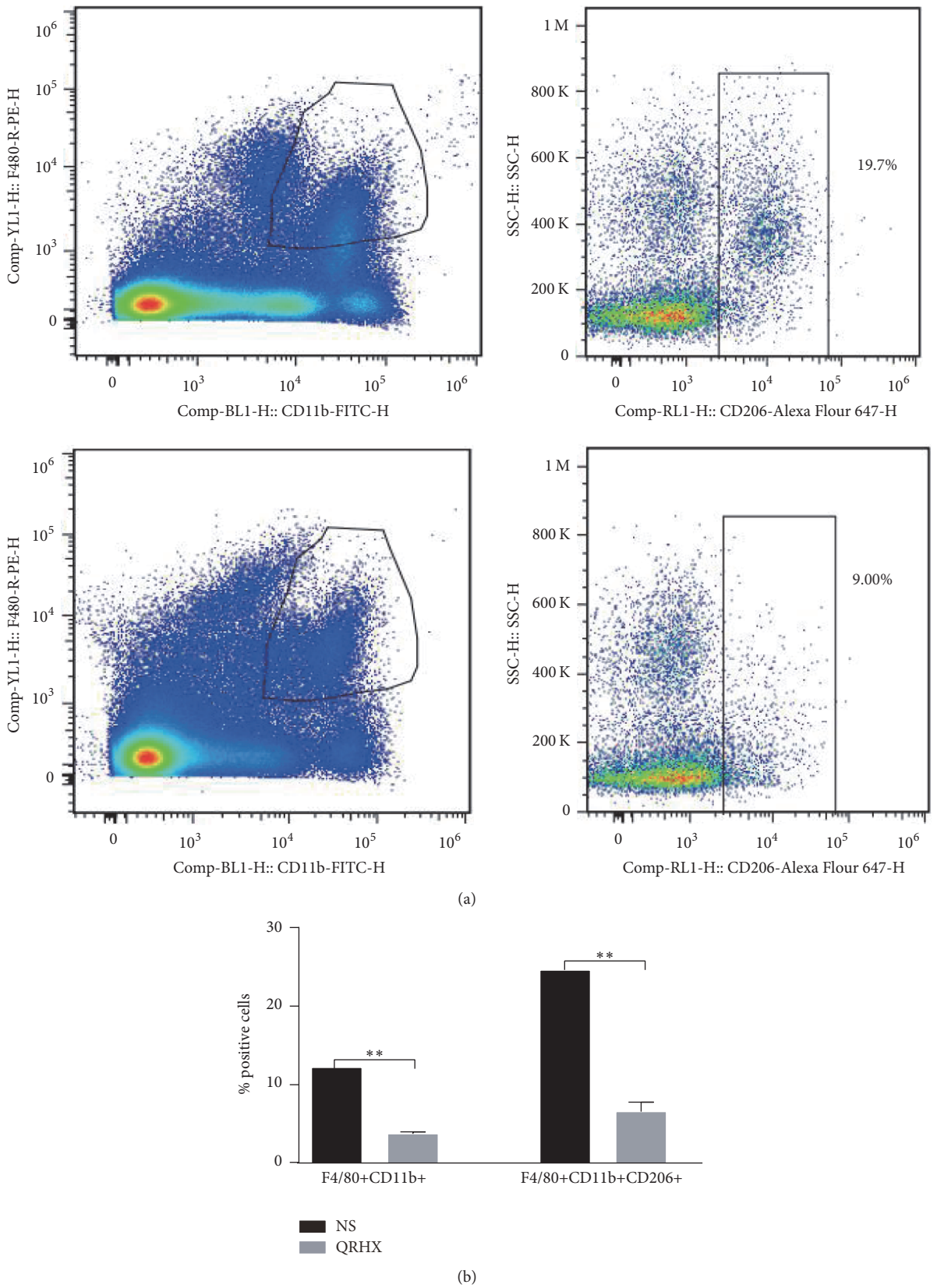

Figure 6: *QRHX decreases the number of TAMs in subcutaneous tumor*. Mice with subcutaneous tumors were dealt with NS and QRHX. Macrophages and TAMs (M2-like subtype) in tumor tissue were measured by flow cytometry. Data represent mean ± SEM; $n = 4$. Compared with NS group, $^{**}P < 0.01$.

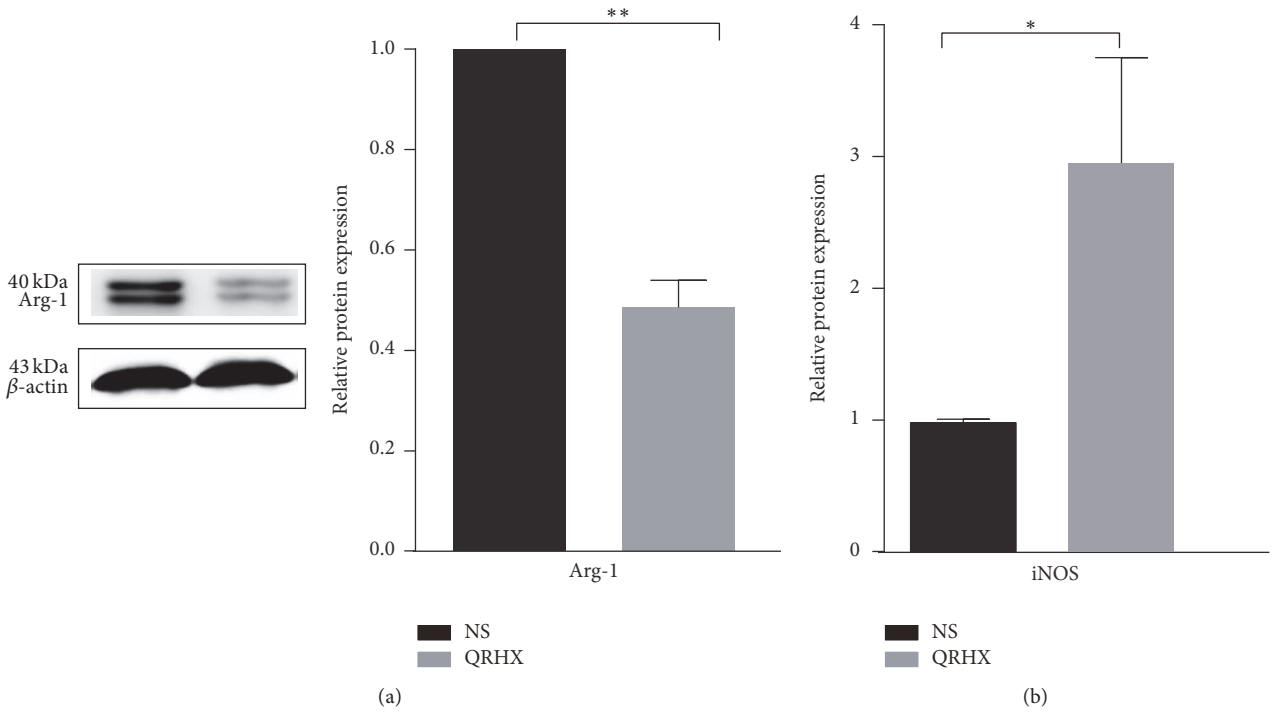

Figure 7: *The expression of M2-related marker (Arg-1) and M1-related marker (iNOS) was detected by western blot and QT-PCR, respectively.* Mice with subcutaneous tumor were dealt with NS and QRHX. Data were presented as means ± SEM ($n = 3$). Compared with NS group, $^{*}P < 0.05$; $^{**}P < 0.01$.

Taking together, the data suggested that QRHX inhibited tumor cell-TAMs interactions possibly through blocking CXCL12/CXCR4/JAK2/STAT3 signaling pathways and then regulated macrophages polarization.

4. Discussion

In the present study, our data demonstrated that QRHX played a more crucial role in inhibiting tumor growth by modulating tumor microenvironment, especially TAMs. QRHX inhibited tumor cell-TAMs interactions via the suppression of cancer-related inflammation and probably blocking the response of macrophages to tumor signals, CXCL12/CXCR4/JAK2/STAT3 axis.

In the nineteenth century, the association between cancer and inflammation was firstly put forward [20]. Large number of studies provided powerful evidence that chronic inflammation can promote tumor development, progression, and metastasis, as well as chemoresistance [16, 21]. Recent studies have confirmed that paeoniflorin, baicalein, and wogonin, important ingredients of QRHX, had the potential to inhibit many types of inflammation [22–24]. Furthermore, baicalein and wogonin exerted obvious inhibitory effects on cancer as well as macrophages and angiogenesis [24, 25]. Paeoniflorin, one of major ingredients, could reduce lung metastasis of LLC through inhibiting the M2 activation [26]. In addition, the cytokines produced by activated innate immune cells in tumor microenvironment can stimulate tumorigenesis, such as IL-6 and TNF-α [27]. Our results showed a remarkable decrease in multiple proinflammatory cytokines such as TNF-a and IL-6 both in serum and tumor tissue of subcutaneous mouse model (Figure 2), suggesting the inhibitory effect of QRHX on cancer-related inflammation.

Tumor microenvironment, created by the tumor and mainly orchestrated by inflammatory cells, contributes to tumor escape, growth, progression, and evolution toward metastasis [28, 29]. Numerous studies in recent decade have presented evidences that TCM have a good effect on regulating tumor microenvironment, such as reversing the immunosuppressive microenvironment [11]. Macrophages, a basic component of the innate immune system, are infiltrated in virtually all malignancies. TAMs, M2-like polarized style, have been regarded as a protumor inflammatory microenvironment, which links inflammation and cancer [15]. Collective evidences demonstrate that TAMs have the ability of enhancing tumor angiogenesis, increasing migration and invasion, and suppressing the antitumor immune responses. It is correlated with the prognosis of patients with malignant tumor, such as lung cancer [30, 31]. Consistent with previous studies, in this study, we detected that the fraction of TAMs was increased in tumor and QRHX inhibited tumor growth in the tumor mice model through decreasing accumulating of TAMs and activation of M2.

CXCR4, which is widely expressed on malignant cells and binds to CXCL12 [32], plays an important role in hematopoiesis, development, and organization of the immune system by directly and indirectly mechanisms [33]. For example, in NSCLC, CXCL12-CXCR4 axis is involved in metastasis and associated with an unfavorable prognosis [34]; in ovarian cancer, it can control accumulation of

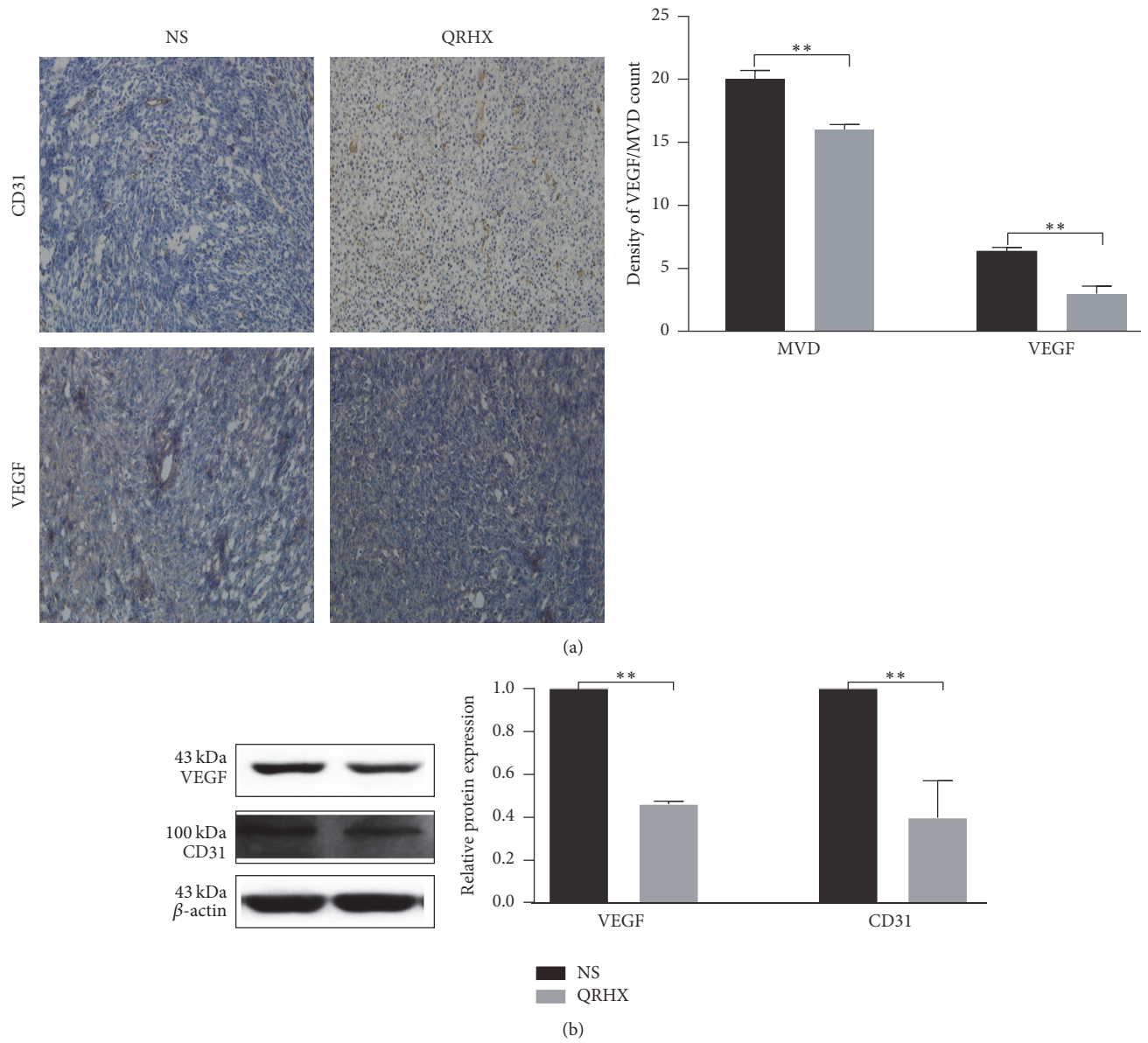

Figure 8: *QRHX inhibits angiogenesis in lung cancer*. Mice with subcutaneous tumors were dealt with NS and QRHX. (a) The nucleus was dyed as blue; CD31 was dyed as brown. MVD were performed at high power field (×200). (b) The VEGF and CD31 protein expression in tumor tissues was detected by western blot. Data was expressed as means ± SEM values ($n = 4$). Compared with NS group, $^{**}P < 0.01$.

human MDSCs and is an independent prognostic factor for tumor progression [35]. Several studies have reported that CXCL12 plays an important role in monocyte recruitment, differentiation, and function [18, 36]. In a mouse model of lung cancer, CXCL12 could recruit tumor-promoting myeloid CD11b+ cells [19]. Besides, powerful evidences indicate a role for CXCR4-CXCL12 axis in promoting macrophages polarization toward the M2 phenotype [37, 38]. In addition, M2 subpopulation is associated with angiogenic factors such as VEGF and CXCL12-CXCR4 axis can also promote tumor vascularization [39]. Excitedly, our results showed QRHX treatment inhibited signaling from tumor cells to macrophages through inducing a remarkable decrease in CXCL12 and CXCR4. Furthermore, QRHX inhibited angiogenesis likely through altering the tumor microenvironment by targeting TAMs.

In STAT family, there are seven proteins; STAT3 is one of them. It is a key transcription factor transducing signals from activated receptors or intracellular kinases to the nucleus and can be activated in tumor cells and immune cells [40]. In tumor, STAT3 could contribute to cancer development and progression, inhibit apoptosis of tumors, and help tumor escape immune system by suppressing the immune response [41]. Evidence indicated that when STAT3 binds to some receptor, it can be activated through Janus Kinases (JAKs), such as JAK2 [42]. Accumulating evidence implicates the important role of JAK2/STAT3 in tumor and macrophage polarization [27]. For instance, IL-6 can contribute to tumor

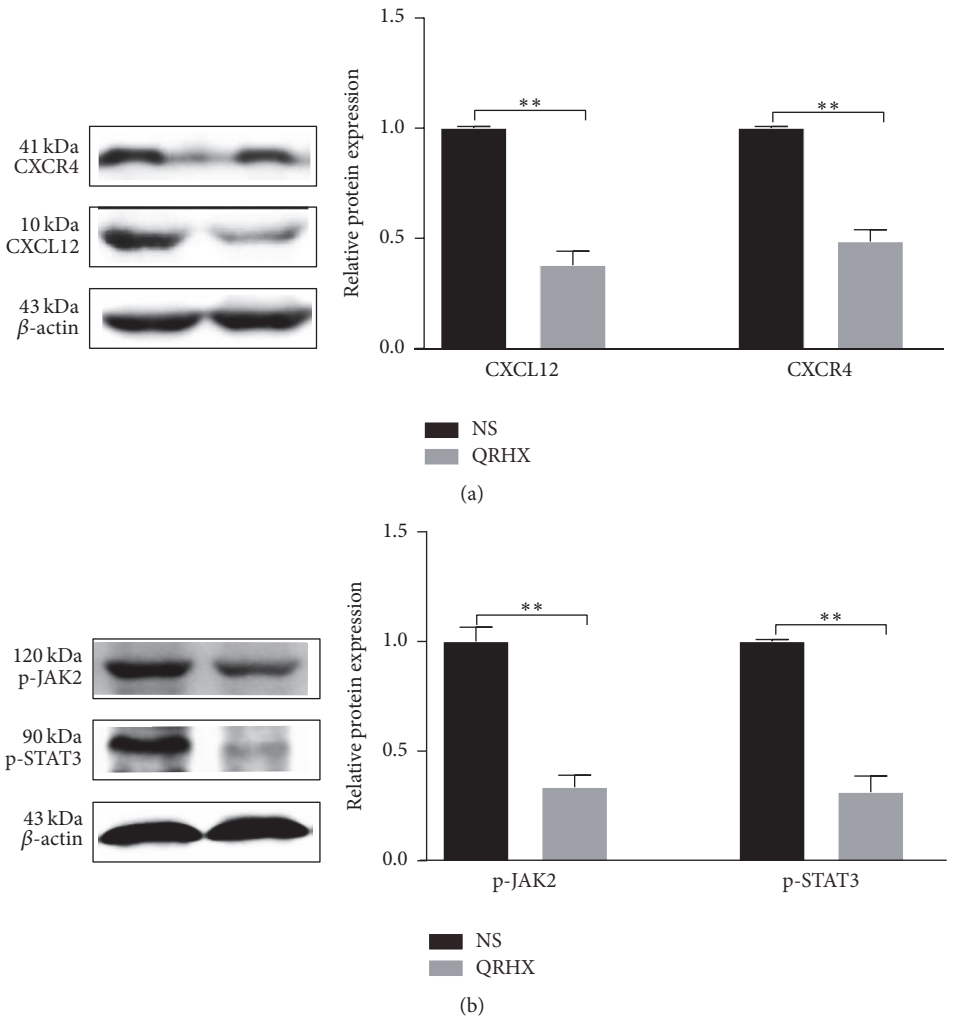

Figure 9: *QRXH regulates TAMs by inhibiting the CXCL12/CXCR4/JAK2/STAT3 signaling pathways*. Mice with subcutaneous tumor were dealt with NS and QRHX. Representative images of western blot and densitometry analysis showing the expressions of CXCL12, CXCR4, p-JAK2, and p-STAT3 in tumor. Compared with NS group, $^{**}P < 0.01$.

cell survival and upregulate the antiapoptotic genes by driving JAK2/STAT3 signal [43]; IFN-ɤ activates macrophage by JAK-STAT signaling pathway [42]. What is more, JAK2 is associated with CXCR4 [39]. Then we can draw that TAMs in malignant tumors tend to M2 subtype possibly through CXCL12/CXCR4/JAK2/STAT3 signaling pathway. QRHX treatment blocked the response of macrophages to tumor signals by suppressing CXCL12/CXCR4/JAK2/STAT3 expression and induced a remarkable decrease of the recruitment of M2 macrophages, suggesting the attenuation of M2 subtype cells function by QRHX.

In TCM theory, TCM formulae have abundant medicinal materials and then regulate diseases through multitargets and multiways. Although the chemical constituents of QRHX have been separated and identified by HPLUNG CANCER-Q/TOF MS-UV method in our team (Supplementary Figure 1 and Table 1), the ingredients are various and their functions are enormous. So, there may be other mechanisms involved in macrophage polarization. What is more, there are diverse types cells in tumor, except for tumor cells and macrophage. Moreover, it is worth mentioning that TAMs were not separated and extracted from tumor tissue. CXCL12, CXCR4, JAK2, and STAT3 can not only play significant role in tumor cell or macrophage, but also other cells, such as T lymphocyte, neutrophils, tumor-associated fibroblast, and endothelial cells. Therefore, QRHX inhibited the CXCL12/CXCR4/JAK2/STAT3 axis possibly through other cells. Taken together, further investigations are needed to identify direct molecular targets of QRHX in macrophages in the context of cancer.

5. Conclusion

In conclusion, data from this study revealed that QRHX could suppress cancer progression by inhibiting the tumor promotion of TAMs in subcutaneous mice model, which could contribute to elucidating the underlying regulatory mode of QRHX on lung cancer treatment.

Abbreviations

ELISA: Enzyme-linked immunosorbent assay
FITC: Fluorescein isothiocyanate
TNF-α: Tumor necrosis factor-α
IL-6: Interleukin-6
iNOS: Inducible nitric oxide synthase
VEGF: Vascular endothelial growth factor
QT-PCR: Quantitative Polymerase Chain Reaction
IF: Immunofluorescence
IHC: Immunohistochemical
TAMs: Tumor-associated macrophages
Arg-1: Arginase 1.

Conflicts of Interest

The authors declare that there are no conflicts of interest.

Authors' Contributions

Fei Xu and Wenqiang Cui contributed equally to this work. Fei Xu and Baojun Liu conceived and designed experiments. Fei Xu and Wenqiang Cui analyzed data and wrote the manuscript. Jingcheng Dong supervised the project. Zhengxiao Zhao and Ying Wei assisted in experimental design and data evaluation. Jiaqi Liu, Mihui Li, Qiuping Li, Chen Yan, and Jian Qiu performed the study. All authors reviewed and approved the manuscript.

Acknowledgments

This study was supported by Natural Science Foundation of China (nos. 81673916 and 81403148); Development Project of Shanghai Peak Disciplines-Integrative Medicine (no. 20150407).

References

[1] I. Ikonomidis, C. A. Michalakeas, J. Parissis et al., "Inflammatory markers in coronary artery disease," *BioFactors*, vol. 38, no. 5, pp. 320–328, 2012.

[2] P. Lee, C. C. Leung, M. I. Restrepo, K. Takahashi, Y. Song, and J. M. Porcel, "Year in review 2015: lung cancer, pleural diseases, respiratory infections, bronchiectasis and tuberculosis, bronchoscopic intervention and imaging," *Respirology*, vol. 21, no. 5, pp. 961–967, 2016.

[3] S. V. Sharma, D. W. Bell, J. Settleman, and D. A. Haber, "Epidermal growth factor receptor mutations in lung cancer," *Nature Reviews Cancer*, vol. 7, no. 3, pp. 169–181, 2007.

[4] D. Leong, R. Rai, B. Nguyen, A. Lee, and D. Yip, "Advances in adjuvant systemic therapy for non-small-cell lung cancer," *World Journal of Clinical Oncology*, vol. 5, no. 4, pp. 633–645, 2014.

[5] M. T. Villanueva, "Microenvironment: the new midfielders in the tumour microenvironment," *Nature reviews. Cancer*, vol. 14, no. 12, p. 765, 2014.

[6] A. Mantovani, S. Sozzani, M. Locati, P. Allavena, and A. Sica, "Macrophage polarization: tumor-associated macrophages as a paradigm for polarized M2 mononuclear phagocytes," *Trends in Immunology*, vol. 23, no. 11, pp. 549–555, 2002.

[7] A. Mantovani and M. Locati, "Tumor-associated macrophages as a paradigm of macrophage plasticity, diversity, and polarization lessons and open questions," *Arteriosclerosis, Thrombosis, and Vascular Biology*, vol. 33, no. 7, pp. 1478–1483, 2013.

[8] W. Hu, X. Li, C. Zhang, Y. Yang, J. Jiang, and C. Wu, "Tumor-associated macrophages in cancers," *Clinical and Translational Oncology*, vol. 18, no. 3, pp. 251–258, 2016.

[9] B. Z. Qian and J. W. Pollard, "Macrophage diversity enhances tumor progression and metastasis," *Cell*, vol. 141, no. 1, pp. 39–51, 2010.

[10] A. Mantovani and P. Allavena, "The interaction of anticancer therapies with tumor-associated macrophages," *Journal of Experimental Medicine*, vol. 212, no. 4, pp. 435–445, 2015.

[11] J. Xu, Z. Song, Q. Guo, and J. Li, "Synergistic effect and molecular mechanisms of traditional Chinese medicine on regulating tumor microenvironment and cancer cells," *BioMed Research International*, vol. 2016, Article ID 1490738, pp. 1–14, 2016.

[12] J. Wu, J. Xu, E. A. Eksioglu et al., "Icariside II induces apoptosis of melanoma cells through the downregulation of survival pathways," *Nutrition and Cancer*, vol. 65, no. 1, pp. 110–117, 2013.

[13] L. Kong, J. Liu, J. Wang et al., "Icariin inhibits TNF-α/IFN-γ induced inflammatory response via inhibition of the substance P and p38-MAPK signaling pathway in human keratinocytes," *International Immunopharmacology*, vol. 29, no. 2, pp. 401–407, 2015.

[14] J. Wu, J. Du, C. Xu et al., "In vivo and in vitro anti-inflammatory effects of a novel derivative of icariin," *Immunopharmacology and Immunotoxicology*, vol. 33, no. 1, pp. 49–54, 2010.

[15] E. M. Conway, L. A. Pikor, S. H. Y. Kung et al., "Macrophages, inflammation, and lung cancer," *American Journal of Respiratory and Critical Care Medicine*, vol. 193, no. 2, pp. 116–130, 2016.

[16] S. Shalapour and M. Karin, "Immunity, inflammation, and cancer: an eternal fight between good and evil," *The Journal of Clinical Investigation*, vol. 125, no. 9, pp. 3347–3355, 2015.

[17] L. Bingle, N. J. Brown, and C. E. Lewis, "The role of tumour-associated macrophages in tumour progression: Implications for new anticancer therapies," *Journal of Pathology*, vol. 196, no. 3, pp. 254–265, 2002.

[18] D. Kim, J. Kim, J. H. Yoon et al., "CXCL12 secreted from adipose tissue recruits macrophages and induces insulin resistance in mice," *Diabetologia*, vol. 57, no. 7, pp. 1456–1465, 2014.

[19] M. C. Schmid, C. J. Avraamides, P. Foubert et al., "Combined blockade of integrin-$\alpha 4\beta 1$ plus cytokines SDF-1α or IL-1β potently inhibits tumor inflammation and growth," *Cancer Research*, vol. 71, no. 22, pp. 6965–6975, 2011.

[20] F. Balkwill and A. Mantovani, "Inflammation and cancer: back to Virchow?" *The Lancet*, vol. 357, no. 9255, pp. 539–545, 2001.

[21] B. B. Aggarwal, S. Shishodia, S. K. Sandur, M. K. Pandey, and G. Sethi, "Inflammation and cancer: how hot is the link?" *Biochemical Pharmacology*, vol. 72, no. 11, pp. 1605–1621, 2006.

[22] W.-L. Jiang, X.-G. Chen, H.-B. Zhu, Y.-B. Gao, J.-W. Tian, and F.-H. Fu, "Paeoniflorin inhibits systemic inflammation and improves survival in experimental sepsis," *Basic and Clinical Pharmacology and Toxicology*, vol. 105, no. 1, pp. 64–71, 2009.

[23] I. D. Kim and B. J. Ha, "The effects of paeoniflorin on LPS-induced liver inflammatory reactions," *Archives of Pharmacal Research*, vol. 33, no. 6, pp. 959–966, 2010.

[24] G.-W. Fan, Y. Zhang, X. Jiang et al., "Anti-inflammatory activity of baicalein in LPS-stimulated RAW264.7 macrophages via estrogen receptor and NF-κB-dependent pathways," *Inflammation*, vol. 36, no. 6, pp. 1584–1591, 2013.

[25] M. Li-Weber, "New therapeutic aspects of flavones: the anticancer properties of Scutellaria and its main active constituents Wogonin, Baicalein and Baicalin," *Cancer Treatment Reviews*, vol. 35, no. 1, pp. 57–68, 2009.

[26] Q. Wu, G.-L. Chen, Y.-J. Li, Y. Chen, and F.-Z. Lin, "Paeoniflorin inhibits macrophage-mediated lung cancer metastasis," *Chinese Journal of Natural Medicines*, vol. 13, no. 12, pp. 925–932, 2015.

[27] W. Lin and M. Karin, "A cytokine-mediated link between innate immunity, inflammation, and cancer," *Journal of Clinical Investigation*, vol. 117, no. 5, pp. 1175–1183, 2007.

[28] T. L. Whiteside, "The tumor microenvironment and its role in promoting tumor growth," *Oncogene*, vol. 27, no. 45, pp. 5904–5912, 2008.

[29] G. Lorusso and C. Rüegg, "The tumor microenvironment and its contribution to tumor evolution toward metastasis," *Histochemistry and Cell Biology*, vol. 130, no. 6, pp. 1091–1103, 2008.

[30] L. Ding, G. Liang, Z. Yao et al., "Metformin prevents cancer metastasis by inhibiting M2-like polarization of tumor associated macrophages," *Oncotarget*, vol. 6, no. 34, pp. 36441–36455, 2015.

[31] A. Yuan, Y. J. Hsiao, H. Y. Chen et al., "Opposite effects of M1 and M2 macrophage subtypes on lung cancer progression," *Scientific Reports*, vol. 5, Article ID 14273, 2015.

[32] F. Balkwill, "Cancer and the chemokine network," *Nature Reviews Cancer*, vol. 4, no. 7, pp. 540–550, 2004.

[33] J. A. Burger and T. J. Kipps, "CXCR4: a key receptor in the crosstalk between tumor cells and their microenvironment," *Blood*, vol. 107, no. 5, pp. 1761–1767, 2006.

[34] R. J. Phillips, M. D. Burdick, M. Lutz, J. A. Belperio, M. P. Keane, and R. M. Strieter, "The stromal derived factor-1/CXCL12-CXC chemokine receptor 4 biological axis in non-small cell lung cancer metastases," *American Journal of Respiratory and Critical Care Medicine*, vol. 167, no. 12, pp. 1676–1686, 2003.

[35] N. Obermajer, R. Muthuswamy, K. Odunsi, R. P. Edwards, and P. Kalinski, "PGE-induced CXCL 12 production and CXCR4 expression controls the accumulation of human MDSCs in ovarian cancer environment," *Cancer Research*, vol. 71, no. 24, pp. 7463–7470, 2011.

[36] L. Sánchez-Martín, A. Estecha, R. Samaniego, S. Sánchez-Ramón, M. Á. Vega, and P. Sánchez-Mateos, "The chemokine CXCL12 regulates monocyte-macrophage differentiation and RUNX3 expression," *Blood*, vol. 117, no. 1, pp. 88–97, 2011.

[37] K. Beider, H. Bitner, M. Leiba et al., "Multiple myeloma cells recruit tumor-supportive macrophages through the CXCR4/CXCL12 axis and promote their polarization toward the M2 phenotype," *Oncotarget*, vol. 5, no. 22, pp. 11283–11296, 2014.

[38] J. M. Mota, C. A. Leite, and L. E. Souza, "Post-sepsis state induces tumor-associated macrophage accumulation through CXCR4/CXCL12 and favors tumor progression in mice," *Cancer Immunology Research*, vol. 4, no. 4, pp. 312–322, 2016.

[39] B. A. Teicher and S. P. Fricker, "CXCL12 (SDF-1)/CXCR4 pathway in cancer," *Clinical Cancer Research*, vol. 16, no. 11, pp. 2927–2931, 2010.

[40] P. C. Heinrich, I. Behrmann, G. Müller-Newen, F. Schaper, and L. Graeve, "Interleukin-6-type cytokine signalling through the gp130/Jak/STAT pathway," *Biochemical Journal*, vol. 334, part 2, pp. 297–314, 1998.

[41] M. Kortylewski, M. Kujawski, T. Wang et al., "Inhibiting Stat3 signaling in the hematopoietic system elicits multicomponent antitumor immunity," *Nature Medicine*, vol. 11, no. 12, pp. 1314–1321, 2005.

[42] X. Hu, J. Chen, L. Wang, and L. B. Ivashkiv, "Crosstalk among Jak-STAT, Toll-like receptor, and ITAM-dependent pathways in macrophage activation," *Journal of Leukocyte Biology*, vol. 82, no. 2, pp. 237–243, 2007.

[43] R. Catlett-Falcone, T. H. Landowski, M. M. Oshiro et al., "Constitutive activation of Stat3 signaling confers resistance to apoptosis in human U266 myeloma cells," *Immunity*, vol. 10, no. 1, pp. 105–115, 1999.

Hindawi
Evidence-Based Complementary and Alternative Medicine
Volume 2017, Article ID 3679295, 10 pages
https://doi.org/10.1155/2017/3679295

Research Article

Boi-ogi-to (TJ-20), a Kampo Formula, Suppresses the Inflammatory Bone Destruction and the Expression of Cytokines in the Synovia of Ankle Joints of Adjuvant Arthritic Rats

Xinwen Zhang,[1] Zhou Wu,[2] Yicong Liu,[2] Junjun Ni,[2] Chunfu Deng,[1] Baohong Zhao,[1] Hiroshi Nakanishi,[2] Jing He,[1] and Xu Yan[3]

[1]*Center of Implant Dentistry, School of Stomatology, China Medical University, Shenyang 110002, China*
[2]*Department of Aging Science and Pharmacology, Faculty of Dental Science, Kyushu University, Fukuoka 812-8582, Japan*
[3]*The VIP Department, School of Stomatology, China Medical University, Shenyang 110002, China*

Correspondence should be addressed to Zhou Wu; zhouw@dent.kyushu-u.ac.jp and Xu Yan; kqyx2003@126.com

Received 23 February 2017; Accepted 10 April 2017; Published 7 May 2017

Academic Editor: Emilio Lizarraga

TJ-20 is a formula consisting of 6 herbs that has been used in the clinical treatment of rheumatoid arthritis (RA) in China and Japan for centuries. However, scientific evidence of the effects of TJ-20 has not been established. In the present study, we focused on the therapeutic effects and investigated the main function of TJ-20 on adjuvant arthritis (AA), an animal model of RA, which was induced with complete Freund's adjuvant (CFA). TJ-20 was administered orally at 600 mg/kg once a day from 0, 7, and 10 days to 8 weeks after the CFA treatment. TJ-20 significantly ameliorated inflammatory progression and bone destruction in AA in a time-dependent manner. Furthermore, TJ-20 significantly reduced the increased changes in a number of macrophages and helper T cells. Moreover, TJ-20 suppressed the expression of TNF-α whereas it augmented the expression of IL-10 and attenuated Th1 cells responses in the synovia of the ankle joint. Therefore, TJ-20 regulated the expression of proinflammatory and anti-inflammatory cytokines in macrophages and Th1/Th2 balance in the synovia of ankle joints in AA rats. These results suggest the positive anti-inflammatory effect of TJ-20 and provide a scientific basis for the clinical use of TJ-20 for RA.

1. Introduction

Rheumatoid arthritis (RA) is a chronic inflammatory disease characterized by recruitment and activation of inflammatory cells such as macrophages and helper T cells in the synovia [1].

Macrophages aggravate the inflammatory process in diseases such as RA by releasing cytokines. Tumor necrosis factor-alpha (TNF-α), a proinflammatory cytokine predominantly produced by macrophages, is actively involved in the inflammatory process and destruction of joints in RA [2, 3]. Evidence has shown that TNF-α exists in the synovial fluid and synovial tissues in patients with RA [4, 5]. TNF-α antibodies and soluble TNF-α receptors are effective in RA patients and animal models of RA [6–8]. IL-10, in turn, acts as anti-inflammatory cytokine to control the production of TNF-α by active macrophages [9, 10].

Helper T cells can be divided into Th1 and Th2 subsets in two ways: the first way is based on their cytokine secretion profile [11]. That is, Th1 cells produce interferon-gamma (IFN-γ) and interleukin-2 (IL-2) but neither IL-4 nor IL-5, while Th2 cells produce IL-4 and IL-5 but not IL-2 or IFN-γ. The second way is by the expression of receptors for chemokines on the cell surface. The CXC chemokine receptor CXCR3 is expressed in Th1 cells, whereas the CC chemokine receptor CCR4 is expressed in Th2 cells [12–14]. An imbalanced Th1/Th2 response has been suggested to be involved in the progression of RA. That is, a predominance of Th1 cells over Th2 cells aggravates the RA [15].

Adjuvant arthritis (AA), a widely studied model of human RA, is also characterized by the recruitment of macrophages and helper T cells to the synovial tissues [16]. The percentage of both macrophages and helper T cells in the mononuclear cell population in the synovia of ankle joints is consistent with

Table 1: Composition of Boi-ogi-to (TJ-20).

Medicinal plants	Weight ratio	Family	Genus	Species
Astragali radix	5	Leguminosae	Astragalus	Astragalus
Sinomenium acutum	5	Menispermaceae	Sinomenium	Sinomenium acutum
Atractylodis Lanceae rhizoma	3	Asteraceae	Atractylodes	Lancea
Jujube fruit	3	Rhamnaceae	Ziziphus	Zizyphus
Glycyrrhizae radix	1.5	Leguminosae	Glycyrrhiza	Glycyrrhiza
Zingiberis Rhizoma	1	Zingiberaceae	Zingiber	Zingiberis Rhizoma

the swelling in the hind paws of AA rats [17]. Studies have suggested that TNF-α and IFN-γ contribute to the progression, whereas IL-10 and IL-4 contribute to the remission, of AA [18, 19].

Boi-ogi-to (TJ-20), a Kampo formula consisting of six ingredients, *Astragali* radix, *Sinomenium acutum*, Atractylodes Lancea rhizoma, *Zizyphi fructus*, *Glycyrrhizae* radix, and *Zingiber* rhizome, has been used for centuries in China and Japan for the treatment of RA. Although an ameliorating effect of *Sinomenium acutum*, a main ingredient of TJ-20 (Table 1), has been reported in rat experimental arthritis and in the treatment of rheumatic diseases [20, 21], the immunological aspect of the effect of TJ-20 in RA is still unclear.

In this study, we examine the therapeutic effects of TJ-20 on the expression of cytokines and the Th1/Th2 balance in the synovia of AA rats, to obtain scientific proof of the clinical effectiveness of TJ-20.

2. Methods

2.1. Induction of AA and Measurement of Paw Swelling. Thirty-six female Lewis rats, weighing 100–110 g, were treated in accordance with the guidelines stipulated by the animal care and use committee of Kyushu University. Twenty-four rats received a single intradermal injection of complete Freund's adjuvant (CFA; heat-killed *Mycobacterium butyricum* were well suspended in mineral oil, 10 mg/ml, 25 mg/kg; Difco Lab., Detroit, MI, USA) at the base of tail under deep ether anesthesia. Twelve rats injected with mineral oil only served as controls (normal rats) for the adjuvant injection. The size (thickness of the ankle from the medial to lateral malleolus) of the hind paws was measured from the day after adjuvant injection (day 0) using digimatic micrometer (Mitutoyo, Kanagawa, Japan). The percent of increase was compared with that of day 0.

2.2. Administration of TJ-20. TJ-20 bulk powder (Tsumura & Co. Ltd., Tokyo, Japan) was dissolved in distilled water (100 mg/ml). Eighteen rats injected with adjuvant were orally administered TJ-20 (600 mg/kg) once a day according to three different schedules (six rats per schedule): schedule I: from day 0 to week 8; schedule II: from day 7 to week 8; schedule III: from day 10 to week 8. Distilled water was orally administered to a group of six rats as adjuvant arthritic controls (AA rats), while TJ-20 was administered to six rats from day 0 as TJ-20 treatment controls (control rats).

2.3. Tissue Preparations. The rats were anesthetized with Nembutal (30 mg/kg) at the end of each experimental schedule, perfused intracardially with 0.01 M phosphate-buffered saline (PBS, pH 7.4), and fixed in PLP fixative (0.01 M sodium metaperiodate; 0.075 M L-lysine-HCl; 2% paraformaldehyde, 0.03 M PB, pH 6.2). Ankle joints, including the tarsal bone and tibia, were excised, immersed in the same fixative for 6 h at 4°C, then washed with PBS, and decalcified in 10% EDTA for 3 weeks at 4°C. After decalcification, specimens were embedded in Optimal Cutting Temperature (OCT) compound (Sakura Finetechnical Co., Ltd., Tokyo, Japan). Serial frozen sections (7 μm) of ankle joints for staining with hematoxylin and eosin and immunohistochemistry were prepared as reported previously [17].

2.4. Immunohistochemistry. Sections were treated with 0.3% H_2O_2 in methanol and then were treated with 10% normal donkey serum for 2 h at 24°C. The sections were incubated with the mouse anti-W3/25 (1 : 200; Harlan Sera-Lab Lid, Loughborough, England), goat anti-IL-4 (1 : 100; BD PharMingen), goat anti-IFN-γ (1 : 100; Santa Cruz Biotechnology), goat anti-ED1 (1 : 500; Santa Cruz Biotechnology), goat anti-TNF-α (1 : 100; Santa Cruz Biotechnology), and goat anti-IL-10 (1 : 100; Santa Cruz Biotechnology) antibodies in a humidified chamber overnight at 4°C. After being washed with cold PBS, the sections were incubated with biotinylated-anti-mouse secondary antibodies (1 : 200; Jackson ImmunoResearch) or biotinylated-anti-goat secondary antibodies (1 : 200; Jackson ImmunoResearch) for 2 h at 24°C and finally with peroxidase conjugated streptavidin (1 : 300; Dako) for 1 h at 24°C. The peroxidase was developed using 3,30-diaminobenzidine (DAB substrate kit; Vector Laboratories), and then the samples were counterstained with Mayer's hematoxylin.

2.5. Double-Immunofluorescence Staining. The sections were hydrated and treated with 10% normal donkey serum for 1 h at 24°C and then incubated with the following antibodies for 2 days at 4°C: goat anti-CXCR3 (1 : 100; Santa Cruz Biotechnology) with mouse anti-W3/25 (1 : 200; Harlan Sera-Lab Lid, Loughborough, England); goat anti-CCR4 (1 : 100; Santa Cruz Biotechnology); and mouse anti-W3/25 (1 : 200; Harlan Sera-Lab Lid, Loughborough, England). The sections were washed with PBS and incubated with a mixture of secondary antibodies conjugated with donkey anti-goat Alexa 488 (1 : 400; Jackson ImmunoResearch) and donkey anti-mouse Cy3 (1 : 400; Jackson ImmunoResearch) for 3 h

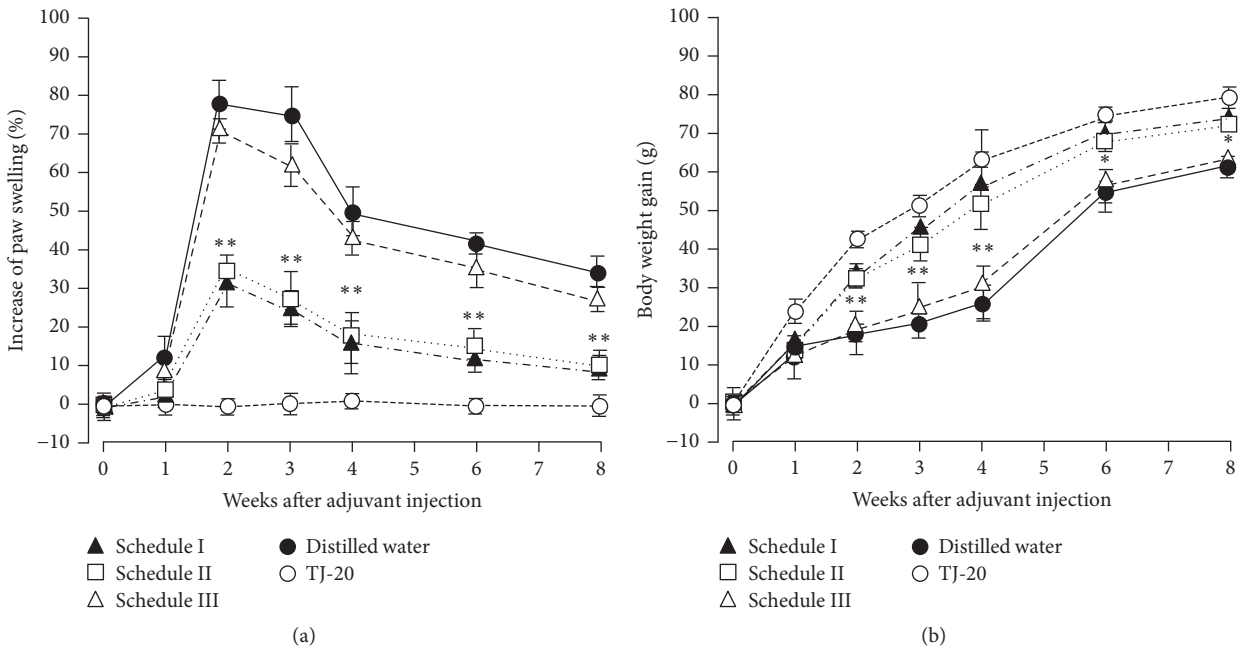

Figure 1: Time course of the suppressive effects of TJ-20 on the clinical parameters of AA rats. AA rats were given TJ-20 according to schedule I (filled triangles), II (open squares), or III (open triangles) or given distilled water (closed circle) orally once a day after adjuvant injection (AA rats). Rats injected with mineral oil alone and given TJ-20 (open circle) served as controls. The hind paw swelling (a) and body weight gain (b) were measured at 1-week intervals. TJ-20 administered according to schedules I and II significantly ameliorated the progression of AA. Data are the mean ± SD for 6 rats in each group. Asterisks indicate a statistically significant difference from AA rats ($^{*}P < 0.05$, $^{**}P < 0.01$).

at 24°C. The sections were washed with PBS and mounted in the antifading medium Vectashield (Vector Laboratories) and examined with a confocal laser-scanning microscope (CLSM) (C2si Confocal Laser Microscope, Nikon).

2.6. Statistical Analysis. The percent increase in hind paw swelling and body weight gain of the rats on each schedule were calculated and expressed as the mean ± SD. Mononuclear cells were counted under a light microscope using the 40x objective and 10x ocular lenses in three areas per section (3 sections per rat). The percentages of ED-positive cells or W3/25-positive cells in mononuclear cells in each area were calculated (the percentage of the positive mononuclear cells) and expressed as the mean ± SD. The data are presented as the means ± SEM. The statistical analyses of the results were performed with Student's unpaired t-tests and one-way ANOVA with a post hoc Tukey's tests using the GraphPad Prism software package. A value of $P < 0.05$ was considered to indicate statistical significance.

3. Results

3.1. Oral Administration of TJ-20 Suppresses the Inflammatory Progression and Bone Destruction of Adjuvant Arthritis. The clinical symptoms, such as redness and swelling of the hind paws in the AA rats, appeared on day 10, peaked at week 2, and remained until week 3. Although the redness and swelling declined thereafter, the hind paws did not recover completely until week 8 (Figure 1(a)). AA rats lost body weight from day 10 to week 3 but gained weight gradually thereafter (Figure 1(b)). The normal rats did not show any clinical symptoms and had gained body weight gradually by week 6 (data not shown). Compared with AA rats, significant reductions in the hind paw swelling and body weight loss were detected at weeks 2 to 3 in the rats given TJ-20 according to schedules I and II, and no significant differences in clinical symptoms were found between these two groups. However, no significant amelioration of swelling and weight loss was detected in the AA rats on schedule III. Control rats did not show any clinical symptoms and gained body weight following a similar time course as the normal rats (Figures 1(a) and 1(b)).

In the histological examination, compared with control rats (Figure 2(a)), a significant recruitment of mononuclear cells was observed at day 7 and the thickness of the synovia reached a maximal level at weeks 2 to 3 (Figure 2(b)). Progress in the destruction of cartilage and bone from weeks 3 to 8 was apparent in AA rats with a decrease of inflammation in synovia (Figure 2(c)). Among the AA rats, we detected a marked suppression of the thickening of the synovia (Figure 2(d)) and of the destruction of bone in the rats treated with TJ-20 according to schedules II and I (data not shown). We did not observe any effects in the AA rats on schedule III (data not shown). These results showed that administration of TJ-20 according to schedules I and II suppressed the progression of arthritis in AA rats.

3.2. Influence of TJ-20 on the Recruitment of Macrophages and Helper T Cells in the Synovia of AA Rats. To investigate whether TJ-20 treatment influences the recruitment

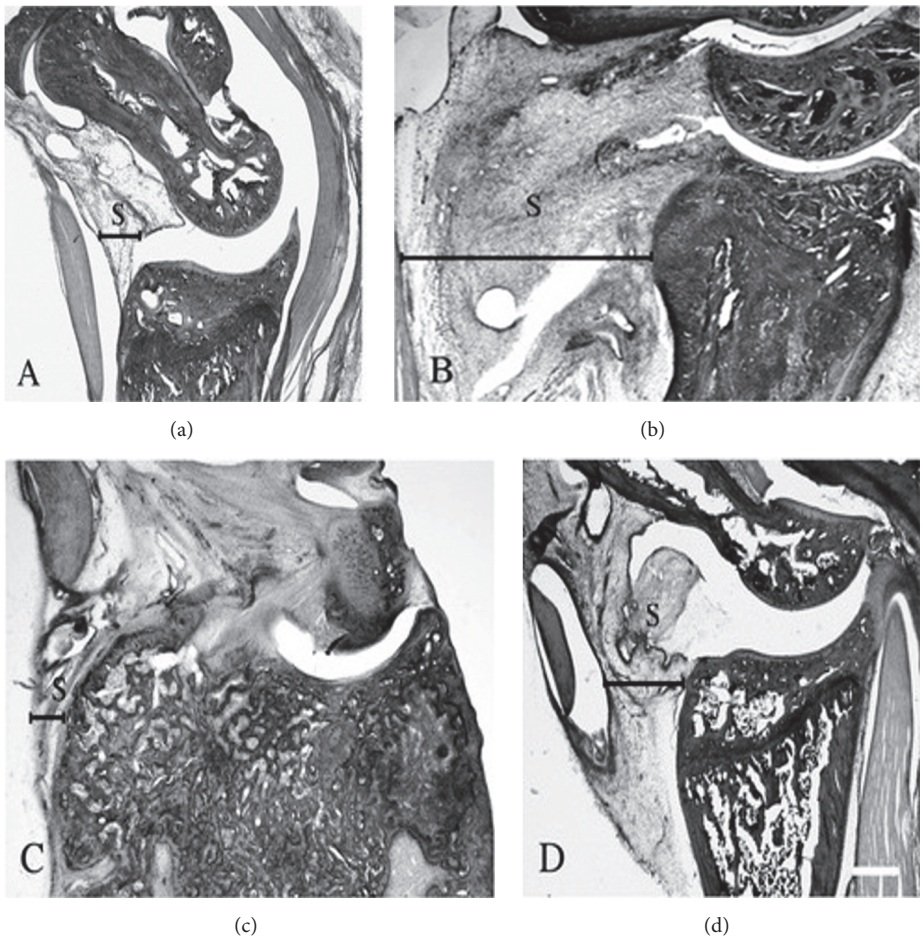

Figure 2: Histological examination of the ankle joints in AA rats. Hematoxylin-eosin staining in ankle joints from control rats (a) and AA rats at week 2 with a remarkable inflammation in synovia (b) and week 8 with the remarkably destruction of cartilage and bone (c) after adjuvant injection. The thickness of the synovia was markedly suppressed in AA rats treated with TJ-20 according to schedule II (d) at week 2 after adjuvant injection. S: synovia; scale bar, 200 μm.

of macrophages and helper T cells in the synovia of AA rats, immunohistochemical staining was carried out using anti-macrophage antibodies (ED1) and anti-T cell antibodies (W3/25). In the synovia of AA rats, we observed a similar time course of change in the percentage of ED1-positive cells and W3/25-positive cells in total mononuclear cells. These cell populations increased significantly from day 10 and reached a maximal level during weeks 2 and 3 (Figures 3(a)–3(c)) and then decreased from week 4 after the adjuvant was injected. Significant reductions in the percentage of ED1-positive mononuclear cells from weeks 2 to 4 (Figures 3(a) and 3(b)) and W3/25-positive mononuclear cells from weeks 2 to 3 (Figures 3(a) and 3(c)) were detected in the synovia of AA rats treated with TJ-20 according to schedules II and I (data not shown). However, no significant decrease in the percentage of ED1-positive or W3/25-positive mononuclear cells was observed in the synovia of AA rats treated with TJ-20 using schedule III (data not shown). These results showed that administration of TJ-20 according to schedules I and II suppressed the infiltration of both macrophages and helper T cells into the synovia of AA rats until week 4 after injection of the adjuvant.

3.3. Influence of TJ-20 on the Expression of Cytokines in the Synovia of AA Rats. To investigate whether TJ-20 treatment influences the expression of proinflammatory cytokines and anti-inflammatory cytokines in the synovia in AA rats, we examined the percentage of TNF-α-and IL-10-positive mononuclear cells in the ankle joints. TNF-α-positive cells were detected from day 7. The percentage of TNF-α-positive cells (Figure 4(a)) in total mononuclear cells increased significantly and reached their maximum at week 2 and then decreased significantly from weeks 3 to 4 (Figure 4(b)). IL-10-positive cells (Figure 4(a)) were also detected from day 7, but the percentage increased gradually from weeks 2 to 4 after injection of adjuvant (Figure 4(c)). In comparison with AA rats, we observed a significant decrease in the percentage of TNF-α-positive mononuclear cells (Figures 4(a) and 4(b)) and in contrast, a significant increase in the percentage of IL-10-positive mononuclear cells from weeks 2 to 4 in the synovia of AA rats treated with TJ-20 according to schedules II (Figures 4(a) and 4(c)) and I (data not shown). No significant change in the percentage of TNF-α- or IL-10-positive mononuclear cells was observed in the AA rats treated with TJ-20 using schedule III (data not shown).

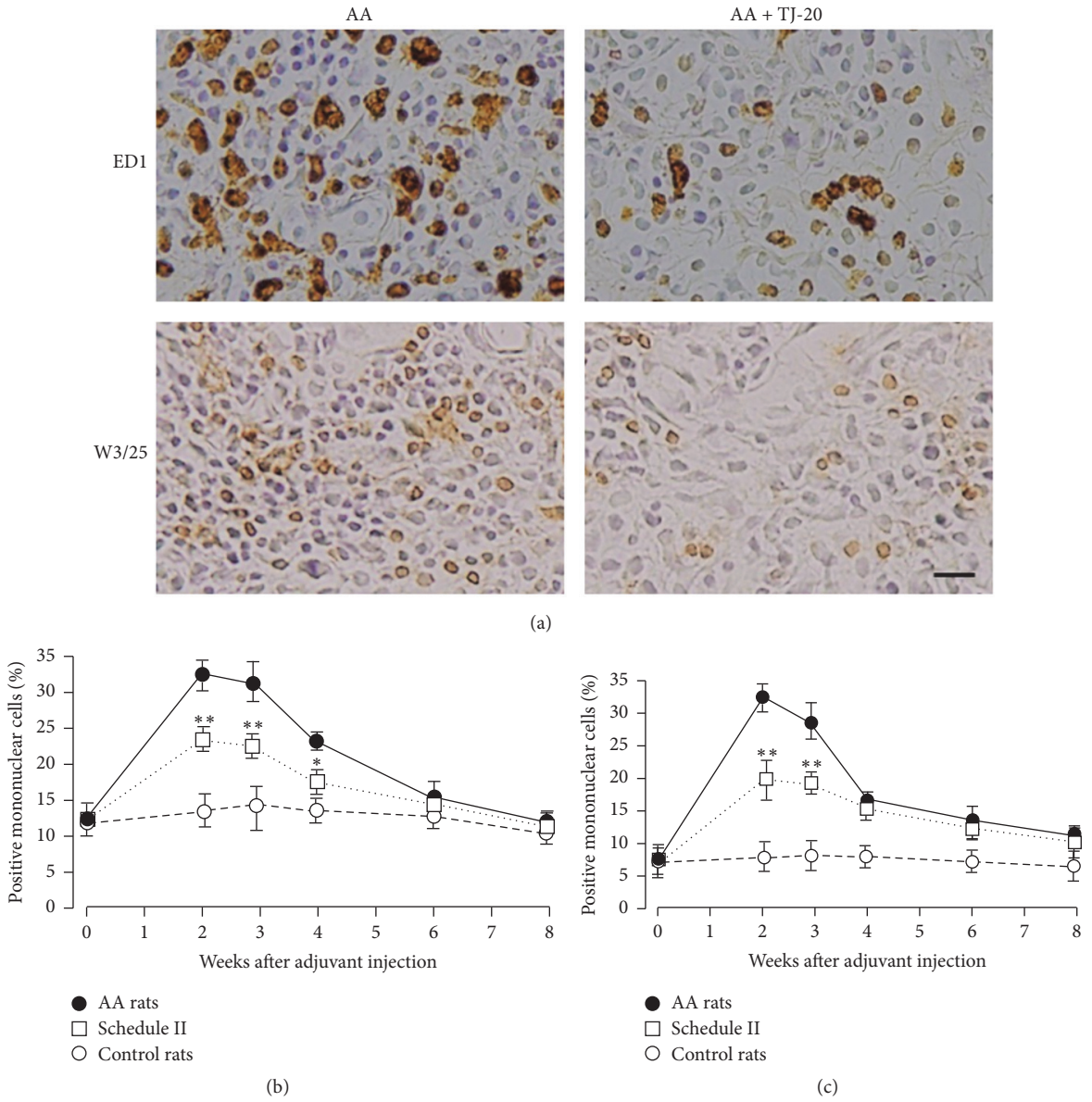

Figure 3: Influence of TJ-20 on the recruitment of macrophages and helper T cells in the synovia of ankle joint in AA rats. Photographs representing ED1-positive macrophages and W3/25-positive helper T cells in the synovia of AA rats at week 2 and AA rats treated with TJ-20 according to schedule II (a), the percentages of ED1-positive macrophages (b), and W3/25-positive helper T cells (c) in AA rats (closed circle), in AA rats treated with TJ-20 according to schedule II (open squares), and in control rats (open circle) were determined by immunohistochemistry. TJ-20 administered according to schedule II significantly lowered the increase in a number of both macrophages and helper T cells. Data are the mean ± SD for 6 rats in each group. Asterisks indicate a statistically significant difference from AA rats ($^{*}P < 0.05$, $^{**}P < 0.01$). Scale bar, 25 μm.

These results showed that administration of TJ-20 according to schedules I and II suppressed the recruitment of TNF-α-expressing cells but increased that of IL-10-expressing cells in the synovia of AA rats.

3.4. Effects of TJ-20 on Th1/Th2 Balance in the Synovia of AA Rats. To investigate whether TJ-20 treatment influences the balance of Th1/Th2 cells in the synovia in AA rats, we examined the percentages of IFN-γ-positive (one of the Th1 cytokines, Figure 4(a)) and IL-4-positive (one of the Th2 cytokines, Figure 4(a)) mononuclear cells and also the percentages of CXCR3 (a marker for Th1 cells)/W3/25-double and CCR4 (a marker for Th2 cells)/W3/25-double positive cells in the synovia of the ankle joints (data not shown). IFN-γ-positive cells were detected on day 7. The percentage among mononuclear cells was increased markedly and reached its maximum at week 2 and then decreased significantly from week 3 (Figure 4(d)). In contrast, the percentage of IL-4-positive mononuclear cells increased significantly from weeks 2 to 4 after the injection of adjuvant (Figure 4(e)). The percentage of CXCR3/W3/25-double positive cells also increased

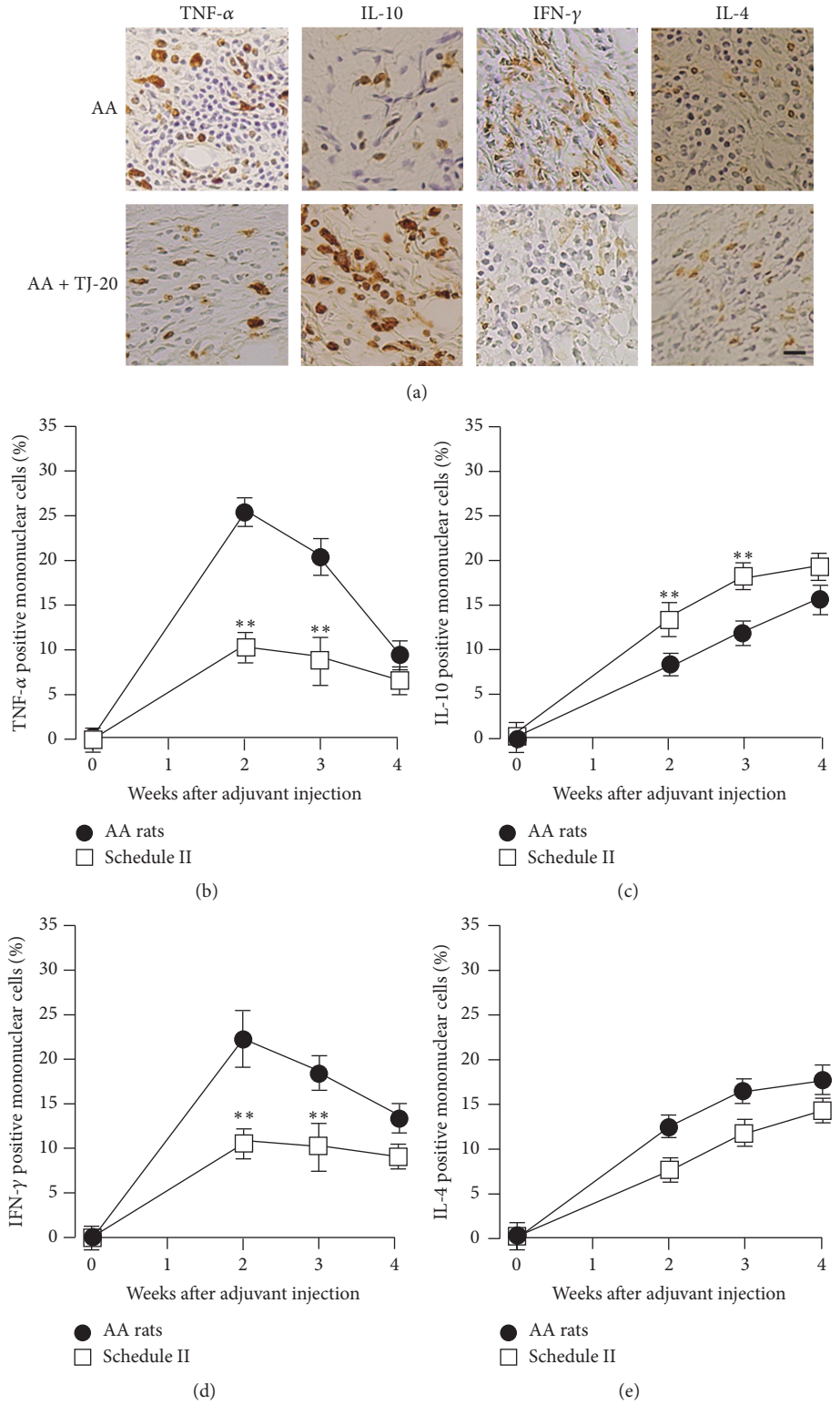

Figure 4: Influence of TJ-20 on the expression of cytokines in the synovia of ankle joint in AA rats. Photographs representing TNF-α-, IL-10-, IFN-γ-, and IL-4-positive mononuclear cells in the synovia of AA rats at week 2 and AA rats treated with TJ-20 according to schedule II (a), the percentages of TNF-α-positive (b), and IL-10-positive (c), IFN-γ-positive (d), and IL-4-positive (e) mononuclear cells in AA rats (closed circle) and AA rats treated with TJ-20 according to schedule II (open squares) were determined by immunohistochemistry. TJ-20 administered according to schedule II significantly suppressed the expression of TNF-α and IFN-γ and augmented the expression of IL-10 but did not augment the expression of IL-4. Asterisks indicate a statistically significant difference from AA rats ($^{*}P < 0.05$, $^{**}P < 0.01$). Scale bar, 25 μm.

Table 2: Effects of TJ-20 on Thl/Th2 balance in the synovia of ankle joint in AA rats.

Time	AA rats			AA rats treated with TJ-20		
	CXCR3 (Th1)	CCR4 (Th2)	CXCR3/CCR4 Th1/Th2 ratio	CXCR3 (Th1)	CCR4 (Th2)	CXCR3/CCR4 Th1/Th2 ratio
2 weeks	60 ± 6.5	27 ± 4.3	2.22	46.9 ± 5.2**	29.8 ± 4.2	1.57
3 weeks	52 ± 5.7	44 ± 7.2	1.18	43.1 ± 6.1*	44.6 ± 3.8	0.97
4 weeks	42 ± 4.8	56 ± 6.7	0.75	38 ± 3.6	61.6 ± 3.1	0.62

By use of doubled-immunofluorescence study, we have determined the percentages of CXCR3/W3/25-double-positive cells and CCR4/W3/25-double-positive cells among total W3/25-positive cells in AA rats and AA rats with TJ-20 administration from day 7 after adjuvant injection. Data are the mean ± SD for 6 rats in each group. Asterisks indicate a statistically significant difference from AA rats ($^{*}P < 0.05$, $^{**}P < 0.01$).

markedly at week 2 but decreased significantly at week 4, while the percentage of CCR4/W3/25-positive cells increased significantly from weeks 2 to 4. The ratio of CXCR3/W3/25- to CCR4/W3/25-double positive cells changed from 2.22 at week 2 to 0.75 at week 4 after injection of the adjuvant (Table 2). In comparison with AA rats, we have detected a significant decrease in both the percentages of IFN-γ-positive mononuclear cells (Figure 4(d)) and the percentage of CXCR3/W3/25-double positive cells from weeks 2 to 3 (Table 2); however we could not detect any significant difference in either the percentage of IL-4-positive mononuclear cells (Figure 4(e)) or the percentage of CCR4/W3/25-double positive cells detected from weeks 2 to 4 in the synovia of AA rats treated with TJ-20 according to schedules II and I (data not shown). The ratio of CXCR3/W3/25- to CCR4/W3/25-double positive cells changed from 1.57 in week 2 to 0.62 in week 4 after injection of the adjuvant (Table 2). These results strongly suggest that the administration of TJ-20 using schedules I and II significantly suppressed the recruitment of Th1 cells into the synovia of AA rats.

4. Discussion

Drugs are metabolized in animals more quickly than in humans [22]. It was reported that the hepatic clearance of drugs in humans was approximately one-seventh of that in other mammals including rats [23]. Furthermore, it is known that the renal clearance rate of mice is about tenfold greater than that of humans [24]. Therefore, in the present study, TJ-20 was administered to rats at a dose of 600 mg per kg of body weight daily, which is equivalent to tenfold the clinical dosage used in humans. Since no body weight loss was observed in the control rats and no significant difference in the body weight gain was detected between the AA rats given TJ-20 on schedule I or II and the normal rats, it is suggested that TJ-20 has few side effects.

Adjuvant arthritis in rats is often used for the assessment of antirheumatic drugs [20, 21, 25]. After injection of adjuvant, mononuclear cells were detected in the synovia as induction phages on day 4, and the swelling of the joints was observed on day 10, as the signs of the onset of AA [26]. From weeks 2 to 3, marked infiltration by mononuclear cells is apparent, represented as the acute phases. After week 4, a significant decrease in the number of mononuclear cells in the synovia was observed, corresponding to the chronic phases of AA [17, 26]. It is suggested that the activation of macrophages and helper T cells as well as the increase in the production of mediators is essential for the onset of AA [27]. In the present study, we found that administration of TJ-20 from day 0 or from day 7 (schedule I and II), but not from day 10 (schedule III), significantly suppressed the progress of AA. Therefore, we hypothesized that TJ-20 affects the infiltration of macrophages and helper T cells into the synovia during the induction stage of AA, but cannot adequately suppress the function of activated macrophages and helper T cells after the onset of AA.

Macrophages and T lymphocytes are considered pivotal to the pathogenesis of RA [1]. Previously, we have reported that the time course of changes in the percentage of both macrophages and helper T cells among mononuclear cells in the synovia is consistent with the swelling in the hind paws of AA rats [17]. Suppression of the activation of both macrophages and T lymphocyte seems as a more effective treatment for RA [28]. Common antirheumatic drugs for RA, such as methotrexate, can inhibit activation of T lymphocytes [29] and macrophages [30]. In this study, we found that TJ-20 administration from induction phases significantly suppressed the percentages of both ED1-positive cells and W3/25-positive cells among mononuclear cells in the synovia of ankle joints of AA rats. These results suggest that TJ-20 can reduce the infiltration of macrophages and T cells into the synovia in AA rats.

The overproduction of TNF-α and IL-10 in the synovia in RA is reported [31]. It has also been reported that the increased level of TNF-α in the synovial fluid and synovia is associated with joint destruction in RA [4, 5]. On the other hand, IL-10 suppresses the production of TNF-α [9, 10] and progression of arthritis [32, 33]. In AA rats, it has been reported that TNF-α is involved in the progression while IL-10 is involved in the remission of AA [18, 19]. In the present study, a significant decrease in the percentage of TNF-α-positive cells and a significant increase of the percentage of IL-10-positive cells were detected in AA rats treated with TJ-20 from the induction phases of AA. Since the suppression of TNF-α production and augmentation of IL-10 expression are thought to be a favorable approach for treating RA [34–36], we speculated that the administration of TJ-20 could be an ideal therapy for arthritis.

An imbalance of Th1/Th2 is also related the progression of RA [37]. IFN-γ, one of the Th1 cytokines, enhanced the aggravation of RA [15, 38]. IL-4, one of the Th2 cytokines,

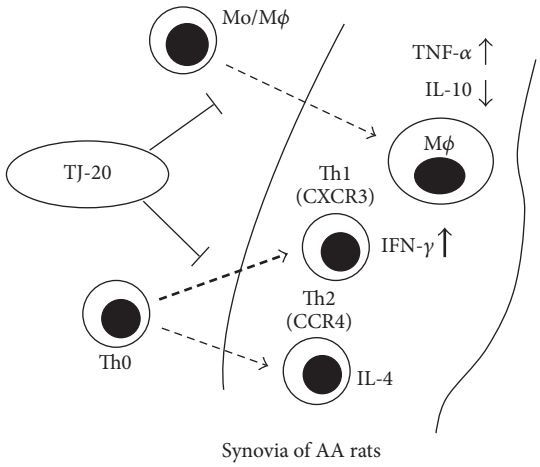

Figure 5: A schematic representation of the effects and the principle molecular mechanisms of TJ-20 on adjuvant arthritis. TJ-20 reduces the recruitment of macrophages and helper T cells into the synovia of ankle joint in AA rats. Consequently, TJ-20 downregulates the production of TNF-α but augments the production of IL-10, which are mainly released by macrophages; TJ-20 also regulates the balance of Th1/Th2 ratio as it suppresses a recruitment of Th1 cells in the synovia of AA rats.

suppressed the inflammation and joint destruction of RA [39]. In AA rats, IFN-γ is shown to be involved in the progression of AA, while IL-4 is involved in the remission of AA, respectively [18, 19]. Chemokines receptors have been reported as markers for Th1 and Th2 cells [12–14]. Using these markers, we have shown that the increase in the number of Th1 cells is highly associated with the progression of AA, while the increase in the number of Th2 cells is involved in its remission [15]. The current study showed that administration of TJ-20 from the induction phases significantly reduced the recruitment of Th1 cells, suggesting that mainly Th1 cells are influenced by TJ-20. Th2 cells have a suppressive effect on Th1 cells through the production of cytokines [40, 41]; however, administration of TJ-20 did not influence either the number of IL-4-expressing cells or that of CCR4-positive helper T cells in the synovia of AA rats. Our observation suggests that the TJ-20 treatment did not affect the recruitment of Th2 cells. Therefore, we speculate that the therapeutic effects of TJ-20 on AA involve regulation of the Th1/Th2 balance. The anti-inflammatory effects of *Sinomenium acutum* and Atractylodes Lancea rhizome, the main ingredients of TJ-20, may contribute to the effects of TJ-20 on AA rats [20, 42].

In conclusion, the current study demonstrated that oral administration of TJ-20 during the induction phase of AA ameliorated the progression of AA in rats. TJ-20 might suppress the recruitment of inflammatory cells, both macrophages and helper T cells, into the synovia. Such pharmacological events could regulate the expression of proinflammatory cytokines/anti-inflammatory cytokines, leading to a modulation of the Th1/Th2 balance in the synovia in AA rats (Figure 5). These results provide a scientific basis for the clinical use of TJ-20 for RA and indicate that TJ-20 is useful for treating at early stages of RA. Further studies are required concerning the effects of TJ-20 on the destruction of bone in the arthritic joints.

Conflicts of Interest

The authors declare that there are no conflicts of interest regarding the publication of this paper.

Acknowledgments

This work was financially supported by grants from the National Natural Science Foundation of China (no. 81500-858), Liaoning Province Doctor Startup Foundation (no. 201501006), and Young Scholars Foundation, School of Stomatology, China Medical University, Shenyang, China (Grant K101593-15-02).

References

[1] G. Janossy, G. Panayi, O. Duke, M. Bofill, L. W. Poulter, and G. Goldstein, "Rheumatoid arthritis: a disease of T-lymphocyte/macrophage immunoregulation," *The Lancet*, vol. 2, no. 8251, pp. 839–842, 1981.

[2] I. B. McInnes and G. Schett, "Cytokines in the pathogenesis of rheumatoid arthritis," *Nature Reviews Immunology*, vol. 7, no. 6, pp. 429–442, 2007.

[3] M. G. Netea, T. Radstake, L. A. Joosten et al., "Salmonella septicemia in rheumatoid arthritis patients receiving anti-tumor necrosis factor therapy: association with decreased interferon-gamma production and Toll-like receptor 4 expression," *Arthritis and Rheumatism*, vol. 48, no. 7, pp. 1853–1857, 2003.

[4] M. C. Genovese, J.-C. Becker, M. Schiff et al., "Abatacept for rheumatoid arthritis refractory to tumor necrosis factor α inhibition," *The New England Journal of Medicine*, vol. 353, no. 11, pp. 1114–1123, 2005.

[5] H. Marotte, W. Maslinski, and P. Miossec, "Circulating tumour necrosis factor-α bioactivity in rheumatoid arthritis patients treated with infliximab: link to clinical response," *Arthritis Research & Therapy*, vol. 7, no. 1, pp. R149–R155, 2005.

[6] R. N. Maini, M. J. Elliott, F. M. Brennan et al., "Monoclonal anti-TNF alpha antibody as a probe of pathogenesis and therapy of rheumatoid disease," *Immunological Reviews*, vol. 144, pp. 195–223, 1995.

[7] K. A. Bush, J. S. Walker, J. Frazier, and B. W. Kirkham, "Effects of a PEGylated soluble TNF receptor type 1 (PEG sTNF-RI) on cytokine expression in adjuvant arthritis," *Scandinavian Journal of Rheumatology*, vol. 31, no. 4, pp. 198–204, 2002.

[8] H.-P. Brezinschek, T. Hofstaetter, B. F. Leeb, P. Haindl, and W. B. Graninger, "Immunization of patients with rheumatoid arthritis with antitumor necrosis factorα therapy and methotrexate," *Current Opinion in Rheumatology*, vol. 20, no. 3, pp. 295–299, 2008.

[9] D. F. Fiorentino, A. Zlotnik, T. R. Mosmann, M. Howard, and A. O'Garra, "IL-10 inhibits cytokine production by activated macrophages," *Journal of Immunology*, vol. 147, no. 11, pp. 3815–3822, 1991.

[10] M. C. D. Trindade, M. Lind, Y. Nakashima et al., "Interleukin-10 inhibits polymethylmethacrylate particle induced interleukin-6 and tumor necrosis factor-α release by human monocyte/macrophages in vitro," *Biomaterials*, vol. 22, no. 15, pp. 2067–2073, 2001.

[11] T. R. Mosmann and R. L. Coffman, "Heterogeneity of cytokine secretion patterns and functions of helper T cells," *Advances in Immunology*, vol. 46, pp. 111–147, 1989.

[12] J. Yamamoto, Y. Adachi, Y. Onoue et al., "Differential expression of the chemokine receptors by the Th1- and Th2-type effector populations within circulating CD4+ T cells," *Journal of Leukocyte Biology*, vol. 68, no. 4, pp. 568–574, 2000.

[13] A. Langenkamp, K. Nagata, K. Murphy, L. Wu, A. Lanzavecchia, and F. Sallusto, "Kinetics and expression patterns of chemokine receptors in human CD4+ T lymphocytes primed by myeloid or plasmacytoid dendritic cells," *European Journal of Immunology*, vol. 33, no. 2, pp. 474–482, 2003.

[14] Z. Wu, K. Toh, K. Nagata, T. Kukita, and T. Iijima, "Effect of the resection of the sciatic nerve on the Th1/Th2 balance in the synovia of the ankle joint of adjuvant arthritic rats," *Histochemistry and Cell Biology*, vol. 121, no. 2, pp. 141–147, 2004.

[15] R. J. Dolhain, A. N. van der Heiden, N. T. ter Haar, F. C. Breedveld, and A. M. Miltenburg, "Shift toward T lymphocytes with a T helper 1 cytokine-secretion profile in the joints of patients with rheumatoid arthritis," *Arthritis & Rheumatology*, vol. 39, no. 12, pp. 1961–1969, 1996.

[16] C. Pelegri, A. Franch, C. Castellote, and M. Castell, "Immunohistochemical changes in synovial tissue during the course of adjuvant arthritis," *Journal of Rheumatology*, vol. 22, no. 1, pp. 124–132, 1995.

[17] Z. Wu, K. Nagata, and T. Iijima, "Immunohistochemical study of NGF and its receptors in the synovial membrane of the ankle joint of adjuvant-induced arthritic rats," *Histochemistry and Cell Biology*, vol. 114, no. 6, pp. 453–459, 2000.

[18] C. B. Schmidt-Weber, D. Pohlers, A. Siegling et al., "Cytokine gene activation in synovial membrane, regional lymph nodes, and spleen during the course of rat adjuvant arthritis," *Cellular Immunology*, vol. 195, no. 1, pp. 53–65, 1999.

[19] A. Hossain, C. L. Zheng, A. Kukita, and O. Kohashi, "Balance of Th1/Th2 cytokines associated with the preventive effect of incomplete Freund's adjuvant on the development of adjuvant arthritis in LEW rats," *Journal of Autoimmunity*, vol. 17, no. 4, pp. 289–295, 2001.

[20] H. Yamasaki, "Pharmacology of sinomenine, an anti-rheumatic alkaloid from Sinomenium acutum," *Acta Medica Okayama*, vol. 30, no. 1, pp. 1–20, 1976.

[21] L. Liu, E. Buchner, D. Beitze et al., "Amelioration of rat experimental arthritides by treatment with the alkaloid sinomenine," *International Journal of Immunopharmacology*, vol. 18, no. 10, pp. 529–543, 1996.

[22] B. B. Brodie, "Difficulties in transposing experimental results obtained with animals to man," *Actualites pharmacologiques*, vol. 17, pp. 1–40, 1964.

[23] H. Boxenbaum, "Interspecies variation in liver weight, hepatic blood flow, and antipyrine intrinsic clearance: extrapolation of data to benzodiazepines and phenytoin," *Journal of Pharmacokinetics and Biopharmaceutics*, vol. 8, no. 2, pp. 165–176, 1980.

[24] R. Dedrick, K. B. Bischoff, and D. S. Zaharko, "Interspecies correlation of plasma concentration history of methotrexate (NSC-740)," *Cancer Chemother Reports*, vol. 54, no. 2, pp. 95–101, 1970.

[25] T. Zhang, H. Li, J. Shi et al., "p53 predominantly regulates IL-6 production and suppresses synovial inflammation in fibroblast-like synoviocytes and adjuvant-induced arthritis," *Arthritis Research & Therapy*, vol. 18, no. 1, p. 271, 2016.

[26] C. M. Pearson and F. D. Wood, "Studies of arthritis and other lesions induced in rats by the injection of mycobacterial adjuvant. VII. Pathologic details of the arthritis and spondylitis," *The American Journal of Pathology*, vol. 42, pp. 73–95, 1963.

[27] J. D. Taurog, G. P. Sandberg, and M. L. Mahowald, "The cellular basis of adjuvant arthritis. II. Characterization of the cells mediating passive transfer," *Cellular Immunology*, vol. 80, no. 1, pp. 198–204, 1983.

[28] O. FitzGerald, "Advances in understanding and novel therapeutic targets in inflammatory arthritis," *Irish Journal of Medical Science*, vol. 164, no. 1, pp. 4–11, 1995.

[29] M. F. Neurath, K. Hildner, C. Becker et al., "Methotrexate specifically modulates cytokine production by T cells and macrophages in murine collagen-induced arthritis (CIA): a mechanism for methotrexate-mediated immunosuppression," *Clinical and Experimental Immunology*, vol. 115, no. 1, pp. 42–55, 1999.

[30] M. D. Smith, M. C. Kraan, J. Slavotinek et al., "Treatment-induced remission in rheumatoid arthritis patients is characterized by a reduction in macrophage content of synovial biopsies," *Rheumatology*, vol. 40, no. 4, pp. 367–374, 2001.

[31] L. Klareskog, J. Rönnelid, and G. Holm, "Immunopathogenesis and immunotherapy in rheumatoid arthritis: an area in transition," *Journal of Internal Medicine*, vol. 238, no. 3, pp. 191–206, 1995.

[32] M. Walmsley, P. D. Katsikis, E. Abney et al., "Interleukin-10 inhibition of the progression of established collagen-induced arthritis," *Arthritis & Rheumatology*, vol. 39, no. 3, pp. 495–503, 1996.

[33] S. Persson, A. Mikulowska, S. Narula, A. O'Garra, and R. Holmdahl, "Interleukin-10 suppresses the development of collagen type II-induced arthritis and ameliorates sustained arthritis in rats," *Scandinavian Journal of Immunology*, vol. 44, no. 6, pp. 607–614, 1996.

[34] D. Hwang and W. Kim, "Rheumatoid arthritis: modelling cytokine signaling networks," *Nature Reviews Rheumatology*, vol. 13, no. 1, pp. 5–6, 2017.

[35] Z. Szekanecz, A. E. Koch, S. L. Kunkel, and R. M. Strieter, "Cytokines in rheumatoid arthritis. Potential targets for pharmacological intervention," *Drugs and Aging*, vol. 12, no. 5, pp. 377–390, 1998.

[36] M. Hisadome, T. Fukuda, H. Sumichika, T. Hanano, and K. Adachi, "A novel anti-rheumatic drug suppresses tumor necrosis factor-α and augments interleukin-10 in adjuvant arthritic rats," *European Journal of Pharmacology*, vol. 409, no. 3, pp. 331–335, 2000.

[37] H. Schulze-Koops and J. R. Kalden, "The balance of Th1/Th2 cytokines in rheumatoid arthritis," *Best Practice and Research: Clinical Rheumatology*, vol. 15, no. 5, pp. 677–691, 2001.

[38] R. Gerli, O. Bistoni, A. Russano et al., "In vivo activated T cells in rheumatoid synovitis. Analysis of Th1- and Th2-type cytokine production at clonal level in different stages of disease," *Clinical and Experimental Immunology*, vol. 129, no. 3, pp. 549–555, 2002.

[39] J. A. van Roon, F. P. Lafeber, and J. W. Bijlsma, "Synergistic activity of interleukin-4 and interleukin-10 in suppression of inflammation and joint destruction in rheumatoid arthritis," *Arthritis & Rheumatology*, vol. 44, no. 1, pp. 3–12, 2001.

[40] J. Zhu, H. Yamane, and W. E. Paul, "Differentiation of effector CD4+ T cell populations," *Annual Review of Immunology*, vol. 28, pp. 445–489, 2010.

[41] M. Peine, S. Rausch, C. Helmstetter et al., "Stable T-bet$^+$GATA-3$^+$ Th1/Th2 hybrid cells arise in vivo, can develop directly from naive precursors, and limit immunopathologic inflammation," *PLoS Biology*, vol. 11, no. 8, Article ID e1001633, 2013.

[42] T. Atsumi, A. Iwashita, I. Ohtsuka et al., "Effects of atractylodis lanceae rhizoma on inflammatory mediator production from the RAW264 macrophage cell line," *Journal of Traditional Medicines*, vol. 30, no. 3, pp. 124–131, 2013.

Hindawi
Evidence-Based Complementary and Alternative Medicine
Volume 2017, Article ID 4951937, 14 pages
https://doi.org/10.1155/2017/4951937

Research Article

Chemicals Compositions, Antioxidant and Anti-Inflammatory Activity of *Cynara scolymus* Leaves Extracts, and Analysis of Major Bioactive Polyphenols by HPLC

Maryem Ben Salem,[1] Hanen Affes,[1] Khaled Athmouni,[2] Kamilia Ksouda,[1] Raouia Dhouibi,[1] Zouheir Sahnoun,[1] Serria Hammami,[1] and Khaled Mounir Zeghal[1]

[1]*Laboratory of Pharmacology, Faculty of Medicine of Sfax, University of Sfax, Sfax, Tunisia*
[2]*Laboratory of Faculty of Sciences of Sfax, University of Sfax, Sfax, Tunisia*

Correspondence should be addressed to Hanen Affes; affeshanen13@yahoo.fr

Received 20 December 2016; Accepted 19 February 2017; Published 30 April 2017

Academic Editor: Valeria Sulsen

Objective. Artichoke (*Cynara scolymus* L.) was one of the plant remedies for primary health care. The present study was focused on the determination of chemical composition, antioxidant activities, and anti-inflammatory activity and on analyzing its major bioactive polyphenols by HPLC. *Methods*. Artichoke Leaves Extracts (ALE) were analyzed for proximate analysis and phytochemical and antioxidant activity by several methods such as DDPH, ABTS, FRAP, and beta-carotene bleaching test. The carrageenan (Carr) model induced paw oedema in order to investigate the anti-inflammatory activity. Identification and quantification of bioactive polyphenols compounds were done by HPLC method. The oxidative stress parameters were determined; CAT, SOD, GSH, MDA, and AOPP activities and the histopathological examination were also performed. *Results*. It was noted that EtOH extract of ALE contained the highest phenolic, flavonoid, and tannin contents and the strongest antioxidants activities including DDPH (94.23%), ABTS (538.75 mmol), FRAP assay (542.62 umol), and β-carotene bleaching (70.74%) compared to the other extracts of ALE. Administration of EtOH extract at dose 400 mg/kg/bw exhibited a maximum inhibition of inflammation induced by Carr for 3 and 5 hours compared to reference group Indomethacin (Indo). *Conclusion*. ALE displayed high potential as natural source of minerals and phytochemicals compounds with antioxidant and anti-inflammatory properties.

1. Introduction

The inflammation reaction is a physiologic response of the body contributed by aggression of microorganism and other soluble products. Polynuclear neutrophils (PN) play an important role in the initiation of inflammation with other molecules named inflammatory mediators released by several cells like cytokines, endotoxins, leukotrienes, prostaglandins, and reactive oxygen species (ROS) [1]. In the beginning for the inflammation reaction, the accumulation of PN in the inflammatory site and tissue and different cell injury are due to participation of proteolysis' enzymes and ROS by activating defense systems [1].

Oxidative stress is a consequence of discrepancy balance between the production of ROS and antioxidants in a system of defense of human organisms [2]. Several studies showed that many of antioxidants systems have the ability to treat some disease like a cancer by scavenging ROS resultant by oxidative stress systems [3].

Carr induced paw oedema model is used to assess the different phases of inflammation reaction. Carr model can induce acute inflammation, release of inflammatory mediators, and production of free radicals [4].

The mechanism of antioxidant enzymatic systems against the inflammatory stress includes superoxide dismutase (SOD), catalase (CAT), and nonenzymatic antioxidants as reduced glutathione (GSH). Recently, several studies showed that lack of antioxidant systems can cause many inflammatory diseases [5]. However, it showed that various roles of enzymatic and nonenzymatic antioxidants help to protect

organisms from excessive generation of ROS in the inflammatory states. Some studies showed that natural herbs could suppress the production of oxidative stress by increasing the antioxidants systems [6]. Plants have rich source of phenolic compounds, carotenoids, vitamins, and terpenoids. These compounds have a potential antioxidant that can be free radical scavenger in order to reduce the development of oxidative stress in many diseases [7].

In order to enhance the Tunisian forest resources and develop new products, we are interested in the family of Asteraceae, particularly *Cynara scolymus*, which characterizes the Mediterranean region and it has been widely used in various hepatic diseases [8].

The objective of this work is designed to evaluate the phytoconstituents of ALE in vitro and the potential anti-inflammatory role of ALE in animal's models.

2. Materials and Methods

2.1. Plant Material and Extraction Method. *C. scolymus* dried leaves were obtained from the region of Bizerte in north of Tunisia; the period of collection was December to March 2014. The plant was authenticated by the Laboratory of Biology and Vegetable Ecophysiology in the Faculty of Science of Sfax. The voucher sample was created by The National Botanical Research Institute of Tunisia. Tunisia. Dried powdered plant material (200 g) was extracted by maceration method (1 L) using different increasing solvent polarities (hexane, butanol, ethyl acetate, 75% EtOH/H_2O, and aqueous). After 48 hours, all extracts were filtered. Then the dried extracts of artichoke were kept in the dark at +4°C in order to evaluate the composition of *C. scolymus* leaves extracts.

2.2. Phytochemical Analysis of Cynara scolymus Leaves Extracts. The analytical tests for identification of different secondary metabolites in *Cynara* leaves extracts were conducted following procedures described by Sofwora and Okwu [9, 10].

2.3. Proximate Analysis of Dried Leaves of C. scolymus. The determination of nutritional composition, crude protein, lipids, fiber, and ash, was obtained using several methods described while the carbohydrate content was obtained by the difference method (calculated by subtracting the sum of crude fat, crude protein, ash content, and crude fiber) [11].

For the determination of crude protein, the concentration of dried samples was determined by micro-Kjeldahl method. The lipid content was estimated by using petroleum ether as a solvent extraction in a Soxhlet at 40–60°C [12]. Total dietary fiber was determined by extraction with petroleum ether. The defatted sample was boiled under reflux with two solvents H_2SO_4 and NaOH, and then they were filtered and washed with boiling water till the filtrates were no longer acidic and basic. The residue of the sample was dried in an oven at 100°C and 600°C, cooled in desiccators, and weighed [13]. The ash content was estimated by heating in a muffle furnace at 600°C.

The quantification of dry matter was performed using one gram of *C. scolymus* leaves heated in 105°C for 1 hour. Then, it was put in desiccators for 30 min. After that, the mass of each content has been noticed. These steps have led to dry leaves and their mass has been noticed again in order to calculate the percentage of humidity in these samples [11]. In addition, the analysis of sugar amounts was obtained by phenol-sulfuric acid reagent [14].

2.4. Quantification of Total Phenolics, Flavonoids, and Tannins Contents of Cynara scolymus Leaves Extracts. The quantification of total phenolics content (TPC) of ALE was determined by Fawole et al. method [15]. 200 μL of ALE was mixed with 1 mL of Folin-Ciocalteu reagent diluted (×10) with distillated water and 0.8 mL of 7.5% of $NaCO_3$ solution in a test tube. 30 min later, the absorbance was measured at 765 nm by using a Jenway 6405 UV-Vis spectrophotometer. TPC was expressed as milligrams of gallic acid equivalents per gram of dry weight (mg GA/g DW). Quantification of total flavonoid content (TFC) was determined spectrophotometrically [16]. 500 μL of ALE was mixed with 1500 μL of water and 150 μL of (5%) $NaNO_2$. After 5 min, 150 μL of $ALCl_3$ (10%, m/v) was added to mixture. After 6 min of incubation at room temperature, a volume of 500 μL of NaOH (4%) was added also. Immediately, the mixture was completely agitated in order to homogenize the contents. The absorbance of solution obtained was measured at 510 nm against a blank. These analyses were expressed as mg of catechin equivalents per gram of dry weight (mg CE/g DW).

The determination of condensed tannin content (TCC) was measured using vanillin method [17]. 50 μL of ALE diluted was added to mixture which was made of 3 mL of 4% methanol-vanillin solution and 1.5 mL of concentrated H_2SO_4. The mixture was incubated to stand for 15 min and the absorbance was measured at 500 nm against methanol as a blank. The amount of TCC was expressed as mg catechin equivalent g^{-1} dry weight (mg CE/g DW).

2.5. Minerals Contents Analysis. The preparation of *C. scolymus* dried leaves was incinerated in a muffle furnace at 550°C for 8 hours [18] and the ashes obtained were digested in nitric acid and dissolved in distilled water for the mineral composition of artichoke leaves [19, 20]. Minerals elements of *C. scolymus* leaves were potassium (K), magnesium (Mg), calcium (Ca), sodium (Na), iron (I), manganese (Mn), zinc (Zn), copper (Cu), and chromium (Cr). These mineral contents were determined by flame atomic absorption spectrometry (Hitachi Z-6100, Japan).

2.6. Analysis In Vitro of Antioxidants Properties

2.6.1. Antioxidant Activity by DPPH Method. The antioxidant activity of DPPH is based on scavenging of DPPH$^{\cdot}$ from antioxidants in the vegetal sample, which produce a spectrophotometric loss in absorbance at 515 nm. The DPPH assay (Sigma Chemical Co., St. Louis, MO) was evaluated as described by Fawole et al. [15]. The mixture was prepared in test tubes by dilution of 50 uL of ALE in 735 mL of 100% methanol.

750 mL of 0.1 mM methanolic DPPH reagent was added to the mixture of ALE-methanol. Then, the mixture was incubated at room temperature in a chamber without any

light during 30 min. After incubation, the estimation of the scavenging ability was performed by measuring at 517 nm in spectrophotometer (T70 UV-Vis).

The capacity of inhibition percentage (PI) of DPPH radicals was calculated as

$$\text{DPPH radicals (PI)} = \left[\frac{(A_b - A_s)}{A_b}\right] \times 100, \quad (1)$$

where A_b refers to the absorbance of control (without plant extract) and A_s to the absorbance of sample (with plant extract). BHT and VC were used as standards at the same concentrations of plant extract.

2.6.2. β-Carotene Bleaching Test. The capacity of ALE to reduce bleaching of beta-carotene was previously determined by Koleva et al. [21]. The mixture of beta-carotene and linoleic acid was prepared; 0.5 mg of β-carotene, 25 uL of linoleic acid, and 200 uL of Tween 40 were dissolved in 1 mL of chloroform solvent. The chloroform was evaporated in a rotator evaporator at 40°C and 100 mL of dH_2O was added; then the mixture was stirred.

Aliquots of 2.5 mL of beta-carotene/linoleic acid emulsion obtained were transferred to test tubes containing different ALE concentrations; then the emulsion of reaction was incubated for 2 h at 50°C and the absorbance of each sample was measured at 470 nm by spectrophotometer. BHT and AA were used as the standards at the same concentrations of the samples.

2.6.3. Antioxidant Activity by $ABTS^{\bullet+}$ Method. The ability to neutralize the $ABTS^{\bullet+}$ was reported by Re et al. [22] using a spectrophotometric, 96-well microplate method. The preparation of $ABTS^{\bullet+}$ free radical solution by incubating a mixture of ABTS (7 mM) and $K_2S_2O_8$ (2.45 mM) dissolved in distillated water to create a stable color of radical solution following 12–16 h of incubation in the dark room at 4°C.

Therefore, the standard $ABTS^{\bullet+}$ solution was prepared by dilution with ethanol to a standard absorbance of 0.7 ± 0.02 at 734 nm.

50 μL of plant extract (1–20 μg/mL) was added to 150 μL of $ABTS^{\bullet+}$. The plates were incubated at room temperature, in the dark room during 15 min; the absorbance was measured at 630 nm. Control wells contained 50 μL of H_2O and 150 μL of $ABTS^{\bullet+}$. Phytochemical interference was accounted by wells containing extract (50 μL) with dH_2O (150 μL), whereas 200 μL of H_2O served as blank. Trolox dissolved in pure MeOH was used as standards.

The antioxidant capacity of ALE was expressed quantitatively as mmol of Trolox Equivalents (TE) (mmol TE/g dry extract).

2.6.4. Ferric Reducing Assay. The potential ability of ALE to reduce the ferric iron was evaluated previously by Fawole et al. [15].

The mixture of FRAP was freshly prepared by 50 mL of 300 mM acetate buffer, 5 mL of 10 mM TPTZ, and 5 mL of 20 mM $FeCl_3$. Prior to its use, the prepared mixture must be incubated in water bath at 37°C during 15 min to stabilize the contents in the reaction mixture.

Exactly, 150 mL of diluted ALE was transferred into different test tubes and then 250 mL of FRAP solution was added in triplicate. The mixture was stirred and incubated in a dark room for 30 min before measuring the absorbance at 515 nm in UV-Vis spectrophotometer. Antioxidant capacity of ALE was expressed as micromoles of Trolox Equivalent per milliliter of sample (mMTE/mL).

2.7. Anti-Inflammatory Activity In Vivo

2.7.1. Chemicals and Reagents. Lambda carrageenan and Indomethacin were purchased from Sigma Aldrich company (France).

2.7.2. Experimental Study. 30 sexually mature male rats, 10–12 weeks old weighing 150–200 g, were obtained from the Institute of Pasteur, Tunisia. Rats were fed with standard laboratory pellets and ad libitum access during the experiment study. The experimental protocol was conducted in accordance with the *Guide for the Care and Use of Laboratory Animals* issued by the University of Sfax, Tunisia, and approved by the Ethics Committee of Animal use, *protocol number 94-1939*. Before the experiment, rats were acclimatized in controlled environmental conditions at 24 ± 4°C with relative humidity (45–55%) and 12 h dark-light cycle. All the groups of animals were randomly divided into the control group and treatment groups.

2.7.3. Carrageenan-Induced Paw Oedema Model. The evaluation of anti-inflammatory activity was reported by Ravi et al. [23]. 0.1 mL of Carr solution (1%) was injected into subplantar surface of the paw of each group of rats to produce acute inflammation. This method was chosen over other methods for the discovery of new therapeutic effects of ALE in inflammation diseases, as it is the most basic method requiring minimal equipment, but much practice.

The experimental study designed 4 groups of six rats. Group (I) was the control group which received isotonic saline solution Nacl (0, 9%) by subplantar injection and had no inflammation and received no treatment. Group (II) was inflamed by carrageenan injection and did not undergo any treatment (Carr). Group (III) was used as reference inflamed rats that were treated with Indomethacin (10 mg/kg/bw) (Carr + Indo) by intraperitoneal injection (i.p.) and Group (IV) was treated with EtOH extract of ALE at dose 400 mg/kg/bw (Carr+ ALE) by i.p. [24]. The doses of ALE and Indo chosen during treatments were proportional to the size of the oedema and covered the whole swelling.

In all treated groups, the oedema paw volumes, up to tibiotarsal articulation, were measured using a digital caliper at 1, 2, 3, 4, and 5 hours after Carr injection.

For each treated group, the size of oedema obtained at these various times (PT) was compared to that obtained before any treatment (P0).

Percentages of oedema inhibition were calculated as

$$\%\ \text{Inhibition (EI)} = \left[1 - \left(\frac{\text{PT}}{\text{P0}}\right)\right] \times 100. \quad (2)$$

Table 1: Phytochemical analysis of *Cynara scolymus* extracts leaves.

Extract	Cardiac glycosides	Triterpenoids	Saponin	Flavonoids	Tannins	Alkaloid
ALE	+	+	+	+	+	+

Sign (+) indicates being present.

Percentages of inflammation inhibition were calculated as

$$\%\ \text{Inhibition (II)} = \left[\text{PT} - \left(\frac{\text{P0}}{\text{P0}}\right)\right] \times 100. \quad (3)$$

2.7.4. Blood Sample Collection. 5 hours after Carr induction, the rats were decapitated and the blood samples were collected in heparin tubes. Plasma samples were obtained after centrifugation at 3000 rpm for 15 min and they were kept in −20°C until analysis on an automatic biochemistry analyzer at the biochemical laboratory of Hedi Chaker Hospital of Sfax.

2.7.5. Inflammatory Biomarkers

(1) Determination of C-Reactive Protein (CRP). CRP was a specific marker following the inflammatory process. It increases in proportion to its intensity [25]. The reactive protein was measured by turbid metric method using an automatic analyzer COBAS INTEGRA 400″ C-reactive. The CRP is expressed with mg/L.

(2) The Fibrinogen Assay of Plasma. Plasma fibrinogen concentration was determined by Clauss clotting method [26] measured on a STA®analyzer. Principle test measures the conversion rate of fibrinogen into fibrin in diluted sample in presence of excess of thrombin and records the clotting time. The clotting time is inversely proportional to the level of fibrinogen in the plasma. The fibrinogen level is expressed with g/L plasma.

(3) Exploring the Antioxidant Enzymatic and Nonenzymatic Status. Oxidative stress parameters were determined in tissues paw oedema homogenates. The supernatants obtained were removed and analyzed for the determination of MDA as described by Draper and Hadley [27]. AOPP levels were quantified by method of Kayali et al. [28]. CAT activity was measured as reported by Aebi [29] and expressed as mmoles of H_2O_2 consumed/(min/mg protein). SOD was assayed spectrophotometrically by colorimetric method of Beyer Jr. and Fridovich [30] and expressed as U/mg protein. GSH activity was assayed according to the method of Carlberg and Mannervik [31] and expressed as mmoles GSS/(min-mg protein) and the protein content was determined using method of Lowry et al. [32].

(4) Histopathological Examination. All the paws oedema tissues of experimental groups were collected for histological examination. First, they were fixed in 10% buffered formalin solution; second, they were embedded in paraffin wax and then cut into 5 mm thick sections and stained with hematoxylin and eosin (H&E). Finally, the slides were photographed with an Olympus U-TU1X-2 camera.

2.8. High Performance Liquid Chromatography (HPLC) Detection and Quantification of Polyphenolic Compounds. The phenolic fractions analysis of EtOH extract of ALE was determined using an Agilent Technologies 1100 series HPLC coupled with a UV-Vis multiwavelength detector. The separation was carried out on a 250 × 4.6 mm. C18 silica column chromatography was chosen at ambient temperature. The mobile phase consisted of C_2H_3N (solvent A) and water with 0.2% of H_2SO_4 (solvent B) and the flow rate was kept at 0.8 mL min^{-1}. For the preparation of calibration curve, a standard stock solution was prepared in methanol (HPLC grade ≥ 99.9% from Sigma Chemical Company) containing Hydroxytyrosol, Tyrosol, 4-hydroxybenzoic acid, verbascoside, apigenin-7-glucoside, Oleuropein, Quercetin, Pinoresinol, cinnamic acid, and apigenin at the same concentration of 1 g/mL. For the preparation of the ethanol extract by dissolving in 1 mL of methanol making a final concentration of 25 mg/mL. Before starting HPLC analysis, all the solutions prepared were filtered with Whatman paper (Ø 0.45 μm). The diluted extract was injected directly and chromatograms were monitored at 280 nm. 20 μL was used for injection. Peaks were identified by the retention times compared with the standards. The analyses of phenolic profiles of ethanol extract were performed in triplicate.

2.9. Statistical Analysis. SPSS program was employed for comparisons between all groups. Comparison between multiple and within groups was analyzed by ANOVA followed by Tukey's tests. Values were shown as mean ± SD. The level of statistical significance was set at p value < 0.05. Pearson's correlation coefficient analysis was calculated using SPSS program also in order to evaluate the statistical relationship between both of polyphenolics compounds and antioxidant activities of ALE.

3. Results

3.1. Phytochemical Analysis of Cynara scolymus Leaves Extracts. ALE revealed the presence of flavonoid, cardiac glycosides, saponin, tannin, terpenoid, and alkaloids (Table 1).

3.2. Proximate Analysis of Dried Leaves of C. scolymus. The results showed that *Cynara* leaves contain high constituents: dry matter (97,03% DW), ash (15,81% DW), carbohydrate (80,05% DW), protein (16,64% DW), lipids (3,41% DW), total sugars (1,97% DW), and dietary fiber (71,60% DW) (Table 2).

3.3. Quantification of Total Phenolic, Flavonoid, and Tannins Contents of Cynara scolymus Leaves Extracts. The TPC, TFC, and TCC were evaluated in different solvents extracts of ALE. All results are shown in Table 3. Maximum content of TPC was obtained using EtOH extract and corresponded to 54.54± 1.26 mg GA/g DW followed by ethyl acetate, aqueous, and

Table 2: Proximate analysis of dried leaves of *Cynara scolymus*.

Constituents	*Cynara scolymus* leaves (percentage dry weight basis)
Dry matter	97.03 ± 0.43
Ash	15.81 ± 0.01
Carbohydrate	80.05 ± 0.69
Protein	16.64 ± 1.79
Lipids	3.41 ± 0.45
Total sugars	1.97 ± 0.10
Dietary fiber	71.60 ± 0.81

Values are expressed as mean ± SD ($n = 3$).

butanol extracts, while TPC of hexane extract was the lowest in comparison with EtOH extract (30.91 ± 9.36 mg GAE/g DW). The EtOH extract showed also the highest content in TFC (12±0.83 CE/g DW), but this value was lower for hexane extract (8.19 ± 0.6 mg CE/g DW), respectively.

The amount of TCC which was evaluated by vanillin assay was the highest in the ethyl acetate and EtOH extract (14.51 and 14.05 mg CE/g DW), but this content was lower than aqueous extract as shown in Table 3.

3.4. Mineral Contents Analysis. The main composition of macroelements and microelements in *C. scolymus* leaves is presented in Table 4.

Elemental analysis in (mg/100 g of dry weight basis) indicated that leaves of artichoke contained the following order of essential minerals compounds: potassium (2886.80), sodium (1762.94), calcium (1359.34), magnesium (433.21), iron (16.17), manganese (13.05), zinc (7.37), copper (1.30), and chromium (0.12).

3.5. Evaluation of Antioxidant Activity. The antioxidant activity of ALE harvested in Tunisia was performed using four methods: DPPH, ABTS, FRAP, and beta-carotene test.

3.5.1. Antioxidant Activity by DPPH Method. DDPH method evaluated the capacity of compounds present in ALE to reduce DDPH radical. The result in Figure 1 showed the scavenging activity of all extracts of *C. scolymus* was concentration dependent. Among all extracts, the EtOH extract displayed the highest free radical scavenging activity at higher concentration (400 ug/mL) (94.23%) compared to the same concentration of vitamin C (9.83%) and BHT (96.23%) followed by ethyl acetate extract (81.51%); the scavenging activity of other extracts was significantly lower when compared to reference standard VC (99.83%).

3.5.2. β-Carotene Bleaching Test. The potential effect of EtOH extract exhibited significantly the highest inhibition rate of β-carotene bleaching (70.74%) compared to BHT and AA (47.94%, 90.59%) ($p < 0{,}001$), respectively (Table 5), whereas hexane and butanol extract showed the lowest rate of β-carotene bleaching 37.38% and 49.39%.

3.5.3. Antioxidant Activity by ABTS$^{\bullet+}$ Method. As evident from Table 5, ALE studied presents a potential capacity

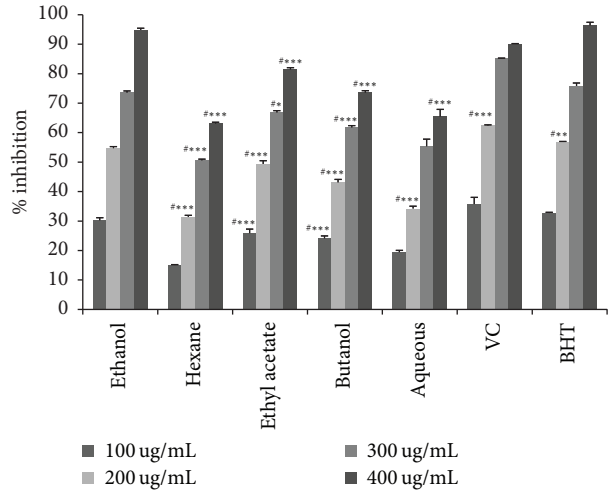

Figure 1: Antioxidant activity by DPPH method of *Cynara scolymus* leaves extracts at different concentrations. Values are mean ± SD ($n = 3$). $^{*}p < 0.05$, $^{**}p < 0.01$, and $^{***}p < 0.001$; $^{\#}$compared to EtOH extract. Butylated Hydroxytoluene (BHT). Vitamin C (VC).

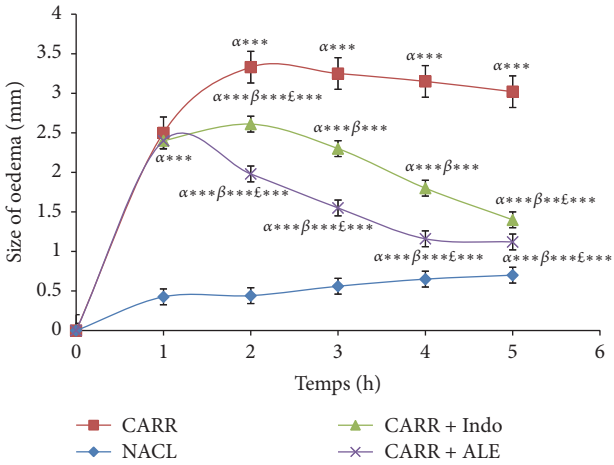

Figure 2: Effect of ALE and Indomethacin on paw oedema induced by carrageenan. Values represent mean ± SD ($n = 6$) in each group. $^{*}p < 0.05$, $^{**}p < 0.01$, and $^{***}p < 0.001$. α: compared to control; β: compared to Carr; £: compared to Carr + Indo.

to scavenge the ABTS radical cation. Among all extracts, EtOH extract was a significantly higher value (499.43 mmol Trolox/g dry extract) than the other extracts, but the lowest level of TEAC was obtained from the hexane extract (104.3 mmol Trolox/g dry extract).

3.5.4. Ferric Reducing Assay. The results in Table 5 showed that, among all extracts of ALE, a higher capacity of reducing ferric capacity was found for EtOH extract (527.79 umol Fe^{2+}/mg dry extract) when compared to other extracts, respectively.

3.6. Anti-Inflammatory Activities. The appearance of Carr induced paw oedema with respective treatments groups was illustrated in Table 7 and Figure 2. The results showed

Table 3: Quantification of total phenolic, flavonoids, and tannins contents of *Cynara scolymus* leaves extracts.

Extracts	Phenolics content (mg GAE/g DW)	Flavonoids content (mg CE/g DW)	Tannins content (mg CE/g DW)
Hexane	39.91 ± 9.36	8.19 ± 0.16	14.05 ± 0.3
Ethyl acetate	53.07 ± 0.47	10.32 ± 0.12	14.51 ± 0.13
Butanol	41.66 ± 2.23	11.21 ± 0.10	13.93 ± 93
Ethanol	54.54 ± 1.26	12.00 ± 0.83	10.99
Aqueous	49.49 ± 0.39	9.49 ± 0.39	4.38 ± 0.45

Values are expressed as mean ± SD ($n = 3$).

Table 4: Mineral contents dried leaves of *Cynara scolymus*.

Elements	*Cynara scolymus* leaves (mg/100 g of dry weight basis)
K	2886.803 ± 12.0
Ca	1359.346 ± 5.05
Na	1762.946 ± 12.0
Mg	433.219 ± 23.4
I	16.176 ± 0.14
Mn	13.051 ± 0.11
Zn	7.371 ± 0.14
Copper	1.30 ± 0.16
Cr	0.124 ± 0.01

Values are expressed as mean ± SD ($n = 3$).

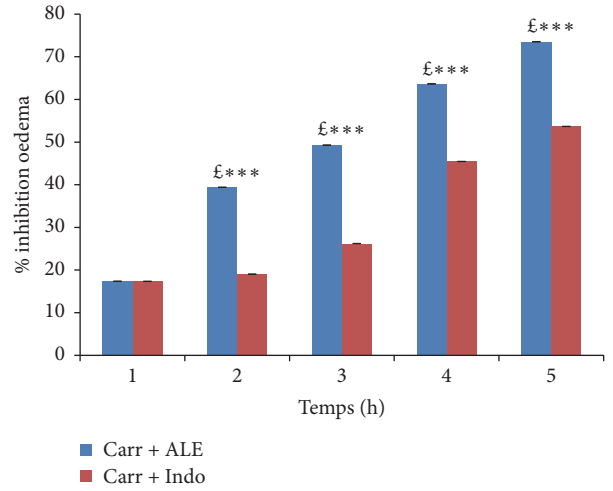

Figure 3: Percentage (%) of oedema inhibition data in all groups. Values represent mean ± SD ($n = 6$) in each group. $^{*}p < 0.05$, $^{**}p < 0.01$, and $^{***}p < 0.001$. £: compared to Carr + Indo.

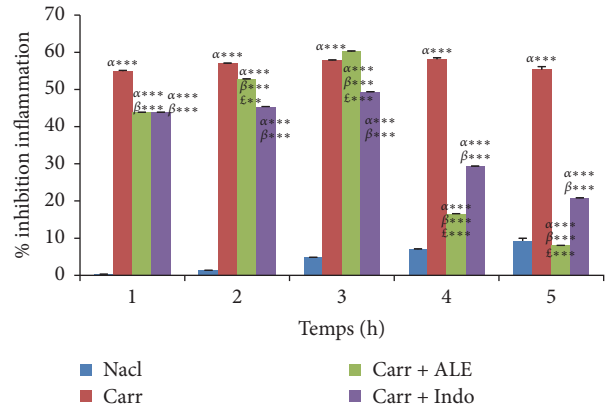

Figure 4: Percentage (%) of oedema inflammation data in all groups. Values represent mean ± SD ($n = 6$) in each group. $^{*}p < 0.05$, $^{**}p < 0.01$, and $^{***}p < 0.001$. α: compared to control group, β: compared to Carr group, and £: compared to Indo group.

that the induction of Carr in rats paw oedema started off by the vascular phase of inflammation which generated an increase in the size of oedema for all groups. This injection generated intense inflammation which peaked after 3 hours. The experimental data showed that ALE presented significant decrease in the size of paw oedema which was time dependent and more important than the reference group Indo and Carr group.

As seen in Figures 3 and 4, EtOH extract at dose (400 mg/kg/bw) has shown a significant percent of oedema inhibition ($p < 0.001$) in the first hour (17.3%) compared with reference group (Indo) and the significant percent of inhibition inflammation was 44,27% in comparison with the control group.

Thus, after five hours, these percentages were 735% for inhibition and 832% for inflammation. For the Indo group, oedema inhibition was significant ($p < 0{,}001$), 53 and 64%, and oedema inflammation was 21 and 86% in comparison with the control group.

These results showed that EtOH extract of ALE had a strong effect as Indo.

3.6.1. Inflammatory Biomarkers: Fibrinogen and CRP. We assayed serum proteins of inflammatory markers in different groups of rats.

(1) Fibrinogen. Carr group caused a significant increase in rate of fibrinogen compared to control group by 19.05% (Figure 5). The rate of fibrinogen decreased significantly ($p < 0.01$) in groups of rats treated with the EtOH extract (16.55%) and Indo (22.90%) compared with Carr group.

Table 5: Antioxidant activities of *Cynara scolymus* leaves extracts.

Sample	FRAP assay (umol Fe (II)/g DW)	β-Carotene bleaching assay (%)	TEAC assay (mmol Trolox/g DW)
Hexane	$223.023 \pm 11.16^{\#***}$	$37.38 \pm 5.24^{\#***}$	$104.3 \pm 10.73^{\#***}$
Ethyl acetate	$508.29 \pm 5.24^{\#***}$	$61.56 \pm 8.17^{\#*}$	$382.60 \pm 5.24^{\#**}$
Butanol	$443.06 \pm 22.98^{\#***}$	$49.393 \pm 2.24^{\#**}$	$251.93 \pm 28.15^{\#***}$
Ethanol	527.79 ± 16.26	70.743 ± 1.29	499.43 ± 39.72
Aqueous	$315.91 \pm 8.36^{\#***}$	$56.11 \pm 5.43^{\#**}$	$210.74 \pm 8.36^{\#***}$
BHT	—	$47.94 \pm 0.75^{\#***}$	—
AA	—	$90.59 \pm 3.25^{\#***}$	—

Values are means ± SD ($n = 3$). Butylated Hydroxytoluene (BHT) and Ascorbic Acid (AA) were used as positive control; $^{\#}$compared with EtOH extract. $^{*}p < 0.05$, $^{**}p < 0.01$, and $^{***}p < 0.001$.

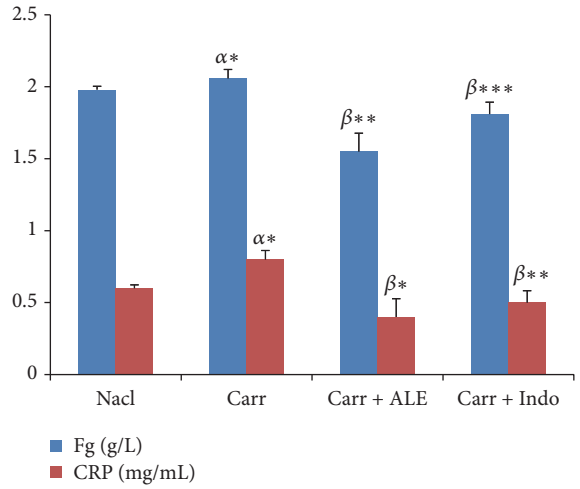

Figure 5: Levels of fibrinogen (Fg) and C-reactive protein (CRP). Values represent mean ± SD ($n = 6$) in each group. $^{*}p < 0.05$, $^{**}p < 0.01$, and $^{***}p < 0.001$. α: compared to control; β: compared to Carr group. Fibrinogen (Fg). C-reactive protein (CRP).

(2) CRP. Analysis showed a significant increase ($p < 0.05$) in CRP level (Figure 5) for Carr group compared to control group (16.73%). However, the injection of EtOH extract and Indo led to a significant decrease ($p < 0{,}001$) (60.86%, 34.23%), respectively, when compared with Carr group.

3.7. Oxidative Stress Parameters. MDA and AOPP levels in oedema paw were illustrated in Table 8. Results showed that Carr induced a significant increase in MDA and AOPP levels; however treatment with EtOH extract of ALE at dose of 400 mg/kg/bw showed a significant decrease ($p < 0{,}001$) (20.80%, 50.23%), compared with Carr group and even Indo group (10 mg/kg) (20.97%, 44.27%), respectively.

3.8. Exploring the Antioxidant Enzymatic and Nonenzymatic Status. CAT, SOD, and GSH levels in the paw oedema tissue of tested groups are shown in Table 8. Treatment of inflamed rats with EtOH extract restored significantly ($p < 0.001$) the SOD activity by 20.75%, the CAT activity by 56.55%, and the GSH activity by 75.66%, respectively, compared to Carr group.

3.9. Histopathological Examination. A microscopic study of paw oedema tissues showed histological changes in Carr group, EtOH extract of ALE (400 mg/kg/pc) group, and Indo (10 mg/kg/bw) group (Figure 6). In the Carr group, we showed a subcutaneous oedema with infiltration of inflammatory cells, especially polynuclear neutrophils at the site of inflamed tissues, and also the presence of spongy-like appearance in the epidermis ((Figure 6(b)) as compared to control group (Figure 6(a))). The EtOH extract group produced a significant decrease in the number of cellular infiltrates and a significant reduced spongy-like appearance in the epidermis (Figure 6(c)), as did reference drug Indo (Figure 6(d)).

3.10. Quantification of Polyphenolic Compounds by HPLC. To the authors' knowledge, the present study identified and quantified the phenolic compounds of ALE from Tunisian origins. Accordingly, the results obtained so far by Folin-Ciocalteu needed to be further complemented to qualify phenolic constituents in EtOH extract under investigation.

The findings revealed the presence of seven phenolic compounds, namely, Hydroxytyrosol, verbascoside, apigenin-7-glucoside, Oleuropein, Quercetin, Pinoresinol, and apigenin. HPLC analysis indicated that ALE have significant amount of verbascoside content 38,1 mg/100 g and Quercetin content (19, 2 mg/100 g) (Figures 7 and 8 and Table 9).

3.11. Correlation between the Polyphenolic Compounds and Antioxidant Capacity. In order to determine the contribution of the phenolic and flavonoid content in ALE on antioxidant capacity, the Pearson correlation coefficient (r) was determined in Table 6. The results showed a significant linear correlation between antioxidant activities determined by using DPPH, ABTS, FRAP, and beta-carotene methods and TPC and TFC, respectively. The strongest correlative value is obtained with DDPH$^{\cdot}$ and TPC ($r = 0.87$). These results indicated a good correlation between TPC and TFC with antioxidant activities of ALE.

4. Discussion

The importance of plants in traditional medicine remedies and the potential of phytochemical constituents were discussed nowadays with respect to their benefit in pharmacotherapy in Tunisia. *Cynara scolymus* was one of these

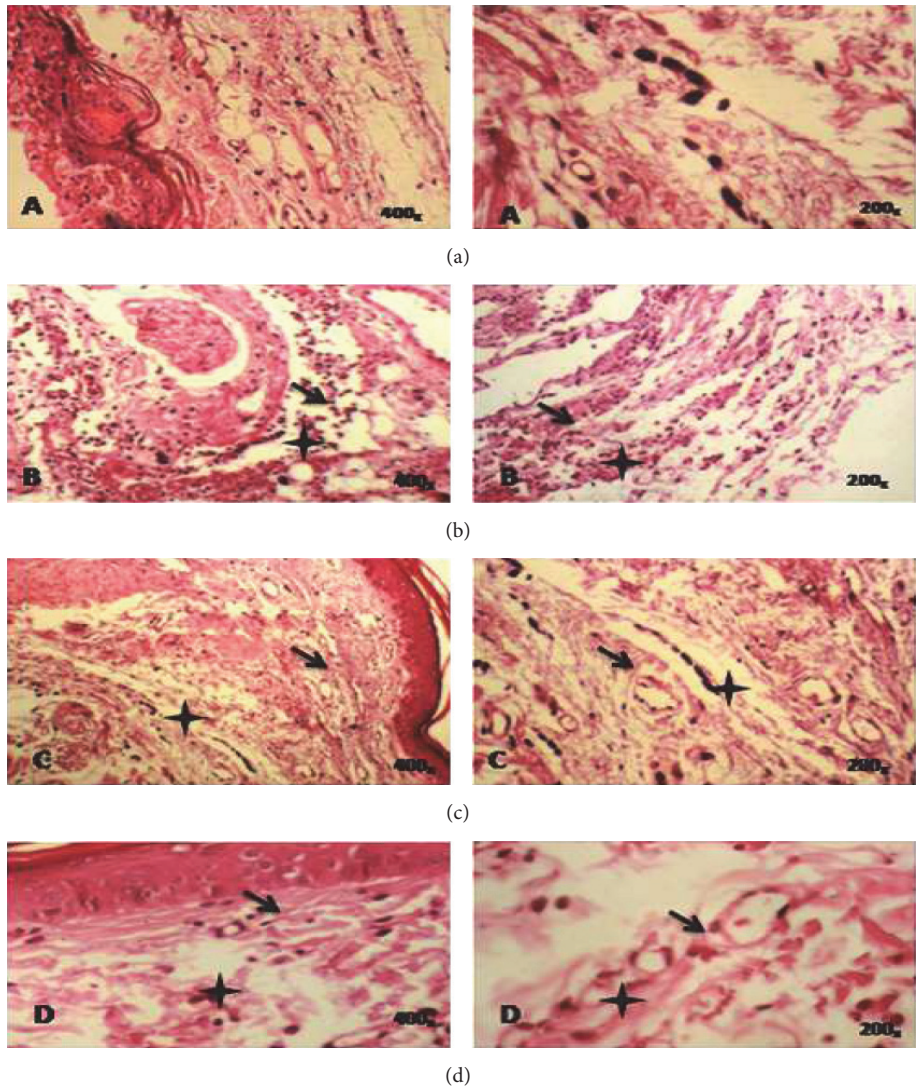

Figure 6: Histopathological slides tissues of paw oedema in experimental groups of rats. (a) Control group; untreated group. (b) Carr group; Carr-treated rat showed heavy infiltration of polynuclear neutrophils (PN) and a spongy-like appearance and bulla in the epidermis. (c) Carr + EtOH extract group; Carr-treated rat that received the EtOH extract (400 mg/kg/bw) reduced significantly the migration of PN and oedematasis in dermis without any spongy-like feature and bulla. (d) Carr + Indo group; Carr-treated rat that received Indomethacin (10 mg/kg/bw) showed a partial protective action. Deparaffinized hematoxylin and eosin (H&E) stained sections (200–400x). Plus sign: infiltration of PN. Arrow: odematasis in the epidermis.

medicinal plants which have a beneficial potential effect attributed to its source of polyphenolic compounds [3].

The selection of this plant was guided by the indications of its traditional use that, at present, there have been very little chemical and biological investigations done. Therefore the present study was to investigate phytochemical composition and their antioxidant capacity and to evaluate in vivo the anti-inflammatory effects of *Cynara scolymus* leaves extracts.

The presence of phenolic compounds is very widely distributed in medicinal plants; several studies showed that these compounds have drawn much attention to their potential antioxidant abilities which demonstrated their beneficial implications for human health.

Regarding the determination of phenolic compounds, the EtOH extract of ALE had the highest amount of these compounds in comparison with other extracts, which were an agreement with the result of Emanue et al. [33], who shows that EtOH extract exhibited the maximum amount of phenolic compounds from the leaves of *Cynara scolymus*, whereas it differs from the reports of Oliveira et al. [34], who proves that aqueous extract of ALE is the most suitable solvent for extraction of phenolic compounds.

The importance of TPC and TFC extraction yields obtained with EtOH extract can be attributed to its good solubility, low toxicity, medium polarity, and high extraction capacity [35].

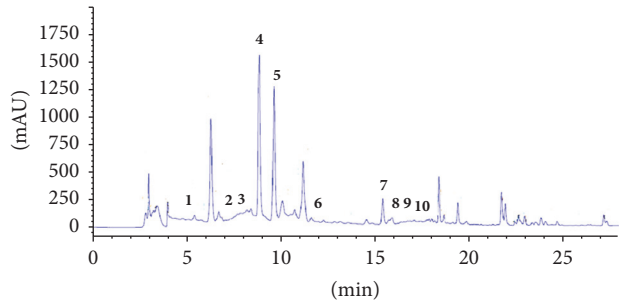

Figure 7: HPLC chromatogram of a standard mixture of polyphenolic compounds. Peaks: **1**, Hydroxytyrosol; **2**, Tyrosol; **3**, 4-hydroxybenzoic acid; **4**, verbascoside; **5**, apigenin-7-glucoside; **6**, Oleuropein; **7**, Quercetin; **8**, Pinoresinol; **9**, cinnamic acid; **10**, apigenin.

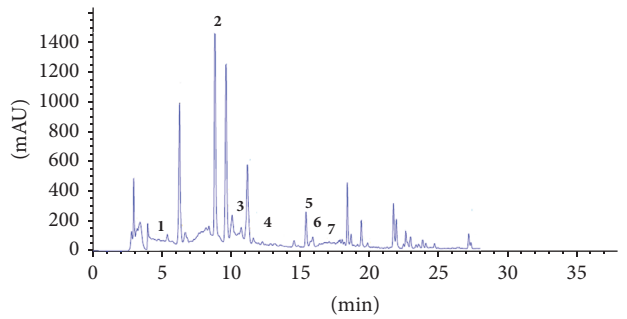

Figure 8: HPLC chromatogram of ethanol extract of *Cynara scolymus leaves extracts*. Peaks: **1**, Hydroxytyrosol; **2**, verbascoside; **3**, apigenin-7-glucoside; **4**, Oleuropein; **5**, Quercetin; **6**, Pinoresinol; **7**, apigenin.

Table 6: Pearson correlation coefficient (r) between the content of phenolic compounds and antioxidant capacity (DDPH$^{\bullet}$, ABTS$^{\bullet+}$, FRAP, and beta-carotene).

Correlation	R
TPC versus DDPH$^{\bullet}$	0,870**
TPC versus ABTS$^{\bullet+}$	0,848**
TPC versus FRAP	0,707**
TPC versus beta-carotene	0,842**
TFC versus DDPH$^{\bullet}$	0,728**
TFC versus ABTS$^{\bullet+}$	0,743**
TFC versus FRAP	0,849**
TFC versus beta-carotene	0,712**

DPPH: 2,2-diphenyl-1-picrylhydrazyl; ABTS: 2,20-azinobis(3-ethylbenzothiazoline-6-sulphonic acid) diammonium salt; FRAP: ferric reducing; TPC: total phenolic content; TFC: total flavonoid content; $^{**}p < 0.01$ significant correlation.

In the first investigation of my study, five solvents of increasing polarities were chosen for the determination of phenolic compounds from leaves of *C. scolymus*, namely, hexane, ethyl acetate, butanol, 75% EtOH/H_2O, and aqueous, in order to determine the variability of TPC and TFC in the aerial part of *Cynara* as a function of each extraction solvent.

This variability of phenolic compounds in ALE can be attributed to the wide range of solubility displayed by various polar compounds within the ALE solvents, the degree of polymerization of phenols and their interaction, genetic factors, geographical variations, and climatic changes [36].

Overall, these findings indicate that EtOH extract of ALE was rich in phenolic and flavonoid contents, which could be the major contributor to their antioxidative properties. Many researches revealed that flavonoids and polyphenols displayed the highest ability of scavenging activity in medicinal plants [37, 38].

The results indicate that EtOH extract of ALE, which contains the highest content of TFC and TPC, displays the highest free radical scavenging activity (94.23%) at concentration of 400 ug/mL. However, Oliveira et al. [34] show that aqueous extract of ALE has good radical scavenging (83.40%) at concentration of 200 ug/mL. Furthermore, our results suggest that some components within EtOH extract are significantly the strongest radical scavenger in comparison with other extracts. The TEAC values of ALE showed also that EtOH extract presents a potential ability to scavenge the ABTS radical cation in accordance with the report of Betancor-Fernández et al. [39].

The FRAP assay shows also that EtOH extract has the highest values (542.62 umol Fe II g/DW). The same result is confirmed by Kukić et al. [40]. Therefore, the results of positive correlation between the TPC, TFC, and the antioxidant methods in vitro suggest that phenolic compounds act as reducing agents, hydrogen donors, and singlet oxygen scavengers [3] and may exert an important in vitro antioxidant capacity of ALE.

The phytochemical screening of ALE has been found to be a rich source of polyphenolic compounds including Quercetin, apigenin-7-glucoside, and verbascoside. These compounds have shown a great potential of antioxidant activity [41].

The research into medicinal plants used as pain relievers' agents should therefore be viewed as new therapy in the inflammatory diseases [42]. The anti-inflammatory activities of EtOH extract of ALE are investigated, applying in vivo experimental Carr model compared with a nonsteroidal anti-inflammatory (Indomethacin); this drug was reported by Higgs et al. [43] who demonstrated the role of Indo to inhibit the biosynthesis of prostaglandins in Carr model rats. The experimental study of anti-inflammatory activity is performed by the Carr test. This phlogiston agent induced tissue oedema characteristic of acute inflammation which is regarded as a crucial parameter in assessing anti-inflammatory activity [44].

The Carr injection produces biphasic states; in the first phase [45], there is an increase in the mRNA synthesis of cyclooxygenase-2 (COX-2) at the first hour. This increase is accompanied by an amplification of synthesis of strong proinflammatory mediator such as prostaglandin, especially the prostaglandin type 2 involved in the inflammatory process [46], serotonin, bradykinin, and leukotrienes, which contribute to the initiation of inflammation reaction. Moreover, the participation of arachidonic metabolites is the main factor responsible for both of phases of Carr induced inflammation.

Table 7: Effect of *Cynara scolymus* leaves extract on carrageenan-induced rat paw oedema.

Treatment	Oedema size (mean ± SD) (mm)					
	0 h	1 h	2 h	3 h	4 h	5 h
Control	0.426 ± 0,00	0.441 ± 0.01	0.56 ± 0.03	0.650 ± 0.05	0.755 ± 0.05	0.70 ± 0.01
Carr	0.426 ± 0,00	$2.8 \pm 0.26^{\alpha***}$	$3.33 \pm 0.28^{\alpha***}$	$3.25 \pm 0.02^{\alpha***}$	$3.15 \pm 0.01^{\alpha***}$	$3.02 \pm 0.09^{\alpha***}$
Carr + Indo (10 mg/kg)	0.426 ± 0,00	$2.46 \pm 0.26^{\alpha***\beta*}$	$2.61 \pm 0.07^{\alpha***\beta***}$	$2.30 \pm 0.02^{\alpha***\beta***}$	$1.8 \pm 0.11^{\alpha***\beta***}$	$1.4 \pm 0.06^{\alpha***\beta***}$
Carr + ALE (400 mg/kg/bw)	0.426 ± 0,00	$2.480 \pm 0.05^{\alpha***\beta***}$	$1.88 \pm 0.04^{\alpha***\beta***£***}$	$1.65 \pm 0.05^{\alpha***\beta***£***}$	$1.16 \pm 0.20^{\alpha***\beta***£***}$	$1.12 \pm 0.1^{\alpha***\beta***£***}$

Values represent means ± SD ($n = 6$) in each group. $^{*}p < 0.05$, $^{**}p < 0.01$, and $^{***}p < 0.001$.
α: compared to control; β: compared to Carr; £: compared to Carr + Indo.

Table 8: Effects of *Cynara scolymus* leaves extract and Indomethacin on CAT, SOD, GSH, AOPP, and MDA activities in carrageenan induced paw oedema.

Groups	CAT (μmoles CAT/min/mg protein)	SOD (unit SOD/min/mg protein)	GSH (nmoles/mg protein)	MDA (nmol MDA/mg protein)	AOPP (nmol/mg protein)
Control	47 ± 2	13.1 ± 4.3	42.1 ± 1.2	23.4 ± 5	48.4 ± 4.3
Carr	$16.2 \pm 0.5^{\alpha***}$	$15.3 \pm 2.6^{\alpha***}$	$13.1 \pm 1.1^{\alpha***}$	$31.4 \pm 7.5^{\alpha***}$	$67.9 \pm 6.9^{\alpha***}$
Carr + Indo (10 mg/kg/bw)	$64.9 \pm 7.1^{\beta***}$	$24.0 \pm 1.3^{\beta***}$	$70.3 \pm 1.1^{\beta***}$	$20.9 \pm 3.0^{\beta***}$	$44.2 \pm 0.6^{\beta***}$
Carr + ALE (400 mg/kg/bw)	$56.5 \pm 2.5^{\beta***£**}$	$20.7 \pm 4.0^{\beta***£**}$	$75.6 \pm 2.5^{\beta***£*}$	$20.8 \pm 6.0^{\beta***}$	$50.2 \pm 4.1^{\beta***£*}$

Values represent means ± SD ($n = 6$) in each group. $^{*}p < 0.05$, $^{**}p < 0.01$, and $^{***}p < 0.001$.
α: compared to control; β: compared to Carr; £: compared to Carr + Indo.
SOD: superoxide dismutase.
CAT: catalase.
GSH: glutathione peroxidase.
MDA: Malondialdehyde.
AOPP: Advanced Oxidation Protein Product.

Table 9: Quantification and identification of phenolic compounds contents in the ethanol extract of *Cynara scolymus* leaves extracts.

Number	Content (mg/100 g of dry extract)	Polyphenolic compound
1	2,8 ± 0,19	Hydroxytyrosol
2	38,1 ± 0,36	Verbascoside
3	9,9 ± 0,02	Apigenin-7-glucoside
4	18 ± 0,1	Oleuropein
5	19,2 ± 0,14	Quercetin
6	5 ± 0,05	Pinoresinol
7	4 ± 0,04	Apigenin

Values represent means ± SD ($n = 3$).

In the second phase, the increase of vascular permeability is observed by release of kinins during 2.30 h. Thereafter from 2.30 h to 5 h, inflammation is mediated by prostaglandins and is also associated with a release infiltration and migration of PN into the inflamed site [47].

Our results indicate that ALE affords protection against the Carr induced acute inflammation in dose dependent manner. EtOH extract of ALE at dose of 400 mg/kg/bw exhibits significant anti-inflammatory activity with 73% inhibition of paw oedema compared with Indo group (53%) and typically reaches a maximum at 5 h; these results obtained suggest the anti-inflammatory effect of EtOH extract of ALE by means of inhibiting the synthesis and the release of inflammatory mediators like histamine, serotonin, and prostaglandins that are involved in acute inflammation. These results revealed the inhibitory effect of EtOH extract on PN migration and it is confirmed through a histological analysis of tissues of paw oedema in experimental groups.

These findings clearly confirm that EtOH extract of ALE has an anti-inflammatory effect by reducing the influx of polymorphonuclear cells to inflammatory tissue following injection of Carr. Most inflammatory markers, such as interleukin-6 (IL-6), tumor necrosis factor-α (TNF-α), CRP, and fibrinogen, increased significantly in response to infection and in active diseases states. CRP is the specific marker of acute inflammation occurring in the body [48]; moreover the fibrinogen is the most relevant indicator of inflammation, and it does not only represent the acute-phase reactant that is increased in inflammatory states. Elevated fibrinogen levels would be associated with higher levels of CRP and would similarly correlate with inflammation reaction.

Therefore the present study showed that EtOH extract of ALE significantly decreases the level of fibrinogen and CRP by value of 22.72% and 34.78% in comparison with Carr group.

The induction of inflammation with Carr is manifested by generation of ROS and has been shown to play an important role in various forms of inflammation [49, 50]. High concentration of reactive free radicals contributes to lipid peroxidation and protein oxidation [3]. Our results showed that there is a significant increase in MDA and AOPP activities in Carr group, when compared to control group, and a highly significant decrease in activities of SOD, CAT, and GSH, also observed at the tissue level compared with the control group ($p < 0.001$). However, the injection of EtOH extract and Indo shows a significant decrease of the levels of MDA and AOPP by 34.27% and 44.27% following a significant increase in antioxidant activities as CAT, SOD, and GSH when compared to Carr group (20.16%, 73.30%, and 75%). From these results, it is implied that the protective effect of EtOH extract may

be attributed to its potential indirectly as a stimulator of the activity and expression of antioxidant enzymes during inflammation.

Thus, the anti-inflammatory activity is due to the individual or synergistic effect of the components in the ALE. In fact, previous studies have found that anti-inflammatory profile of ALE could be related to polyphenolic compounds according to the phytochemical analysis. We performed HPLC analysis to justify the correlation between phytochemical compounds and anti-inflammatory activity of this plant. Among these polyphenolic compounds, verbascoside has been reported in several reports and showed a potential spectrum of many activities including antioxidant and anti-inflammatory. Particular, verbascoside presents antiedematogenic activities in animal models of Carr induced inflammation [51] and the responses exhibited the maximum activity for the fourth hour of treatment. Such activities may be derived from inhibitory action of chemical mediators of the inflammatory process such as histamine and bradykinin. A significant antioxidant effect of verbascoside has been recently reported by Aleo et al. [52] in an experimental study [53]. Other authors reported that anti-inflammatory activity of verbascoside has been evaluated by an in vitro test performed on cell cultures of primary human keratinocytes [54] in which it was able to reduce the release of proinflammatory markers such as chemokines.

Apigenin-7-glucoside was found to block the release of several varieties of enzymes involved in inflammation including especially lipoxygenases and cyclooxygenases [55, 56] leading to inhibition of proinflammatory molecules NF-kB activation and inhibits neutrophil infiltration in tissues.

From these results, we suggest that anti-inflammatory activity observed is due to a synergic action of these phenolic components contained in EtOH extract of ALE.

C. scolymus is one of the few herbal remedies which have been verified through experimental studies. Further the toxicity studies of ALE are required in order to confirm the safety of this medicinal plant in the treatment of inflammation diseases.

5. Conclusion

The present study showed clearly the advantages of *C. scolymus* leaves extracts which have safer anti-inflammatory profile with potent antioxidant activity attributed to the phenolic compounds. Furthermore, in the future studies, we are interested to characterize the action mechanisms of active phenolic compounds of ALE responsible for anti-inflammatory and antioxidants activities.

Conflicts of Interest

The authors declare no conflicts of interest.

Acknowledgments

This research was supported by the Tunisian Ministry of Higher Education and Scientific Research.

References

[1] C. Pasquier, "Stress oxidative et inflammation," *Blool*, vol. 4, pp. 1–6, 1996.

[2] M. A. Abuashwashi, O. M. Palomino, and M. P. Gómez-Serranillos, "Geographic origin influences the phenolic composition and antioxidant potential of wild *Crataegus monogyna* from Spain," *Pharmaceutical Biology*, vol. 54, no. 11, pp. 2708–2713, 2016.

[3] M. B. Salem, H. Affes, K. Ksouda et al., "Pharmacological studies of artichoke leaf extract and their health benefits," *Plant Foods for Human Nutrition*, vol. 70, no. 4, pp. 441–453, 2015.

[4] M.-H. Huang, B.-S. Wang, C.-S. Chiu et al., "Antioxidant, antinociceptive, and anti-inflammatory activities of *Xanthii Fructus* extract," *Journal of Ethnopharmacology*, vol. 135, no. 2, pp. 545–552, 2011.

[5] G.-J. Huang, S.-S. Huang, S.-S. Lin et al., "Analgesic effects and the mechanisms of anti-inflammation of ergostatrien-3β-ol from *antrodia camphorata* submerged whole broth in mice," *Journal of Agricultural and Food Chemistry*, vol. 58, no. 12, pp. 7445–7452, 2010.

[6] C. Tohda, N. Nakayama, F. Hatanaka, and K. Komatsu, "Comparison of anti-inflammatory activities of six *Curcuma rhizomes*: a possible curcuminoid-independent pathway mediated by *Curcuma phaeocaulis* extract," *Evidence-Based Complementary and Alternative Medicine*, vol. 3, no. 2, pp. 255–260, 2006.

[7] K. Goksel, K. Murat, Y. Murat, E. Sevil, and H. Fidan, "Antioxidant activities of ethanol extracts of *Hypericum triquetrifolium* and *Hypericum scabroides*," *Pharmaceutical Biology*, vol. 46, no. 4, pp. 231–242, 2008.

[8] R. Gebhardt and M. Fausel, "Antioxidant and hepatoprotective effects of artichoke extracts and constituents in cultured rat hepatocytes," *Toxicology in Vitro*, vol. 11, no. 5, pp. 669–672, 1997.

[9] A. Sofwora, *Medicinal Plants and Traditional Medicine in Africa*, John Wiley & Sons, Ann Arbor, Mich, USA, 1982.

[10] D. E. Okwu, "Phytochemicals, vitamins and mineral contents of two Nigerian medicinal plants," *International Journal of Molecular Medicine and Advances Sciences*, vol. 1, pp. 375–381, 2005.

[11] N. Tsevegsuren, G. Davaakhuu, and T. S. Udval, "Phytochemical analysis of *Cynara scolymus* L. cultivated in Mongolia," *Mongolian Journal of Chemistry*, vol. 15, no. 41, pp. 40–42, 2014.

[12] AACC, *Approved Methods of the AACC*, American Association of Cereal Chemists, St. Paul, Minn, USA, 8th edition, 1984.

[13] S. C. Lee, L. Prosky, and J. W. DeVries, "Determination of total, soluble, and insoluble, dietary fiber in foods—enzymatic-gravimetric method, MES-TRIS buffer: collaborative study," *Journal of the Association of Official Analytical Chemists*, vol. 75, pp. 395–416, 1992.

[14] M. Dubois, K. A. Gilles, J. K. Hamilton, P. A. Rebers, and F. Smith, "Colorimetric method for determination of sugars and related substances," *Analytical Chemistry*, vol. 28, no. 3, pp. 350–356, 1956.

[15] O. A. Fawole, U. L. Opara, and K. I. Theron, "Chemical and phytochemical properties and antioxidant activities of three pomegranate cultivars grown in South Africa," *Food and Bioprocess Technology*, vol. 5, no. 7, pp. 2934–2940, 2012.

[16] V. Dewanto, X. Wu, K. K. Adom, and R. H. Liu, "Thermal processing enhances the nutritional value of tomatoes by increasing total antioxidant activity," *Journal of Agricultural and Food Chemistry*, vol. 50, no. 10, pp. 3010–3014, 2002.

[17] B. Sun, J. M. Ricardo-da-Silva, and I. Spranger, "Critical factors of vanillin assay for catechins and proanthocyanidins," *Journal*

of Agricultural and Food Chemistry, vol. 46, no. 10, pp. 4267–4274, 1998.

[18] AOAC, *Official Methods of Analysis*, vol. 1, AOAC, Washington, DC, USA, 15th edition, 1990.

[19] D. Pljevljakušić, K. Šavikin, T. Janković et al., "Chemical properties of the cultivated *Sideritis raeseri Boiss.* & *Heldr. subsp. raeseri*," *Food Chemistry*, vol. 124, no. 1, pp. 226–233, 2011.

[20] M. M. Özcan, A. Ünver, T. Uçar, and D. Arslan, "Mineral content of some herbs and herbal teas by infusion and decoction," *Food Chemistry*, vol. 106, no. 3, pp. 1120–1127, 2008.

[21] I. I. Koleva, T. A. Van Beek, J. P. H. Linssen, A. De Groot, and L. N. Evstatieva, "Screening of plant extracts for antioxidant activity: a comparative study on three testing methods," *Phytochemical Analysis*, vol. 13, no. 1, pp. 8–17, 2002.

[22] R. Re, N. Pellegrini, A. Proteggente, A. Pannala, M. Yang, and C. Rice-Evans, "Antioxidant activity applying an improved ABTS radical cation decolorization assay," *Free Radical Biology and Medicine*, vol. 26, no. 9-10, pp. 1231–1237, 1999.

[23] V. Ravi, T. S. M. Saleem, S. S. Patel, J. Raamamurthy, and K. Gauthaman, "Anti-inflammatory effect of methanolic extract of *Solanum nigrum Linn. Berries*," *International Journal of Applied Research in Natural Products*, vol. 2, pp. 33–36, 2009.

[24] D. Chattopadhyay, G. Arunachalam, A. B. Mandal, T. K. Sur, S. C. Mandal, and S. K. Bhattacharya, "Antimicrobial and anti-inflammatory activity of folklore: *Mallotus peltatus* leaf extract," *Journal of Ethnopharmacology*, vol. 82, no. 2-3, pp. 229–237, 2002.

[25] L. R. Morse, K. Stolzmann, H. P. Nguyen et al., "Association between mobility mode and c-reactive protein levels in men with chronic spinal cord injury," *Archives of Physical Medicine and Rehabilitation*, vol. 89, no. 4, pp. 726–731, 2008.

[26] A. Clauss, "Gerinnungsphysiologische schnellmethode zur bestimmung des fibrinogens," *Acta Haematologica*, vol. 17, no. 4, pp. 237–246, 1957.

[27] H. H. Draper and M. Hadley, "Malondialdehyde determination as index of lipid peroxidation," *Methods in Enzymology*, vol. 186, pp. 421–431, 1990.

[28] R. Kayali, U. Çakatay, T. Akçay, and T. Altug, "Effect of alpha-lipoic acid supplementation on markers of protein oxidation in post-mitotic tissues of ageing rat," *Cell Biochemistry and Function*, vol. 24, no. 1, pp. 79–85, 2006.

[29] H. Aebi, "Catalase in vitro," *Methods in Enzymology*, vol. 105, pp. 121–126, 1984.

[30] W. F. Beyer Jr. and I. Fridovich, "Assaying for superoxide dismutase activity: some large consequences of minor changes in conditions," *Analytical Biochemistry*, vol. 161, no. 2, pp. 559–566, 1987.

[31] I. Carlberg and B. Mannervik, "Glutathione reductase," in *Glutamate, Glutamine, Glutathione, and Related Compounds*, vol. 113 of *Methods in Enzymology*, pp. 484–490, Elsevier, 1985.

[32] O. H. Lowry, N. J. Rosebrough, A. L. Farr, and R. J. Randall, "Protein measurement with the Folin phenol reagent," *The Journal of Biological Chemistry*, vol. 193, no. 1, pp. 265–275, 1951.

[33] V. Emanue, V. Adrian, N. A. Sultana, and C. Svetlana, "Antioxidant and antimicrobial activities of ethanol extracts of *Cynara scolymus* (*Cynarae folium*, Asteraceae family)," *Tropical Journal of Pharmaceutical Research*, vol. 10, no. 6, pp. 777–783, 2011.

[34] G. L. D. S. Oliveira, R. A. M. O. Francisco, O. B. A. Vinícius et al., "Evaluation of antioxidant capacity of the aqueous extract of *Cynara scolymus* L. (Asteraceae) *in vitro* and in Saccharomyces cerevisiae," *African Journal of Pharmacy and Pharmacology*, vol. 8, pp. 136–147, 2014.

[35] K. Horiuchi, S. Shiota, T. Hatano, T. Yoshida, T. Kuroda, and T. Tsuchiya, "Antimicrobial activity of oleanolic acid from Salvia officinalis and related compounds on vancomycin-resistant enterococci (VRE)," *Biological and Pharmaceutical Bulletin*, vol. 30, no. 6, pp. 1147–1149, 2007.

[36] A. Daoud, D. Malika, S. Bakari et al., "Assessment of polyphenol composition, antioxidant and antimicrobial properties of various extracts of Date Palm Pollen (DPP) from two Tunisian cultivars," *Arabian Journal of Chemistry*, 2015.

[37] D. Krishnaiah, B. Awang, S. Rosalam, and S. M. Anisuzzaman, "Antioxidant activity and total phenolic content of an isolated *Morinda citrifolia* L. methanolic extract from Polyethersulphone (PES) membrane separator," *Journal of King Saud University—Engineering Sciences*, vol. 1, pp. 63–66, 2015.

[38] F. Sharififar, G. Dehghn-Nudeh, and M. Mirtajaldini, "Major flavonoids with antioxidant activity from Teucrium polium L.," *Food Chemistry*, vol. 112, no. 4, pp. 885–888, 2009.

[39] A. Betancor-Fernández, A. Pérez-Gálvez, H. Sies, and W. Stahl, "Screening pharmaceutical preparations containing extracts of turmeric rhizome, artichoke leaf, devil's claw root and garlic or salmon oil for antioxidant capacity," *Journal of Pharmacy and Pharmacology*, vol. 55, no. 7, pp. 981–986, 2003.

[40] J. Kukić, V. Popović, S. Petrović et al., "Antioxidant and antimicrobial activity of *Cynara cardunculus* extracts," *Food Chemistry*, vol. 107, no. 2, pp. 861–868, 2008.

[41] S. Konyalıoğlu, H. Sağlam, and B. Kırvçak, "α-Tocopherol, flavonoid, and phenol contents and antioxidant activity of *Ficus carica*. leaves," *Pharmaceutical Biology*, vol. 43, no. 8, pp. 683–686, 2005.

[42] D. U. Bawankule, P. Trivedi, A. Pal et al., "Protective mechanism of lignans from Phyllanthus amarus against galactosamine/lipopolysaccharide-induced hepatitis: an in-vivo and in-silico studies," *Current Topics in Medicinal Chemistry*, vol. 14, no. 8, pp. 1045–1055, 2014.

[43] G. A. Higgs, R. J. Flower, and J. R. Vane, "A new approach to anti-inflammatory drugs," *Biochemical Pharmacology*, vol. 28, no. 12, pp. 1959–1961, 1979.

[44] A. A. Hemmati, H. Kalantari, A. Siahpoosh, B. Ghorbanzadeh, and H. Jamali, "Anti-inflammatory Effect of Hydroalcoholic Extract of the *Washingtonia filifera* Seeds in Carrageenan-Induced Paw Edema in Rats," *Jundishapur Journal of Natural Pharmaceutical Products*, vol. 10, no. 1, pp. 19–25, 2015.

[45] I. Posadas, M. Bucci, F. Roviezzo et al., "Carrageenan-induced mouse paw oedema is biphasic, age-weight dependent and displays differential nitric oxide cyclooxygenase-2 expression," *British Journal of Pharmacology*, vol. 142, no. 2, pp. 331–338, 2004.

[46] K. Pundarikakshudu, D. H. Shah, A. H. Panchal, and G. C. Bhavsar, "Anti-inflammatory activity of fenugreek (*Trigonella foenum-graecum Linn*) seed petroleum ether extract," *Indian Journal of Pharmacology*, vol. 48, no. 4, pp. 441–444, 2016.

[47] S. Cuzzocrea, G. Costantino, E. Mazzon, B. Zingarelli, A. De Sarro, and A. P. Caputi, "Protective effects of Mn(III)tetrakis (4-benzoic acid) porphyrin (MnTBAP), a superoxide dismutase mimetic, in paw oedema induced by carrageenan in the rat," *Biochemical Pharmacology*, vol. 58, no. 1, pp. 171–176, 1999.

[48] M. A. Mendall, P. Patel, M. Asante et al., "Relation of serum cytokine concentrations to cardiovascular risk factors and coronary heart disease," *Heart*, vol. 78, no. 3, pp. 273–277, 1997.

[49] A. Ialenti, A. Ianaro, S. Moncada, and M. Di Rosa, "Modulation of acute inflammation by endogenous nitric oxide," *European Journal of Pharmacology*, vol. 211, no. 2, pp. 177–182, 1992.

[50] D. Salvemini, Z.-Q. Wang, D. M. Bourdon, M. K. Stern, M. G. Currie, and P. T. Manning, "Evidence of peroxynitrite involvement in the carrageenan-induced rat paw edema," *European Journal of Pharmacology*, vol. 303, no. 3, pp. 217–220, 1996.

[51] E. E. S. Schapoval, M. R. Winter De Vargas, C. G. Chaves, R. Bridi, J. A. Zuanazzi, and A. T. Henriques, "Antiinflammatory and antinociceptive activities of extracts and isolated compounds from *Stachytarpheta cayennensis*," *Journal of Ethnopharmacology*, vol. 60, no. 1, pp. 53–59, 1998.

[52] E. Aleo, R. Ricci, S. Passi, and S. A. Cataudella, "Novel cyt-H2O2-chemiluminescenes assay for measuring the reducing/antioxidant capacity on hydrophilic and lipophilic antiooxindants and biological samples," *Progress in Nutrition*, vol. 3, pp. 154–182, 2005.

[53] E. Mazzon, E. Esposito, R. Di Paola et al., "Effects of verbascoside biotechnologically produced by *Syringa vulgaris* plant cell cultures in a rodent model of colitis," *Naunyn-Schmiedeberg's Archives of Pharmacology*, vol. 380, no. 1, pp. 79–94, 2009.

[54] E. J. Middleton, "Effect of plant flavonoids on immune and inflammatory cell function," *Advances in Experimental Medicine and Biology*, vol. 439, pp. 175–182, 1998.

[55] J. Baumann, F. Von Bruchhausen, and G. Wurm, "Flavonoids and related compounds as inhibitors of arachidonic acid peroxidation," *Prostaglandins*, vol. 20, no. 4, pp. 627–639, 1980.

[56] M. D. Dos Santos, M. C. Almeida, N. P. Lopes, and G. E. P. De Souza, "Evaluation of the anti-inflammatory, analgesic and antipyretic activities of the natural polyphenol chlorogenic acid," *Biological and Pharmaceutical Bulletin*, vol. 29, no. 11, pp. 2236–2240, 2006.

Hindawi
Evidence-Based Complementary and Alternative Medicine
Volume 2017, Article ID 2694261, 10 pages
https://doi.org/10.1155/2017/2694261

Research Article

Icariin Prevents H_2O_2-Induced Apoptosis via the PI3K/Akt Pathway in Rat Nucleus Pulposus Intervertebral Disc Cells

Xiangyu Deng,[1] Sheng Chen,[2] Dong Zheng,[1] Zengwu Shao,[1] Hang Liang,[1] and Hongzhi Hu[1]

[1]*Department of Orthopaedic Surgery, Union Hospital, Tongji Medical College, Huazhong University of Science and Technology, Wuhan 430022, China*
[2]*Tongji Medical College, Huazhong University of Science and Technology, Wuhan 430022, China*

Correspondence should be addressed to Dong Zheng; xhzhengdong@163.com

Received 29 December 2016; Revised 20 March 2017; Accepted 27 March 2017; Published 27 April 2017

Academic Editor: Nilufar Mamadalieva

Icariin is a prenylated flavonol glycoside derived from the Chinese herb *Epimedium sagittatum*. This study investigated the mechanism by which icariin prevents H_2O_2-induced apoptosis in rat nucleus pulposus (NP) cells. NP cells were isolated from the rat intervertebral disc and they were divided into five groups after 3 passages: (A) blank control; (B) 200 μM H_2O_2; (C) 200 μM H_2O_2 + 20 μM icariin; (D) 20 μM icariin + 200 μM H_2O_2 + 25 μM LY294002; (E) 200 μM H_2O_2 + 25 μM LY294002. LY294002 is a selective inhibitor of the phosphoinositide 3-kinase (PI3K)/Akt signaling pathway. NP cell viability, apoptosis rate, intracellular reactive oxygen species levels, and the expression of AKT, p-AKT, p53, Bcl-2, Bax, caspase-3 were estimated. The results show that, compared with the control group, H_2O_2 significantly increased NP cell apoptosis and the level of intracellular ROS. Icariin pretreatment significantly decreased H_2O_2-induced apoptosis and intracellular ROS and upregulated p-Akt and BCL-2 and downregulated caspase-3 and Bax. LY294002 abolished the protective effects of icariin. Our results show that icariin can attenuate H2O2-induced apoptosis in rat nucleus pulposus cells and PI3K/AKT pathway is at least partly included in this protection effect.

1. Introduction

Low back pain (LBP) is a frequent musculoskeletal disorder worldwide that affects approximately 70% of the adult population sometime in their lives, and most result in musculoskeletal disability. LBP can cause an enormous economic burden every year. The societal cost (converted into 2008 prices) of back pain is estimated at £12.3 billion in the United Kingdom (£1.6 billion for direct healthcare resources, £1.6 billion related to informal care, and indirect costs of £9.1 billion through loss of productivity due to morbidity) and €16.5–50 billion in Germany [1–7]. Therefore, LBP is a major disease that severely impacts human health and results in an enormous strain on limited medical resources [6].

Intervertebral disc (IVD) degeneration is considered to be one of the main reasons for LBP [8]. Nucleus pulposus (NP) cells are of critical importance in maintaining the biomechanical properties of IVDs. A decreased number of NP cells and changes in the extracellular matrix composition are early pathologic signs of IVD degeneration. Moreover, reversal of IVD degeneration is almost impossible due to the poor self-repairing ability of NP tissues.

Icariin is one the most frequently prescribed medicinal herbs in traditional Chinese medicine. Qianggu Capsule, which contains icariin, is used to treat postmenopausal and posttraumatic osteoporosis. An increasing number of articles have reported that icariin possesses multiple biological activities, such as improvement of drug resistance to chemotherapy [9], tumor-suppression, and antioxidation. Additionally, we find that icariin has an initiative pathophysiological effect on the reversal of IVD degeneration. We speculate that this results from a protective effect of the icariin on NP cells. Icariin can prevent apoptosis and oxidative stress in several cell models. Because the selective phosphoinositide 3-kinase (PI3K) inhibitor, LY294002, can reverse this effect; the protection seen with icariin appears to occur through activation of the PI3K/Akt signaling pathway [10], implying that icariin activates this pathway.

In the current study, H_2O_2 was used to induce apoptosis of NP cell with or without pretreatment with icariin. Our findings suggest that H_2O_2 induces apoptosis in NP cells and icariin prevents it through the PI3K/AKT signaling pathway. Our results provide an initiative method for the treatment of IVD degeneration disease.

2. Materials and Methods

2.1. General Supplies. Instruments, reagents, and experimental animals were provided by the animal center of Tongji Medical College and Huazhong University of Science and Technology. H_2O_2 was purchased from Thermo Fisher Scientific (Waltham, MA, USA). Icariin (purity ≥ 98%) was purchased from Nanjing Zelang Pharmaceutical Technology (Nanjing, China). Fetal bovine serum was purchased from Thermo Fisher. F12-Dulbecco's modified Eagle medium was purchased from HyClone (Logan, UT, USA). Cell counting kit-8 (CCK8) was purchased from Kaiji Bioengineering Institute (Jiangsu, China). LY294002 was purchased from Sigma-Aldrich (St. Louis, MO, USA). The reactive oxygen species (ROS) detection kit was purchased from Nanjing Jiancheng Bioengineering Institute (Nanjing, China). The Annexin V-FITC/propidium iodide detection kit was purchased from Nanjing KeyGen Biotech (Nanjing, China). β-Actin, Bcl-2, bax, caspase-3, phospho(p)-Akt, rabbit monoclonal antibodies, and the p53, Akt mouse monoclonal antibody, were purchased from Abcam (Cambridge, UK). Goat anti-rabbit and goat anti-mouse IgG were purchased from Proteintech (Wuhan, China). Microplate Reader was purchased from Thermo. Inverted fluorescence microscope was from Olympus, Japan.

2.2. Culture and Synchronization of the NP Cells and the Detection of Cell Density and Morphology. The density and morphology of NP cells under different treatments were observed and photographed with an inverted phase-contrast microscope. NP cells were isolated using about 200 g NP tissue of rats. Briefly, NP tissue was aseptically removed in a Petri dish containing 0.25% (w/v) type II collagenase and cut into pieces 0.1 mm × 0.1 mm. Then samples were digested with 0.25% (w/v) type II collagenase for 15–20 min and serum was used to stop the reaction. After centrifugation at 1200 rpm for 7 min, the supernatant was discarded and the pellet was resuspended in F12-Dulbecco's modified Eagle medium supplemented with 20% fetal bovine serum, 100 U/mL penicillin, and 100 mg/L streptomycin. Cell cultures were maintained at 37°C and 5% CO_2. Medium was changed 3–5 days later when the cells had been attached and then changed every other day. When NP cells reached approximately 80% confluence, each primary culture was subcultured at a 1 : 3 ratio with a 0.25% (w/v) trypsin solution.

2.3. Experimental Protocols. First cells were tested for the ability of icariin to activate the PI3K/AKT pathway. Kinetics of the phosphorylation of AKT were estimated by Western blot analysis at 0 h, 1 h, 2 h, 3 h, 4 h, and 5 h. Other cells were randomly separated into five groups with at least three replicates: (A) blank control; (B) 200 μM H_2O_2; (C) 20 μM icariin + 200 μM H_2O_2; (D) 20 μM icariin + 25 μM LY294002 + 200 μM H_2O_2; (E) 25 μM LY294002 + 200 μM H_2O_2. Treatment with LY294002, icariin, and H_2O_2 was performed for 2 h, 24 h, and 6 h, respectively.

2.4. Detection of Icariin Cytotoxicity and Cell Viability and Proliferation. NP cells at passage 3 were replated in 96-well plates at a density 1×10^5 cells per well, and the culture medium was plated after synchronization. Cells were then treated with icariin for 24 h at various concentrations (0.1, 0.5, 1, 5, 10, 20, 40, and 50 μM). Cell viability was detected according to the instructions of the CCK8 assay. Then cells were treated according to the aforementioned experimental groupings. Cell viability was detected according to the manufacturer's instructions.

2.5. Apoptosis Assay. Cells were harvested and washed with PBS twice at 4°C. Next, cells were resuspended in 200 μL of binding buffer and incubated with 10 μL of Annexin V-FITC solution (15 min, room temperature) in the dark. Then cells were incubated with 10 μL PI and 300 μL Binding Buffer and immediately analyzed in a BD FACSCalibur cytometer to separate living cells, apoptotic cells, and necrotic cells in different periods.

2.6. Detection of Intracellular ROS Levels by Flow Cytometry. Cells were treated differently according to the aforementioned experiment grouping design. Then 200 μL of culture medium from each group was gathered to detect intracellular ROS levels. Experimental steps were strictly executed according to the manufacturer's instructions.

2.7. Expression of Akt, p-Akt, p53, Bcl-2, Bax, and Caspase-3 by Western Blot Analysis. Proteins were extracted according to the instructions of the Total Extraction Sample Kit. Equal amounts of proteins (10 μg) were loaded onto 10% sodium dodecyl sulfate polyacrylamide gels, electrophoresed, and then transferred to polyvinylidene fluoride membranes. The membranes were incubated with 5% nonfat milk for 2 h followed by incubation with primary antibodies overnight at 4°C (0.5 μg/mL Akt, p53, p-Akt, Bcl-2, and caspase-3; 1 : 5000). After washing in TBST, membranes were incubated with the secondary antibody for 1.5 h at room temperature (rabbit anti-mouse or goat anti-rabbit, 1 : 5000). Bands were visualized by incubating with enhanced chemiluminescence reagent for 2 min after membranes were washed with TBST. Densitometry of p-Akt, Akt, p53, Bcl-2, and bax as well as caspase-3 levels was performed using ImageJ software (National Institutes of Health, Bethesda, MD, USA).

2.8. Statistical Analysis. Data are presented as means ± standard deviation. For group-wise comparisons, a one-way ANOVA with the LSD or Dunnett's *T*3 test was performed using SPSS 19.0 (IBM, Chicago, IL, USA). Values were considered significantly different for $p < 0.05$.

3. Results

3.1. H_2O_2 Induced Apoptosis in NP Cells. H_2O_2 can lead to cell dead and icariin alone has no cytotoxicity in NP cells;

what is more, icariin can protect against the H_2O_2-induced cytotoxicity. Our date revealed the best concentration of H_2O_2 which can lead to a favourable cell apoptosis is 200 μM (Figure 1(a)). The viability and proliferation of cells treated with icariin for 24 h at various concentrations (0.1, 0.5, 1, 5, 10, 20, 40, and 50 μM) were not significantly different ($p > 0.05$) compared to the control group (Figure 1(b)). In addition, icariin provided significant protection when NP cells were exposed to 200 μM H_2O_2 (Figure 1(c)). The results of the above are detected by CCK8.

3.2. The Apoptosis Rate of Different Tests. The protective effect was weakened by a 1 h pretreatment with 20 μM of the PI3K/Akt pathway inhibitor, LY294002 (Figure 2). As shown in Figure 2, cells treated with H_2O_2 had a smaller size than control cells and a high percentage of dead cells in the population. This observation was confirmed by fluorescence microscopy and flow cytometry after Annexin V/PI staining of the cells (Figure 2(a)). Morphologic changes and apoptosis were also evident by fluorescence microscopy and flow cytometry with Annexin V/propidium iodide staining (Figure 2(b)). When cells were pretreated with icariin, the number of dead cells was decreased and cell morphology was similar to that of control cells. Groups (D) (200 μM H_2O_2 + 20 μM Ica) and (E) (200 μM H_2O_2 + 20 μM Ica + 25 μM LY294002) reveal that the cells became shrunk and there were many dead cells. This revealed that the protection by icariin was prevented by inhibiting the PI3K/Akt pathway ($p < 0.05$).

3.3. The Intracellular ROS Rate of Different Tests. With the different interventions of the (A)–(E) groups, ROS levels in NP cells varied in parallel with the extent of apoptosis (Figure 3). Similar results were observed by both fluorescence microscopy and flow cytometry. Compared to the control group, cells treated with 200 μM H_2O_2 showed a significant increase of intracellular ROS levels ($p < 0.05$). Cells pretreated with icariin showed intracellular ROS levels significantly lower compared to group (B) ($p < 0.05$). Intracellular ROS levels of group (D) cells (200 μM H_2O_2 + 20 μM Ica +25 μM LY294002) were risen compared to group (C) ($p < 0.05$), which demonstrates that the PI3K/AKT pathway participates in the process. Group (E) cells (25 μM LY294002 + 200 μM H_2O_2) showed the highest ROS levels among all groups ($p < 0.05$), which indicates that blocking the PI3K/Akt pathway itself can be deleterious for the cells.

3.4. The Activation of PI3K/AKT Pathway. We observed a time-dependent activation of the PI3K/AKT pathway when NP cells were treated with icariin ($p < 0.05$) (Figure 4). Also, with different interventions, p-AKT and p53, the iconic molecules of PI3K/AKT, showed the inverse variation trendy with apoptosis rate, indicating that the activation of PI3K/AKT is a protection factor in the H_2O_2-induced apoptosis (Figure 4(b)).

3.5. The Expression of Proteins in Apoptosis Pathway. The expression of caspase-3, Bax, and Bcl-2 proteins is shown in Figure 5. The antiapoptosis protein bcl-2 decreased when tested with H_2O_2 and increased when pretreated with icariin and decreased when the PI3K/AKT pathway was blocked ($p < 0.05$). In contrast, proapoptotic proteins caspase-3 and Bax were decreased in icariin-treated cells. Together, these results showed that icariin had a significant protective effect when NP cells were exposed to H_2O_2 and this protection could be impaired by LY294002.

4. Discussion

Intervertebral disc degeneration is the most important reason for LBP. There are extensive reports about the pathogenesis of spinal degeneration and the primary therapies currently in use. These include Western medicine, surgical operations, and IVD tissue engineering [11–13]. However, there are few reports on the effect of traditional Chinese medicines, such as icariin, on NP and annulus fibrosus cells, although, as an old Chinese traditional medicine, icariin has been reported to benefit osteogenesis in vivo [14], accelerate the differentiation of osteoblast and mesenchymal stem cells [15], and protect neurocytes [16]. Additional effects are described in numerous review articles [9, 15, 17–24].

The current study is the first report of the effect and the possible mechanism of icariin in NP cells exposed to H_2O_2. We believe the mechanism of the protective effect of icariin may involve activation of the PI3K/Akt pathway. Icariin attenuates cigarette smoke-mediated oxidative stress in human lung epithelial cells [17], inhibits neurotoxicity in PC12 cells [16], and activates rat bone marrow cells [15]. These results suggest an activation effect of icariin on the PI3K/Akt pathway.

The IVD has no blood vessels to provide nutrition. Thus, degeneration will ensue if it is exposed to acid or oxidative stress. There are reports that oxidative stress caused by H_2O_2 can lead to apoptosis of NP cells [25–33]. In this work, we chose H_2O_2 to simulate the physiopathological environment with oxidative stress in vitro, because, actually, the NP cells have to face the oxidative stress in vivo. We chose the concentration of 200 μM because this is the lowest concentration that can induce apoptosis of NP cells. We found that, even at 600 μM of H_2O_2, NP cells presented the state of necrosis and that, as the concentration of H_2O_2 increased from 200 μM to 600 μM, the NP cells showed similar apoptosis state. Related results had also been measured by the methods of CCK8.

Then we found that icariin provides substantial concentration-dependent protection to NP cells exposed to H_2O_2 by means of the CCK8 assay. The greatest protection was seen at 40 μM when these cells were exposed to 200 μM H_2O_2. Protection could also be observed by light microscopy. Importantly, icariin alone elicited no cytotoxic effect on NP cells at concentrations up to 50 μM.

We used Western blotting to explore the pathways activated in NP cells treated with icariin. We observed an increase in p-Akt, which is the active form in the PI3K/Akt signaling pathway. Because icariin activated the PI3K/AKT pathway in NP cells, we conducted a series of experiments including measurements of ROS levels, apoptosis, apoptosis-related molecules (caspase-3, Bcl-2, and Bax), and the proteins included in PI3K/AKT pathway such as p-AKT and p53.

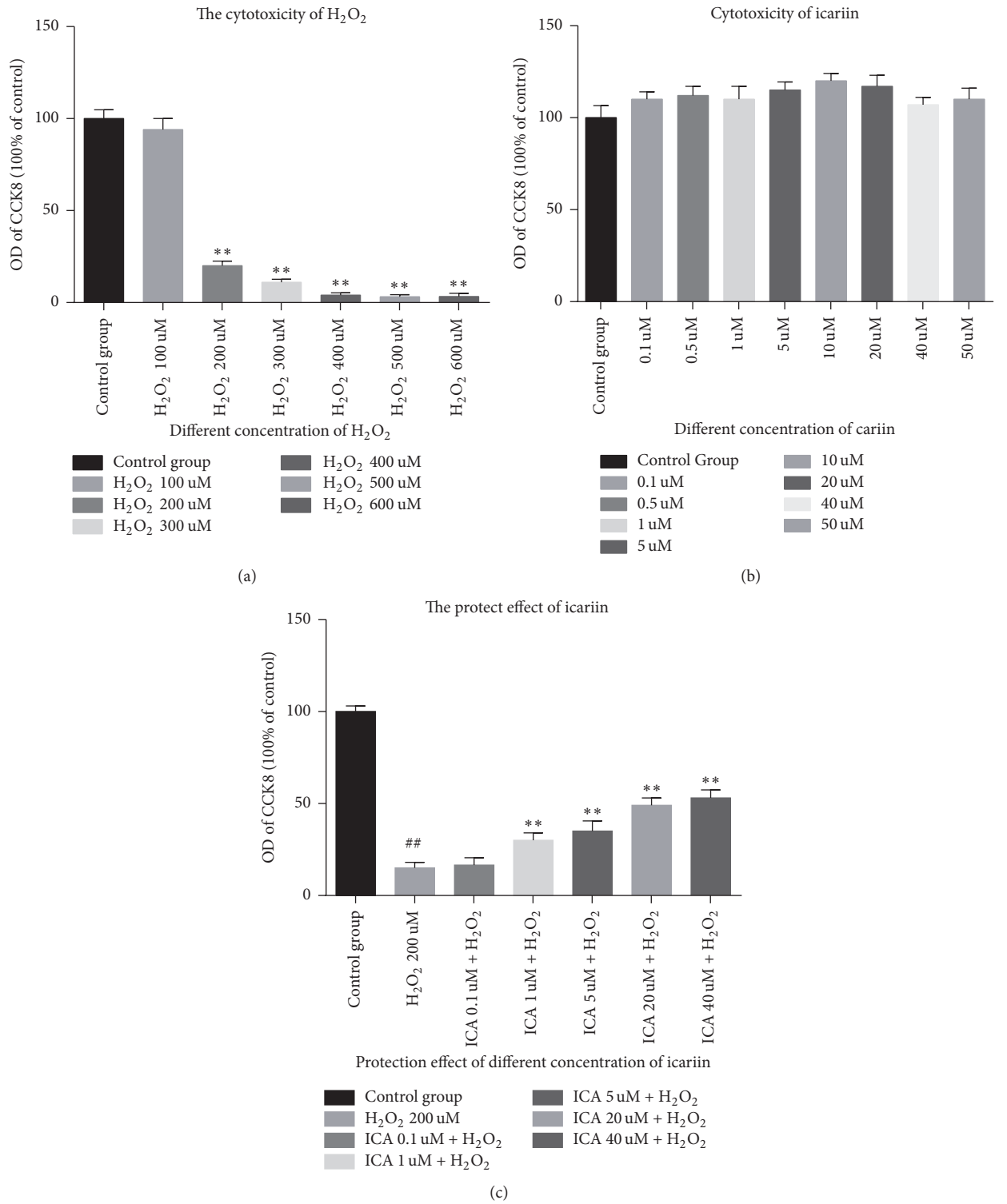

Figure 1: Icariin have no cytotoxicity in NP cells and had a significant protective effect on NP cells exposed to H_2O_2 at the concentration of 200 uM and this protective effect was attenuated by the PI3K/AKT pathway inhibitor LY294002. (a) H_2O_2 led to obvious cell death at the concentration of 200 uM to 600 uM. Results are presented as mean ± SD ($^{**}p < 0.01$ versus control group). (b) Icariin alone has no effect on the viability and proliferation of NP cells at concentrations up to 50 μM. (c) Icariin protects NP cells against H_2O_2-induced toxicity ($^{\#\#}p < 0.01$ versus control group, $^{**}p < 0.01$ versus H_2O_2 group).

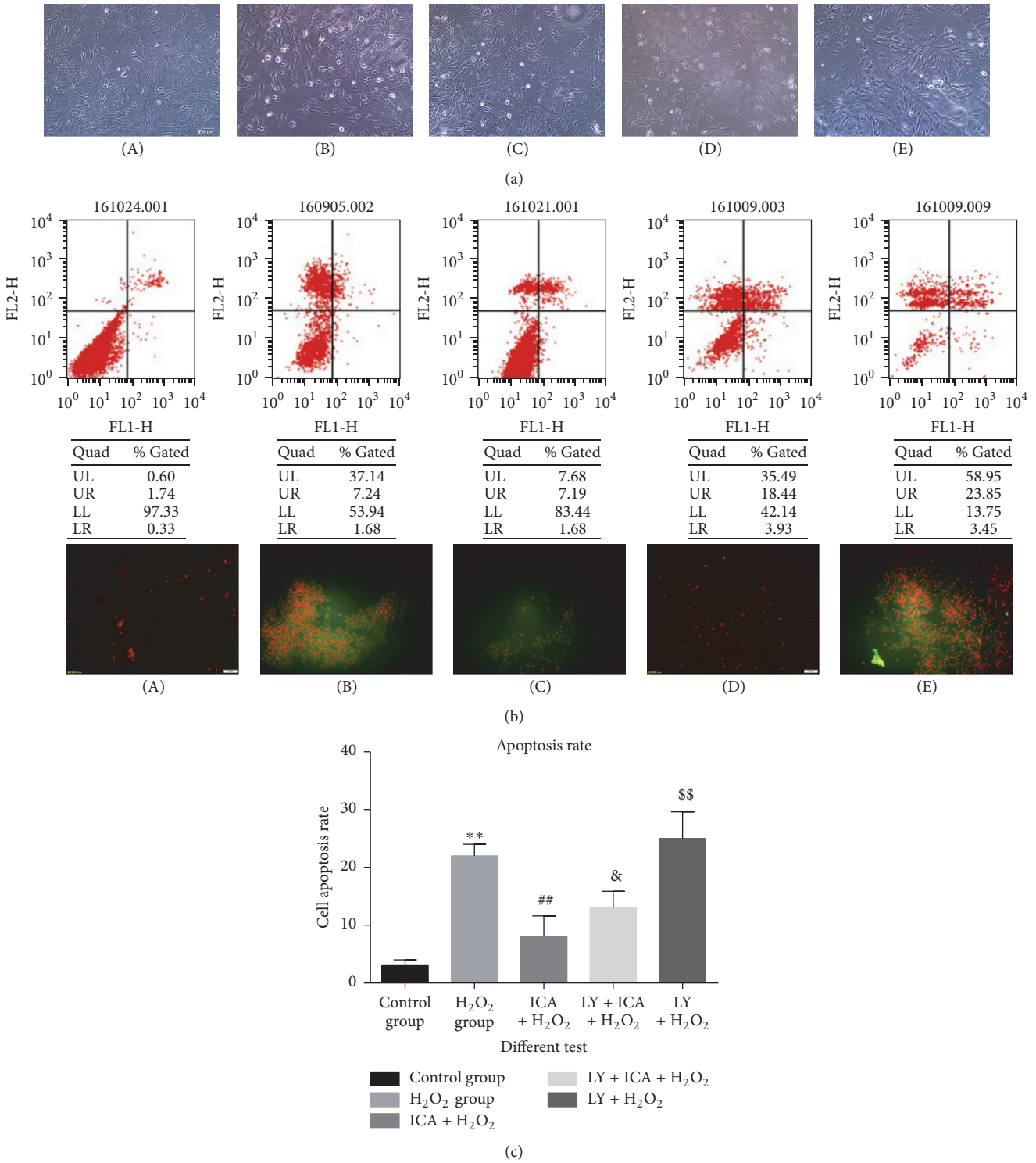

FIGURE 2: The sectionalization: (A) blank control. (B) 200 μM H_2O_2. (C) 200 μM H_2O_2 + 20 μM icariin (Ica). (D) 200 μM H_2O_2 + 20 μM Ica. (E) 200 μM H_2O_2 + 20 μM Ica + 25 μM LY294002. (a) Phase-contrast light microscopy observations: the cell number of group (B) is decreased, cells are more shrunk, and there were many round dead cells. In group (C), there were fewer dead cells and the cell morphology was more normal than in group (B). However, in group (D), cells shrank and there were many dead cells. (b) Apoptosis detected by flow cytometry and fluorescence microscope: the extent of apoptosis significantly declined in group (C) compared with group (B). In group (D), the extent of apoptosis increased compared with group (C). Group (E) exhibited the most apoptotic cells of all groups. (c) Apoptosis rate: the apoptosis rate of H_2O_2 group increased significantly and the cytotoxicity of H_2O_2 is weakened by icariin ($^{**}p < 0.01$ versus control group; $^{\#\#}p < 0.01$ versus H_2O_2 group). In addition, the lock of PI3/AKT pathway made a dent in the protection effect of icariin ($^{\&}p < 0.05$ versus group (C)). Group (E) (25 μM LY294002 + 200 μM H_2O_2): this group exhibited more apoptotic cells ($^{\$\$}p < 0.01$ versus group (D)).

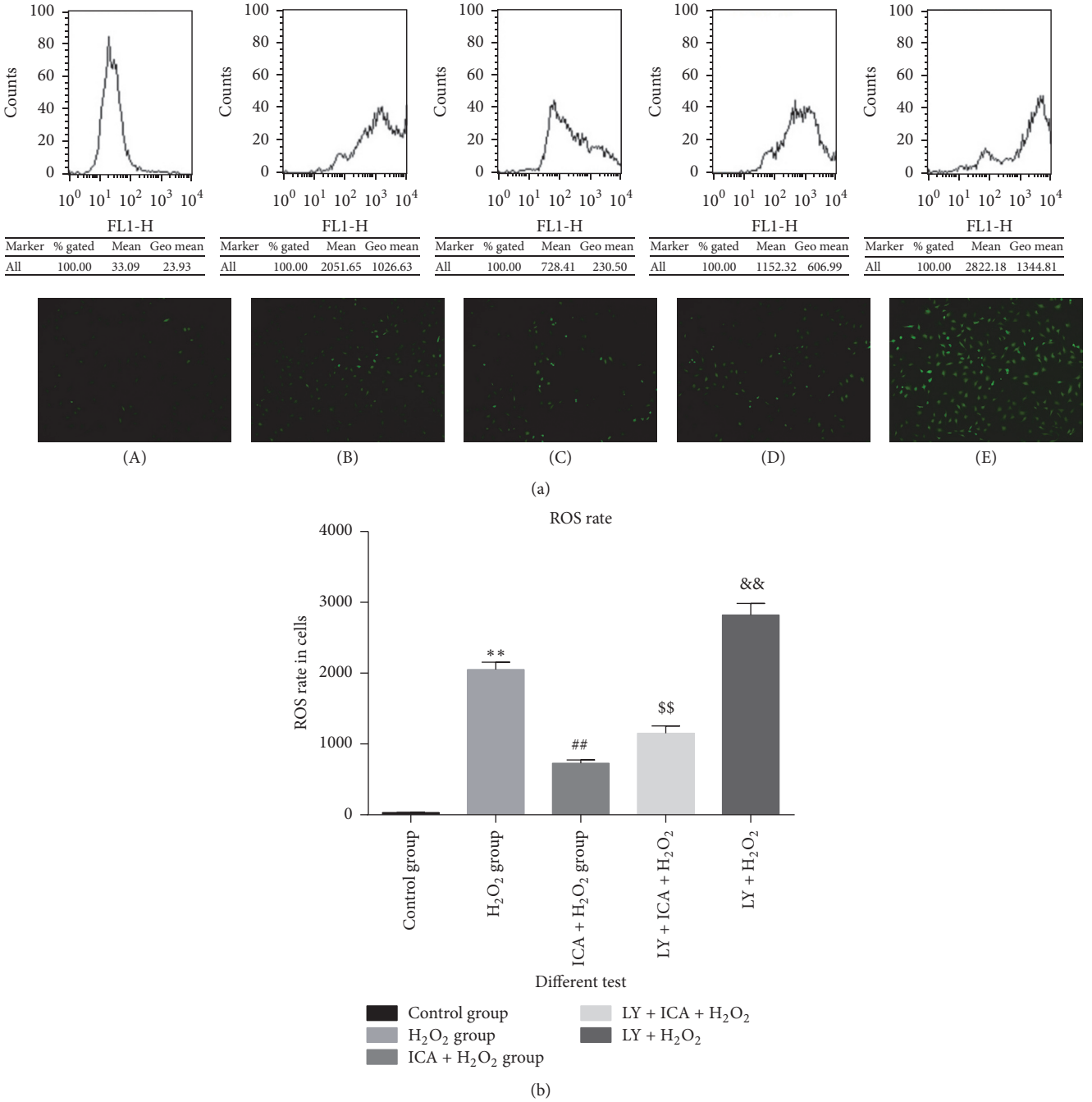

Figure 3: The sectionalization: (A) blank control. (B) 200 μM H_2O_2. (C) 200 μM H_2O_2 + 20 μM icariin (Ica). (D) 200 μM H_2O_2 + 20 μM Ica. (E) 200 μM H_2O_2 + 20 μM Ica + 25 μM LY294002. (a) Flow cytometry detection and fluorescence microscope observations: the intracellular ROS dye of group (B) rises. In group (C), there were fewer intracellular ROS than in group (B). However, in groups (D) and (E), intracellular ROS dye increased. (b) ROS rate: the ROS rate of H_2O_2 group increased significantly and the cytotoxicity of H_2O_2 is weakened by icariin ($^{**}p < 0.01$ versus control group; $^{\#\#}p < 0.01$ versus H_2O_2 group). In addition, the lock of PI3/AKT pathway made a dent in the protection effect of icariin ($^{\$\$}p < 0.01$ versus group (C)). Group (E) showed the highest ROS levels among all groups, which indicates LY294002 acts synergistically to H_2O_2 in elevating intracellular ROS ($^{\&\&}p < 0.01$ versus group (B)).

Changes in each of these parameters reflected the protective effect of icariin when NP cells were exposed to 200 μM H_2O_2. Importantly, all changes were diminished in cells treated with LY294002, an inhibitor of PI3K. Although the results with a single pharmacologic agent are insufficient to conclude that the PI3K/Akt pathway is the most important or only mechanism involved in the protective effect of icariin, it is clear that this pathway is a factor. The potential role of other pathways and cytokines requires more research, such as MAPK [34, 35] and HIF-1α [36] and NF-kappaB

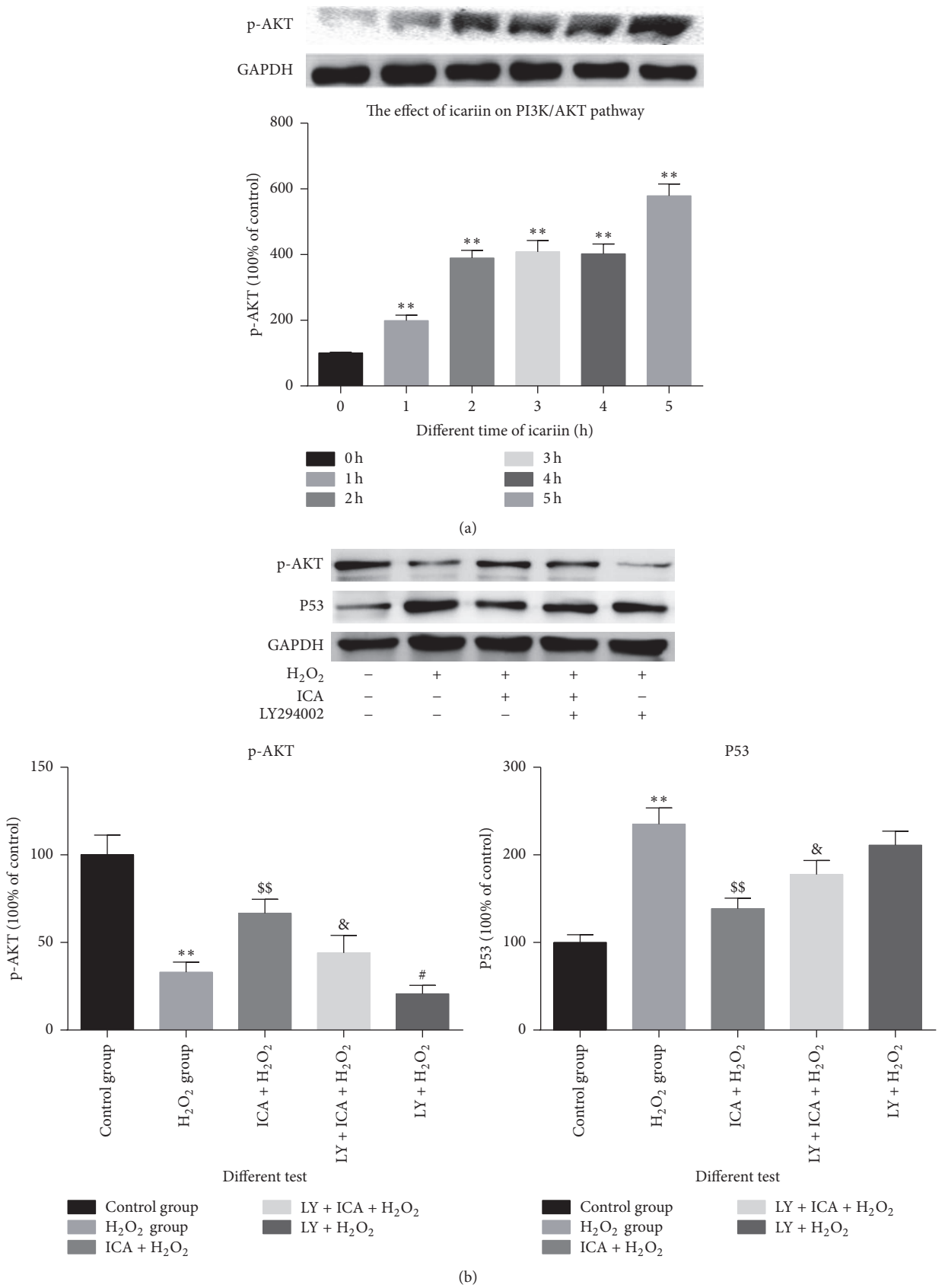

Figure 4: The effect of icariin on the PI3K/Akt pathway. (a) Prolonged culturing of NP cells with icariin increases the expression of p-Akt ($^{**}p < 0.01$ versus control group). (b) p-Akt and p53 levels in NP cells treated with different agents ($^{**}p < 0.01$ versus control group; $^{\$\$}p < 0.01$ versus H_2O_2 group; $^{\&}p < 0.05$ versus group (C); $^{\#}p < 0.05$ versus group (B)). Data are expressed as means ± SD ($n = 3$).

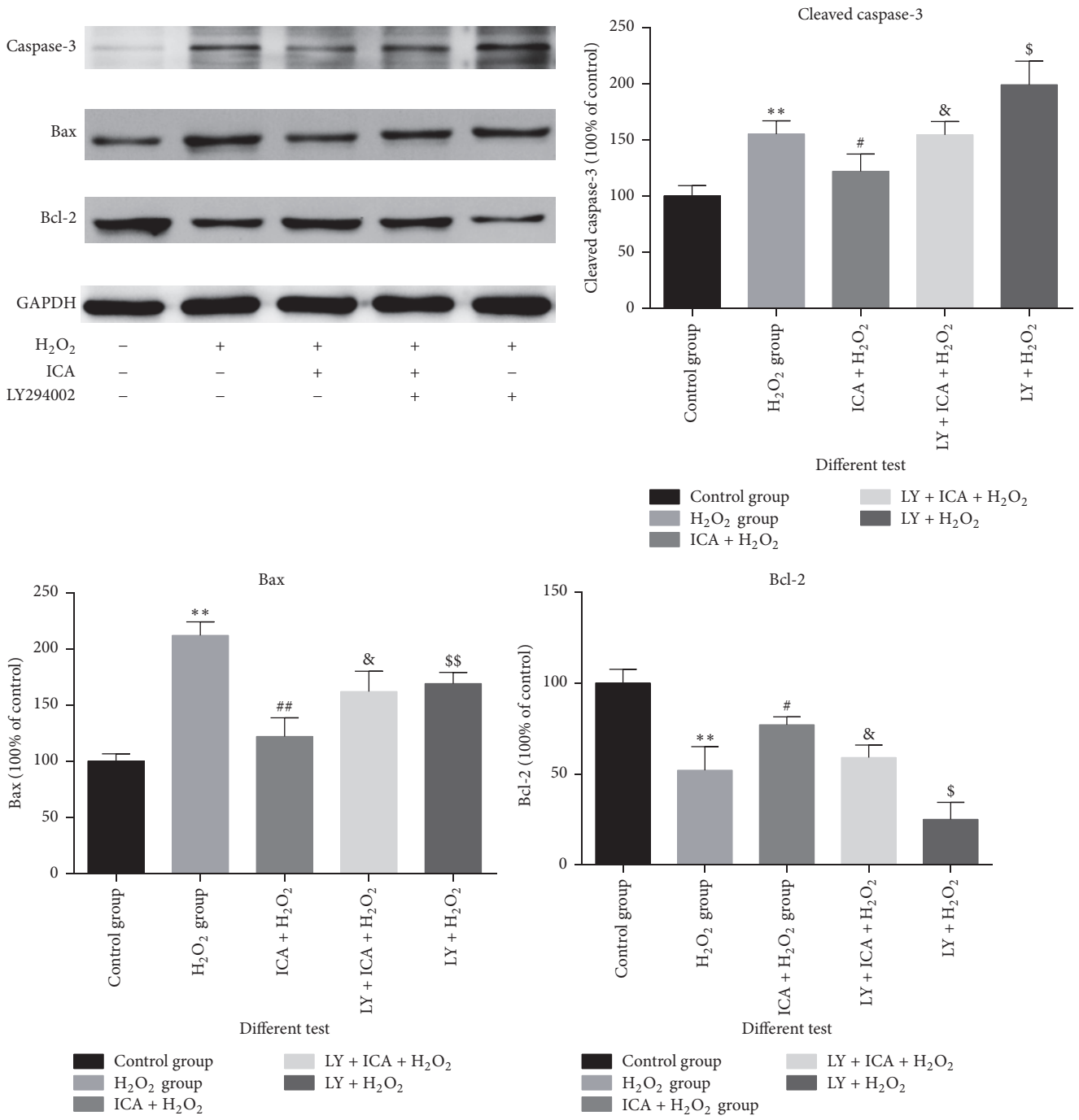

Figure 5: Icariin protects nucleus pulposus (NP) cells from H_2O_2-induced apoptosis. Bcl-2, Bax, and caspase-3 were detected by Western blotting. Bcl-2 levels are descended in NP cells treated with H_2O_2 ($^{**}p < 0.01$ versus control group) and Bcl-2 levels are increased in NP cells treated with H_2O_2 and icariin when compared with the H_2O_2 alone group ($^{\#}p < 0.05$ versus H_2O_2 group) and decreased when the PI3K/Akt pathway is blocked with LY294002 ($^{\$}p < 0.05$ versus group (C)). Caspase-3 and Bax are decreased in icariin-treated cells ($^{**}p < 0.05$ versus control group). The protective effect of icariin could be impaired by the presence of LY294002 to block the PI3K/Akt pathway ($^{\#\#}p < 0.01$ versus H_2O_2 group, $^{\&}p < 0.05$ versus group (C)). In addition, LY294002 alone exacerbates H_2O_2-induced damage ($^{\$\$}p < 0.01$, $^{\$}p < 0.05$ versus H_2O_2 group).

and AF-1 [37],which reportedly can be stimulated by icariin. Furthermore, the extracellular matrix of NP cells has not been examined and there may be some differences between the control and experimental groups.

In summary, this is the first report demonstrating the protective effect of icariin on NP cells exposed to H_2O_2. In addition, we have proposed a possible mechanism for this protection involving the PI3K/Akt pathway. These results

may suggest new approaches to prevent spinal degeneration and decrease the damage that is caused by the imbalance of oxidative stress.

Conflicts of Interest

The authors declare that there are no conflicts of interest regarding the publication of this paper.

Acknowledgments

This work was supported by the National Natural Science Foundation of China (no. 81472134).

References

[1] Y.-C. Huang, V. Y. L. Leung, W. W. Lu, and K. D. K. Luk, "The effects of microenvironment in mesenchymal stem cell-based regeneration of intervertebral disc," *Spine Journal*, vol. 13, no. 3, pp. 352–362, 2013.

[2] M. O. Karl and T. A. Reh, "Regenerative medicine for retinal diseases: activating endogenous repair mechanisms," *Trends in Molecular Medicine*, vol. 16, no. 4, pp. 193–202, 2010.

[3] S. Dagenais, J. Caro, and S. Haldeman, "A systematic review of low back pain cost of illness studies in the United States and internationally," *The Spine Journal*, vol. 8, no. 1, pp. 8–20, 2008.

[4] J. Hong, C. Reed, D. Novick, and M. Happich, "Costs associated with treatment of chronic low back pain: an analysis of the UK general practice research database," *Spine*, vol. 38, no. 1, pp. 75–82, 2013.

[5] N. Maniadakis and A. Gray, "The economic burden of back pain in the UK," *Pain*, vol. 84, no. 1, pp. 95–103, 2000.

[6] M. Juniper, T. K. Le, and D. Mladsi, "The epidemiology, economic burden, and pharmacological treatment of chronic low back pain in France, Germany, Italy, Spain and the UK: a literature-based review," *Expert Opinion on Pharmacotherapy*, vol. 10, no. 16, pp. 2581–2592, 2009.

[7] H. Breivik, E. Eisenberg, and T. O'Brien, "The individual and societal burden of chronic pain in Europe: the case for strategic prioritisation and action to improve knowledge and availability of appropriate care," *BMC Public Health*, vol. 13, no. 1, article 1229, 2013.

[8] G. Fontana, E. See, and A. Pandit, "Current trends in biologics delivery to restore intervertebral disc anabolism," *Advanced Drug Delivery Reviews*, vol. 84, pp. 146–158, 2015.

[9] Z. Wang, L. Yang, Y. Xia, C. Guo, and L. Kong, "Icariin enhances cytotoxicity of doxorubicin in human multidrug-resistant osteosarcoma cells by inhibition of ABCB1 and down-regulation of the PI3K/Akt pathway," *Biological and Pharmaceutical Bulletin*, vol. 38, pp. 277–284, 2015.

[10] R. H. Xie et al., *Mechanism of chlorogenic acid on apoptosis of rat nucleus pulposus cells induced by oxidative stress. Zhong Yao Cai*, 37, 465-469, 2014.

[11] P. Colombier, A. Camus, L. Lescaudron, J. Clouet, and J. Guicheux, "Intervertebral disc regeneration: a great challenge for tissue engineers," *Trends in Biotechnology*, vol. 32, no. 9, pp. 433–435, 2014.

[12] J. Silva-Correia, S. I. Correia, J. M. Oliveira, and R. L. Reis, "Tissue engineering strategies applied in the regeneration of the human intervertebral disk," *Biotechnology Advances*, vol. 31, no. 8, pp. 1514–1531, 2013.

[13] R. D. Bowles, H. H. Gebhard, R. Härtl, and L. J. Bonassar, "Tissue-engineered intervertebral discs produce new matrix, maintain disc height, and restore biomechanical function to the rodent spine," *Proceedings of the National Academy of Sciences of the United States of America*, vol. 108, no. 32, pp. 13106–13111, 2011.

[14] J. Wang, Y. Tao, Z. Ping et al., "Icariin attenuates titanium-particle inhibition of bone formation by activating the Wnt/β-catenin signaling pathway in vivo and in vitro," *Scientific Reports*, vol. 6, Article ID 23827, 2016.

[15] Y. K. Zhai, X. Y. Guo, B. F. Ge et al., "Icariin stimulates the osteogenic differentiation of rat bone marrow stromal cells via activating the PI3K–AKT–eNOS–NO–cGMP–PKG," *Bone*, vol. 66, pp. 189–198, 2014.

[16] K.-W. Zeng, H. Ko, H. O. Yang, and X.-M. Wang, "Icariin attenuates β-amyloid-induced neurotoxicity by inhibition of tau protein hyperphosphorylation in PC12 cells," *Neuropharmacology*, vol. 59, no. 6, pp. 542–550, 2010.

[17] J. Wu, H. Xu, P. F. Wong, S. Xia, J. Xu, and J. Dong, "Icaritin attenuates cigarette smoke-mediated oxidative stress in human lung epithelial cells via activation of PI3K-AKT and Nrf2 signaling," *Food and Chemical Toxicology*, vol. 64, pp. 307–313, 2014.

[18] H. Koizumi, J. Yu, R. Hashimoto, Y. Ouchi, and T. Okabe, "Involvement of androgen receptor in nitric oxide production induced by icariin in human umbilical vein endothelial cells," *FEBS Letters*, vol. 584, no. 11, pp. 2440–2444, 2010.

[19] M.-C. Jiang, X.-H. Chen, X. Zhao, X.-J. Zhang, and W.-F. Chen, "Involvement of IGF-1 receptor signaling pathway in the neuroprotective effects of Icaritin against MPP+-induced toxicity in MES23.5 cells," *European Journal of Pharmacology*, vol. 786, pp. 53–59, 2016.

[20] C.-Q. Xu, B.-J. Liu, J.-F. Wu et al., "Icariin attenuates LPS-induced acute inflammatory responses: involvement of PI3K/Akt and NFκB signaling pathway," *European Journal of Pharmacology*, vol. 642, no. 1–3, pp. 146–153, 2010.

[21] D. Zhang, Z. Wang, C. Sheng et al., "Icariin prevents amyloid beta-induced apoptosis via the pi3k/akt pathway in pc-12 cells," *Evidence-Based Complementary and Alternative Medicine*, vol. 2015, Article ID 235265, 2015.

[22] X. Meng, H. Pei, and C. Lan, "Icariin exerts protective effect against myocardial ischemia/reperfusion injury in rats," *Cell Biochemistry and Biophysics*, vol. 73, no. 1, pp. 229–235, 2015.

[23] M. Zhai, L. He, X. Ju et al., "Icariin acts as a potential agent for preventing cardiac ischemia/reperfusion injury," *Cell Biochemistry and Biophysics*, vol. 72, no. 2, pp. 589–597, 2015.

[24] X.-H. Duan, C.-Q. Xu, J.-H. Huang, W.-J. Zhou, and B. Sun, "Icariin delays homocysteine-induced endothelial cellular senescence involving activation of the PI3K/AKT-eNOS signaling pathway," *Pharmaceutical Biology*, vol. 51, no. 4, pp. 433–440, 2013.

[25] H. Chu, H. Yu, D. Ren, K. Zhu, and H. Huang, "Plumbagin exerts protective effects in nucleus pulposus cells by attenuating hydrogen peroxide-induced oxidative stress, inflammation and apoptosis through NF-κB and Nrf-2," *International Journal of Molecular Medicine*, vol. 37, no. 6, pp. 1669–1676, 2016.

[26] A. Dimozi, E. Mavrogonatou, A. Sklirou, and D. Kletsas, "Oxidative stress inhibits the proliferation, induces premature senescence and promotes a catabolic phenotype in human nucleus pulposus intervertebral disc cells," *European Cells & Materials*, vol. 30, pp. 89–103, 2015.

[27] B. He, H. Tao, S. Liu, and A. Wei, "Protective effect of carboxymethylated chitosan on hydrogen peroxide-induced apoptosis in nucleus pulposus cells," *Molecular Medicine Reports*, vol. 11, no. 3, pp. 1629–1638, 2015.

[28] L. Yang, Z. Rong, M. Zeng et al., "Pyrroloquinoline quinone protects nucleus pulposus cells from hydrogen peroxide-induced apoptosis by inhibiting the mitochondria-mediated pathway," *European Spine Journal*, vol. 24, no. 8, pp. 1702–1710, 2015.

[29] J.-W. Chen, B.-B. Ni, B. Li, Y.-H. Yang, S.-D. Jiang, and L.-S. Jiang, "The responses of autophagy and apoptosis to oxidative stress in nucleus pulposus cells: implications for disc degeneration," *Cellular Physiology and Biochemistry*, vol. 34, no. 4, pp. 1175–1189, 2014.

[30] R. H. Xie, M. Yin, C. C. Yin et al., "Mechanism of chlorogenic acid on apoptosis of rat nucleus pulposus cells induced by oxidative stress," *Zhong Yao Cai*, vol. 37, no. 3, pp. 465–469, 2014.

[31] X. Yang, L. Jin, L. Yao, F. H. Shen, A. L. Shimer, and X. Li, "Antioxidative nanofullerol prevents intervertebral disk degeneration," *International Journal of Nanomedicine*, vol. 9, no. 1, pp. 2419–2430, 2014.

[32] D. Yang, D. Wang, A. Shimer, F. H. Shen, X. Li, and X. Yang, "Glutathione protects human nucleus pulposus cells from cell apoptosis and inhibition of matrix synthesis," *Connective Tissue Research*, vol. 55, no. 2, pp. 132–139, 2014.

[33] J. Xie, P.-J. Tong, L.-T. Shan, and C.-L. Wu, "Reseach of oxidative stress nduces aging in rabbit intervertebral disc nucleus pulposus cells injured by H_2O_2," *China Journal of Orthopaedics and Traumatology*, vol. 26, no. 4, pp. 332–335, 2013.

[34] L. Ding, X.-G. Liang, D.-Y. Zhu, and Y.-J. Lou, "Icariin promotes expression of PGC-1α, PPARα, and NRF-1 during cardiomyocyte differentiation of murine embryonic stem cells in vitro," *Acta Pharmacologica Sinica*, vol. 28, no. 10, pp. 1541–1549, 2007.

[35] Y. Wu, L. Xia, Y. Zhou, Y. Xu, and X. Jiang, "Icariin induces osteogenic differentiation of bone mesenchymal stem cells in a MAPK-dependent manner," *Cell Proliferation*, vol. 48, no. 3, pp. 375–384, 2015.

[36] P. Wang, F. Zhang, Q. He et al., "Flavonoid compound icariin activates hypoxia inducible factor-1α in chondrocytes and promotes articular cartilage repair," *PLoS ONE*, vol. 11, no. 2, Article ID e0148372, 2016.

[37] Y. Wo, D. Zhu, Y. Yu, and Y. Lou, "Involvement of NF-κB and AP-1 activation in icariin promoted cardiac differentiation of mouse embryonic stem cells," *European Journal of Pharmacology*, vol. 586, no. 1-3, pp. 59–66, 2008.

Hindawi
Evidence-Based Complementary and Alternative Medicine
Volume 2017, Article ID 3285394, 7 pages
https://doi.org/10.1155/2017/3285394

Research Article

The Impacts of *Chrysanthemum indicum* Extract on Oxidative Stress and Inflammatory Responses in Adjuvant-Induced Arthritic Rats

Mei Dong,[1] Dongsheng Yu,[2] Naif Abdullah Al-Dhabi,[3] and Veeramuthu Duraipandiyan[3]

[1]*Infectious Immune Department of Rheumatism, Tianjin Hospital, Jiefangnan Road 406, Tianjin 300211, China*
[2]*Department of Rehabilitation Medicine, Tianjin Medical University, Tianjin 300070, China*
[3]*Addiriyah Chair for Environmental Studies, Department of Botany and Microbiology, College of Science, King Saud University, P.O. Box 2455, Riyadh 11451, Saudi Arabia*

Correspondence should be addressed to Dongsheng Yu; yudongshengdm@126.com

Received 30 December 2016; Revised 24 March 2017; Accepted 30 March 2017; Published 10 April 2017

Academic Editor: Valeria Sulsen

Chrysanthemum indicum has been used as a therapeutic agent against inflammation, hypertension, and respiratory conditions for many years. This research's aim has been to examine the antioxidant impacts that *Chrysanthemum indicum* extract (CIE) has on the oxidative stress and inflammatory responses in adjuvant-induced arthritic (AA) rats. 40 rats were categorised into 4 groups according to a completely randomized approach: Group I involved normal control rats (CTRL) that received a basal diet; Group II involved arthritic control rats (CTRL-AA) that received the same diet; Group III involved rats that received a basal diet and 30 mg/kg CIE; and Group IV involved arthritic rats with the same diet as Group III rats (CIE-AA). After injection with complete Freund's adjuvant, body weight, arthritis score, and the serum levels of TNF-α, IL-1β, IL-6, myeloperoxidase (MPO), malondialdehyde (MDA), superoxide dismutase (SOD), and glutathione peroxidase (GSH-PX) were assessed. The results demonstrated that CIE delayed the onset time of arthritis and decreased the clinical arthritis severity score ($P < 0.05$). Observations of CIE-AA and CTRL-AA rats demonstrated that CIE alleviates oxidative stress and inflammatory responses in CIE-AA group. In conclusion, CIE alleviated oxidative stress and inflammatory responses, thereby highlighting its potential use as a candidate for clinical treatments of rheumatoid arthritis.

1. Introduction

The cardinal symptoms of rheumatoid arthritis (RA), an autoimmune disease, are chronic synovitis and the impairment of articular cartilage and the underlying bone in joints. It is classified as a systemic inflammatory disease which targets the joints by generating proliferative synovitis. Over time, RA has the potential to lead to the malformation or destruction of affected joints, and this has been found to lead to working disability and higher mortality rates [1]. Research shows that approximately 1% of the global population suffers from the condition, and it has been identified in patients ranging from 35 to 50 [1].

Disequilibrium regarding pro- and anti-inflammatory cytokines has been found to initiate autoimmunity and lasting inflammation, and this is the factor that contributes to the RA's characteristic joint impairment [2]. After observing the way in which joint destruction and levels of proinflammatory cytokines in the serum or arthritic tissues of RA patients are positively related, researchers identified that a range of proinflammatory cytokines, including tumour necrosis factor- (TNF-) α, interleukin- (IL-) 1β, and IL-6, perform a significant function in the condition's biological process [3].

For transgenic mice displaying the overexpression of TNF-α, acute inflammatory responses and the rapid onset of destructive arthritis are consistently observed [4]. In contrast to this, IL-1 deficient mice [5] or IL-6 deficient mice [6], in the context of experimental animal models of human RA, display reduced synovial infiltrate and tissue impairment. It is worthwhile to note the evidence to suggest that biologic medications for TNF-α, IL-1, and IL-6 lower the radiographic onset of joint disease at the same time as they hinder the condition's

activity [7]. Also notable are the findings demonstrating that the nuclear factor-κB (NF-κB), which is primarily constituted of p65 and p50 complex, performs an important function in transcriptionally regulating proinflammatory gene expression in the context of RA [8]. Furthermore, it is necessary for the inhibitor of NF-κB (IκB)α to degrade if NF-κB is to be activated, and this drives the nuclear transport of NF-κBp65 [9]. The regulation of cytokine gene expression takes place based on NF-κB activation, and in contrast to this, appropriate receptors can be drawn on by cytokines to facilitate IκBα degradation and NF-κB activation. The consequence of this is the enhancement of RA's inflammation development. An important finding to consider for the present study is the way in which significant oxidative stress, in a similar way to the rise of proinflammatory cytokines, functions as a central risk factor for joint damage in RA. The stimulation of inflammatory cells, including neutrophils and macrophages, to discharge reactive oxygen species (ROS) in the synovial fluid takes place in view of cytokine overproduction, the relevance of which is emphasised insofar as this serves as an intermediary of tissue damage [10].

Contemporary clinical practice primarily draws on disease-modifying antirheumatic drugs, among other means, for RA treatment. Other commonly employed agents range from nonsteroidal anti-inflammatory drugs and corticosteroids to biologic medications. In view of this, it is important to acknowledge that several damaging secondary effects result from the use of many of these approaches, the most notable of which include ruptured gastrointestinal blood vessels, cardiovascular complications, and liver conditions [11, 12]. Given the commonality of these side effects, survey evidence has been published to suggest that 60–90% of individuals receiving these treatments look for supplementary or substitute therapies [13].

Innovative medications sourced from curative plants have historically offered significant treatment options for various conditions, including RA. Consequently, researchers have taken as their subject the attempt to identify botanically derived drugs. The inflorescence or bud of *Chrysanthemum indicum* has found extensive usage throughout the historical practice of TCM, and it has primarily been applied in treating inflammation, hypertension, and respiratory diseases. Phytochemical profile of CIE has identified flavonoids, terpenoids, and phenolic compounds [14], and other studies have published findings to highlight its antiviral, antioxidant, anti-inflammatory, antibacterial, and immunomodulatory characteristics [15]. Given the organic nature of the therapeutic agent in combination with the widespread usage it enjoys in traditional medicine and the culinary sphere, *Chrysanthemum indicum* constitutes a promising candidate for alternative medical practice, particularly regarding the alleviation of RA's symptoms and other organ manifestations.

Therefore, it is important to account for the gap in the literature with regard to the matter of investigating the anti-inflammatory and immunomodulatory features of the plant's active components, and this constitutes the primary intention of this study. Specifically, the author will examine the impact that CIE has on paw swelling, joint impairment, the generation of inflammatory mediators, and NF-κB activation in adjuvant arthritis (AA) rats.

2. Materials and Methods

2.1. Chrysanthemum indicum Extract Preparation. After gathering *Chrysanthemum indicum* Linné (Asteraceae) flowers at a nearby market, authentication was conducted by examining microscopic and macroscopic features. 70% ethanol (with a 2-hour reflux) was used to extract the *Chrysanthemum indicum*'s dried flowers two times, and a reduced pressure was subsequently used to concentrate the extract. Prior to storing the concentrated extract at 4°C, it was subject to filtering and lyophilization. The dried extract's yield from the initial resources equaled 12.35%. Then the lyophilized powder was suspended in 10% dimethyl sulfoxide (DMSO) to lyse the cells, filtered with a 0.2 μm syringe filter, and subsequently lyophilized.

2.2. Laboratory Animals and Adjuvant Arthritis. After obtaining 40 2-month-old adult male Wistar rats weighing between 180 and 200 g from the Tianjin Laboratory Animal Centre (Tianjin, China), conventional environmental conditions were used for maintenance: namely, a 12-hour light/dark cycle, 25 ± 2°C, and 50% humidity. Food and drinking water were freely available for the animals. The research protocol received approval based on Tianjin Hospital's regulatory requirements for the care and use of experimental animals, and the experiment was conducted in accordance with relevant provisions.

A completely randomized approach was used to allocate 10 rats to one of 4 groups. The features of each group are listed as follows: the first group (Group I) involved normal control rats (CTRL) managed with a basal diet; the second group (Group II) involved arthritic control rats (CTRL-AA) managed with the same diet; the third group (Group III) involved rats managed with a basal diet and 30 mg/kg CIE; and the fourth group (Group IV) involved arthritic rats managed with the same diet as Group III rats (CIE-AA).

These distinct diets were maintained for each group for a period of 7 days and, following this, the arthritic rats in the CTRL-AA and CIE-AA groups were subject to anaesthetisation using isoflurane. Arthritis was brought about with one intradermal injection of 4 mg heat-killed *Mycobacterium butyricum* in Freud's adjuvant with 0.1 ml of paraffin oil. With 7-day intervals, the body weight was logged three times from day 0 to day 14 following induction by injection. The mice were sacrificed after the treatment process had finished on day 14, and then the arthritis index for each specimen was evaluated by examining the paws. The evaluation scale ranged from 0 to 4, where 0 was equivalent to no erythema or swelling; 1 to moderate erythema or swelling of a single or multiple digits; 2 to a wholly swollen paw; 3 to erythema and ankle swelling; and 4 to ankylosis (namely, the inability for ankle bending). A severity score was derived as the composite of the sum of each paw's score. Day 14 also involved the extraction of tissues for homogenate preparation from joint, and after extraction, the tissues were subject to immediate freezing and storage at −80°C for further analysis.

2.3. Measurement of Serum Indicators. ELISA determination kits were employed to identify the levels of TNF-α, IL-1β, and IL-6, and this was carried out based on the conventional curve (Beyotime Institute of Biotechnology, China) [16]. A Bio-Rad microplate reader (Bio-Rad Laboratories, Inc., Hercules, CA, USA) was used to log the optical density at 405 nm, and the process articulated by Liu et al. [17] was conducted to analyse myeloperoxidase (MPO), malondialdehyde (MDA), superoxide dismutase (SOD), and glutathione peroxidase (GSH-PX) activity.

2.4. Preparation of Whole Cell Extract for NF-κB Determination. Following the experimental process, 10 mg joint tissue samples were extracted. Incubation then took place with a 100 μL tissue lysis buffer (Thomas Scientific, Swedesboro, NJ, USA) for a duration of 30 minutes on ice. A BCA kit (Bio-Rad Laboratories, Inc.) was used to assess the protein concentration, and a TransAM NF-κB p65 Transcription Factor Assay Kit facilitated the monitoring of NF-κB activation. Quantity One software, version 4.4.0 (Bio-Rad Laboratories, Inc.), was employed to measure absorbance, and this was identified as 450 nm. The recorded outcomes were articulated in the form of absorbance per milligram of total protein.

2.5. Statistical Analysis. SPSS 21.0 for Windows was used to facilitate data analysis with a nonparametric Mann–Whitney test. For each of the four groups, the researcher carried out a one-way analysis of variance, and the results were articulated in the form of mean ± standard error of the mean (SEM). Intergroup comparative analysis was facilitated by employing the post hoc least squared differences (LSD) test with $P < 0.05$ being regarded as statistically significant.

3. Results

Figure 1(a) presents the observed increase in body weight over the course of the experiment, and it shows that the weight of the arthritic control rats decreased significantly while the normal control rats' body weight increased ($P < 0.05$). On day 7, the recorded body weight increase for the CTRL-AA group was considerably lower when compared to the CTRL and CIE groups ($P < 0.05$), and the body weight increase for the CIE-AA group was not significantly different than the other three. On day 14, the recorded body weight increase for the CTRL-AA and CIE-AA groups was considerably lower when compared to the other two groups ($P < 0.05$), while the body weight for the CIE-AA group was considerably lower than the CTRL-AA group ($P < 0.05$, see Figure 1(a)). Figure 1(b) displays the progression of the arthritis score index. Over the course of the initial phase of the condition (namely, until the eighth day following adjuvant injection), an examination of the arthritic rats revealed a minor inflammatory reaction in the injected paw; the arthritis scores for the injected paws ranged between 2 and 3 for the CTRL-AA and CIE-AA groups. Inflammation was seen to commence on day 9, and for the CTRL-AA group, arthritis scores rose to the highest end of the scale on day 14. For the CTRL-AA and CIE-AA groups, the arthritis scores were notably greater than those of the other two groups from day 7 ($P < 0.05$), and the CTRL-AA group's arthritis sores were notably greater than that of the CIE-AA group at day 10 ($P < 0.05$).

As demonstrated in Figures 2(a) and 2(b), when considering the CTRL and CIE groups in relation to the CTRL-AA and CIE-AA groups, the MPO and MDA levels in the serum were significantly higher for the latter ($P < 0.05$). Additionally, the CIE-AA group displayed notably lower MPO and MDA levels ($P < 0.05$) when considered in relation to the CTRL-AA group (Figures 2(a) and 2(b)). As seen in Figures 2(c) and 2(d), a significant inhibition in the level of GSH-Px and SOD ($P < 0.05$) in the CTRL-AA and CIE-AA groups was observed by way of comparison with the CTRL and CIE groups. Furthermore, when comparing the CIE-AA group with the CTRL-AA group, the activity of GSH-Px and SOD for the former was notably higher than the latter ($P < 0.05$).

This study took measures to derive a quantitative measure of the levels for TNF-α, IL-1β, and IL-6, primarily because this information is key to an accurate understanding of the function that *Chrysanthemum indicum* performed in the experimental rat model. Figure 3 shows that, for the CTRL and CIE groups, TNF-α, IL-1β, and IL-6 levels are virtually identical. Dissimilarly, when comparing the CTRL-AA group to the CTRL and CIE groups, it was observed that TNF-α, IL-1β, and IL-6 levels were greater for the former ($P < 0.05$). Therefore, the results indicate a clear causation between the consumption of CIE for the CIE-AA mice and a fall in TNF-α, IL-1β, and IL-6 levels ($P < 0.05$).

Through the assessment of nuclear NF-κB (p65), it was possible for the researcher to identify NF-κB activation in cell extracts from joint. In turn, this information facilitated the identification of whether suppression of NF-κB activation pathways resulted in the protective impact of isoflavones with regard to arthritis. Figure 4 illustrates that, for the CTRL-AA and CIE-AA groups, nuclear NF-κB (p65) were considerably greater than in the other two groups ($P < 0.05$). In addition to this, the collected data demonstrated that when comparing the CTRL-AA group with the CIE-AA group, nuclear NF-κB (p65) was considerably greater in the former ($P < 0.05$).

4. Discussion

Aside from a recently conducted study, which found evidence to suggest that the butanol-soluble component of *Chrysanthemum indicum* resulted in the inhibition of auricle edema in mice [18], research addressing the anti-inflammatory function of *Chrysanthemum indicum* and, moreover, its molecular mechanism is not extensive. This research demonstrates that *Chrysanthemum indicum* extract was a key contributing factor in facilitating a rise in body weight gain and a reduction in arthritis scores is, therefore, a valuable addition to the extant literature.

Dietary factors play essential roles in body health, disease status, and inflammatory responses [19]. This study has examined the potential that CIE has to play an important role in treating and preventing adjuvant arthritis, and the results are promising regarding its therapeutic role as a therapeutic agent against inflammatory conditions. Lee et al. examined the phagocytic activity of macrophages using a mouse model,

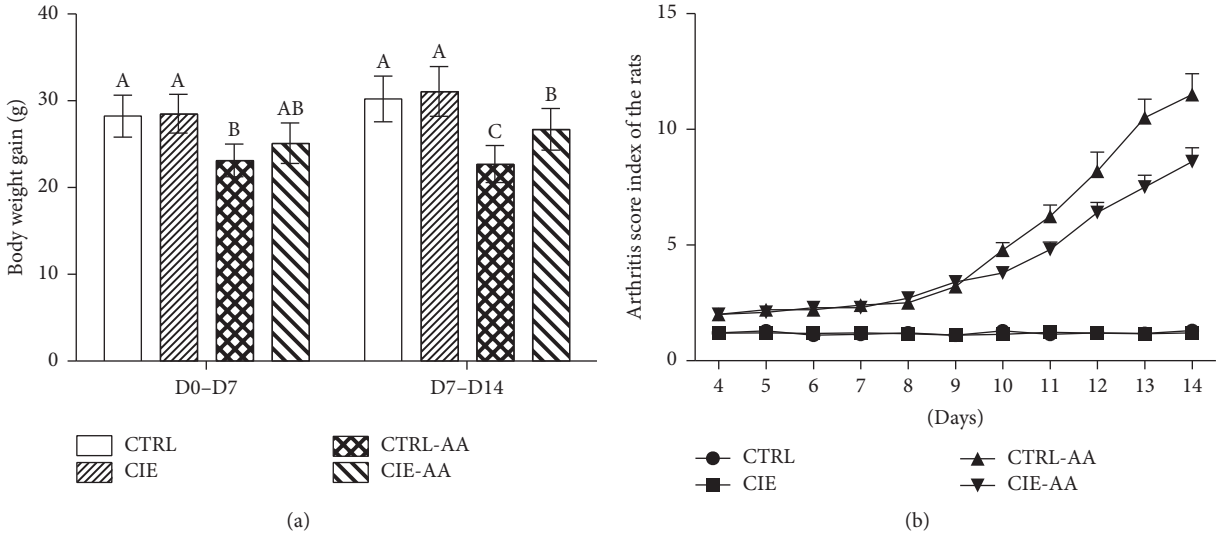

Figure 1: Body weight gain and arthritis index scores for Groups I–IV. (a) Body weight gain on day 7 and day 14; (b) arthritis index score from day 0 to day 14 following adjuvant injection. Arthritis was found to lower body weight gain while IF-AA treatment facilitated a rise in body weight gain when considered in relation to the CTRL-AA group. Data are expressed as means ± SEM ($n = 10$). ^{A,B}Different from each other ($P < 0.05$).

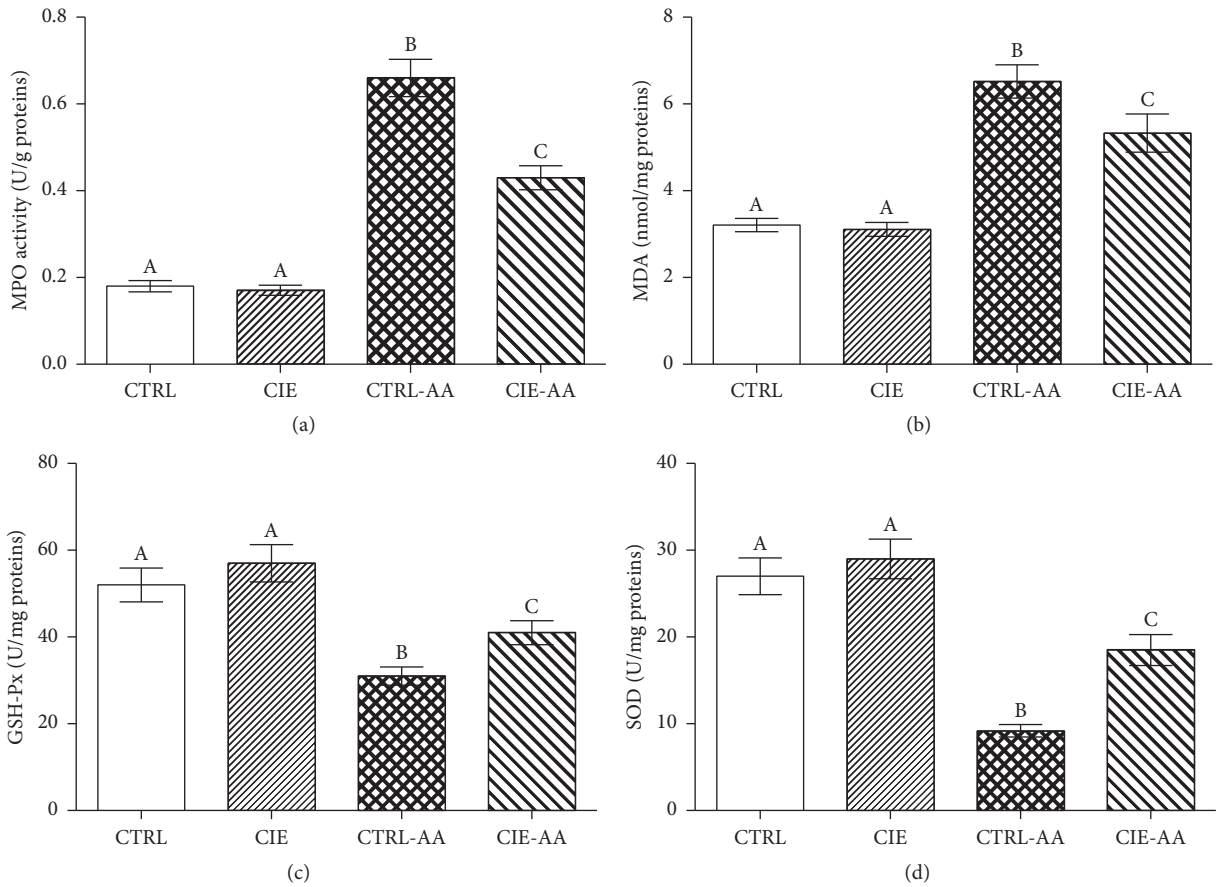

Figure 2: The preventative impact of CIE on the level of (a) MPO, (b) MDA, (c) GSH-Px, and (d) SOD values for the AA model. Data indicated with different superscript letters were statistically dissimilar ($P < 0.05$; $n = 10$).

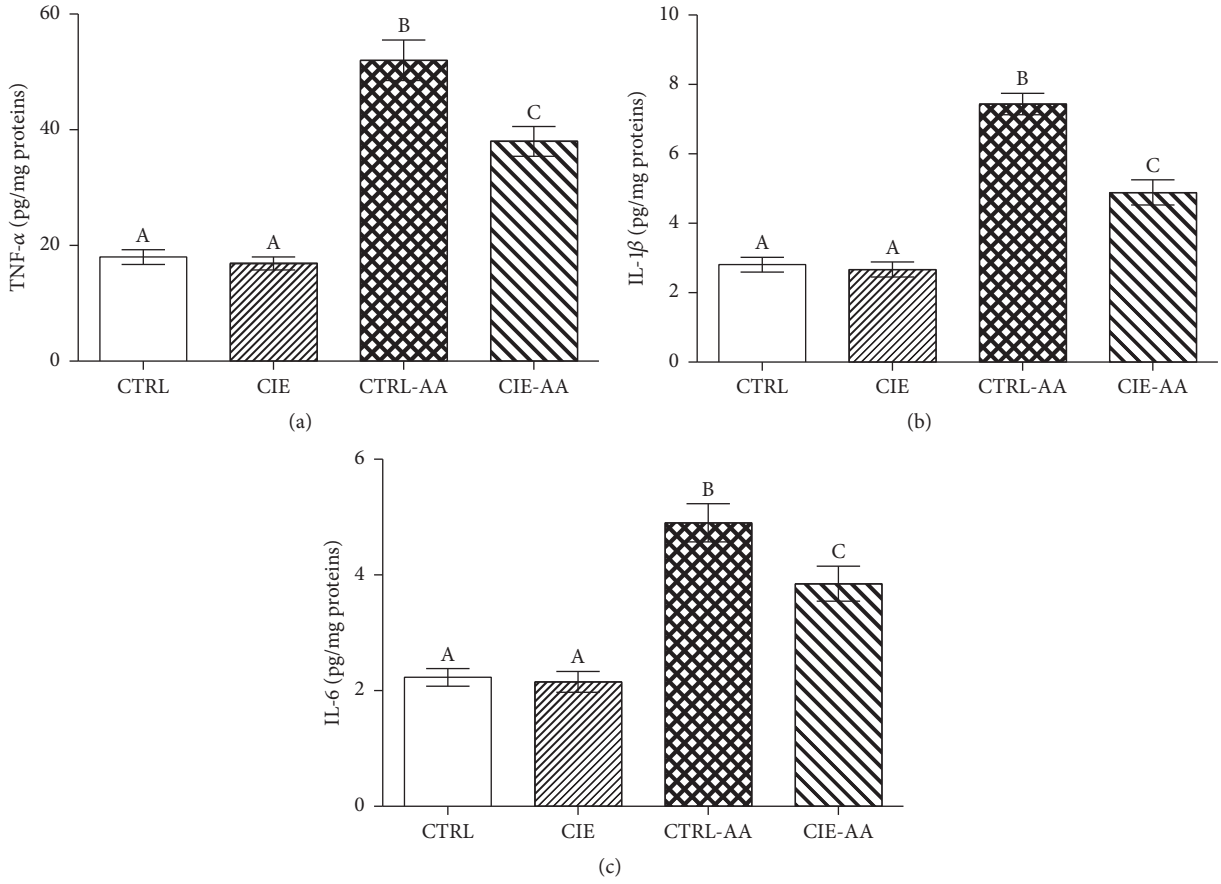

Figure 3: The preventative impact of CIE on the level of (a) TNF-α, (b) IL-1β, and (c) IL-6 values for the AA model. Data indicated with different superscript letters were statistically dissimilar ($P < 0.05$; $n = 10$).

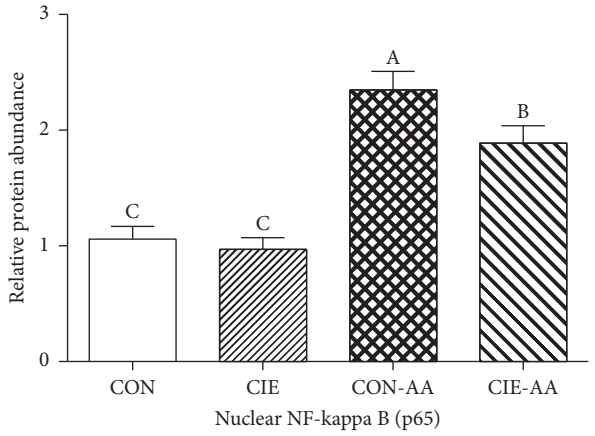

Figure 4: The impact of CIE on NF-κB activation. NF-κb were evaluated by assessing p65 DNA binding in joint. Data indicated with different superscript letters were statistically dissimilar ($P < 0.05$; $n = 10$).

and the findings revealed that CIE had a positive impact [20]. Another study, that of Cheng et al., published further findings to support the way in which CIE and its fractions may be beneficial for its anti-inflammatory features; specifically, Cheng et al.'s study addressed mouse auricle edema [18]. Nevertheless, although the extant findings provide insight into the degree to which *Chrysanthemum indicum* has anti-inflammatory properties, information regarding its precise mechanisms in vivo model system is scant. Our previous research showed that CIE had beneficial effects on the inflammation responses and oxidative stress in a ankylosing spondylitis model in mice [21]. However, the extant literature contains no studies which address the anti-inflammatory impacts in an adjuvant arthritis model. Consequently, the present research constitutes the only study published to date on the topic of CIE's anti-inflammatory activity and its action mechanisms among adjuvant arthritis rats.

Adjuvant arthritis is a widely used rodent model in studies addressing rheumatoid arthritis owing to similarity of its pathological characteristics to human RA [22]. As noted in this study, the appearance of pannus formation, inflammatory cells infiltration, cartilage degradation, and bone erosion are core features of adjuvant arthritis, and this constitutes the central rationale as to why adjuvant arthritis is popular in fundamental RA research and anti-RA therapeutic research. The present research has examined the positive impacts that CIE has on oxidative stress in the serum of AA rats, and it is therefore relevant to note that recently published reports have noted the link between RA and oxidative stress in human

and animal populations [23, 24]. Furthermore, regarding sufferers of RA, studies have reported on increased lipid peroxidation, oxidative stress, and a decrease in enzymatic antioxidants, such as GSH-Px and SOD [23, 24]. Additional research demonstrates that MPO constitutes a frequent in vivo index of granulocyte infiltration and inflammation and, moreover, it functions as an indicator of oxidative stress [25].

This study found that oxidative stress was higher in the serum of AA rats when considered in relation to the control groups, and a correlation was identified between the presence of dietary CIE and the suppression of MPO activity; the latter finding indicates the alleviation of oxidative stress among AA rats. These findings reinforce the experimental outcomes of Comar et al. [26], which indicate a link between increased ROS content in the liver of arthritic rats and a stimulated prooxidant system in combination with an insufficient antioxidant defence mechanism. In view of the integral part that ROS plays in RA, a connection can be established between the serum's biochemical and histological modifications and variance in the oxidative state. Our previous data also showed that CIE significantly increased the activities of catalase (CAT), SOD, and GSH-Px in ankylosing spondylitis mice [21]. In view of this, alleviating oxidative stress could serve as a viable way to facilitate the prevention and treatment of the liver complications associated with arthritis. By focusing on the serum of arthritic rats, this study also examined the impact that CIE had on the oxidative stress parameters; one of the key findings is that the consumption of CIE among AA rats resulted in higher GSH-Px and SOD activities in the long-term. The author suggests that CIE, owing to its effect of heightening antioxidant enzyme activity, alleviated oxidative stress in the liver.

A series of papers have found evidence for the relevance of NF-κB in RA [27, 28], and the degree to which it is inhibited by CIE has been identified as an indicator of CIE's promise as therapeutic agent. A number of recently conducted experimental models have found that mediators of this kind have the capacity to gather leukocytes, including neutrophils [29, 30]. This study's findings emphasise the potential of CIE insofar as it can facilitate the significant inhibition of inflammatory response and, moreover, decrease NF-κB, TNF-α, IL-1β, and IL-6 levels. Therefore, there is reason to suppose that the anti-inflammatory capacity of CIE could be applied to inhibit inflammatory mediators including NF-κB, TNF-α, IL-1β, and IL-6. The same trends were also observed in our previous report; CIE modulated NF-κB pathway and further altered the levels of TNF-α, IL-1β, and IL-6 [21]. Inflammatory cytokine generation is a critical process in the regulation of inflammation and the advancement of tumours, and this study's findings corroborate CIE's capacity to inhibit TNF-α and IL-1β. Consequently, the body of evidence to suggest that CIE constitutes an effective therapeutic agent against tumour progression and inflammatory response is growing.

As aforementioned, this study's findings, derived from experimentation with AA rats, demonstrate that CIE improved oxidative stress and, furthermore, facilitated a fall in the serum levels of IL-1β, IL-6, and TNF-α. An equally critical finding stems from the indication that CIE has the capacity to suppress NF-κB activation in the AA rats' joints. In view of these considerations, CIE may yet emerge as a viable and highly effective way to prevent and treat RA.

Conflicts of Interest

The authors declare that there are no conflicts of interest regarding the publication of this article.

Acknowledgments

The authors would like to extend their sincere appreciation to the Deanship of Scientific Research at King Saud University for its funding of this research through the Research Group Project no. RGP-213.

References

[1] Y. Choi, J. R. Arron, and M. J. Townsend, "Promising bone-related therapeutic targets for rheumatoid arthritis," *Nature Reviews Rheumatology*, vol. 5, no. 10, pp. 543–548, 2009.

[2] I. B. McInnes and G. Schett, "Cytokines in the pathogenesis of rheumatoid arthritis," *Nature Reviews Immunology*, vol. 7, no. 6, pp. 429–442, 2007.

[3] S. Siebert, A. Tsoukas, J. Robertson, and I. McInnes, "Cytokines as therapeutic targets in rheumatoid arthritis and other inflammatory diseases," *Pharmacological Reviews*, vol. 67, no. 2, pp. 280–309, 2015.

[4] J. Keffer, L. Probert, H. Cazlaris et al., "Transgenic mice expressing human tumour necrosis factor: a predictive genetic model of arthritis," *EMBO Journal*, vol. 10, no. 13, pp. 4025–4031, 1991.

[5] M. I. Koenders, E. Lubberts, B. Oppers-Walgreen et al., "Induction of cartilage damage by overexpression of T cell interleukin-17A in experimental arthritis in mice deficient in interleukin-1," *Arthritis and Rheumatism*, vol. 52, no. 3, pp. 975–983, 2005.

[6] M. Sasai, Y. Saeki, S. Ohshima et al., "Delayed onset and reduced severity of collagen-induced arthritis in interleukin-6-deficient mice," *Arthritis and Rheumatism*, vol. 42, no. 8, pp. 1635–1643, 1999.

[7] P. Emery, A. Sebba, and T. W. J. Huizinga, "Biologic and oral disease-modifying antirheumatic drug monotherapy in rheumatoid arthritis," *Annals of the Rheumatic Diseases*, vol. 72, no. 12, pp. 1897–1904, 2013.

[8] K. D. Brown, E. Claudio, and U. Siebenlist, "The roles of the classical and alternative nuclear factor-κB pathways: potential implications for autoimmunity and rheumatoid arthritis," *Arthritis Research and Therapy*, vol. 10, no. 4, article 212, 2008.

[9] C. F. Spurlock, J. T. Tossberg, B. K. Matlock, N. J. Olsen, and T. M. Aune, "Methotrexate inhibits NF-κB activity via long intergenic (noncoding) RNA-p21 induction," *Arthritis and Rheumatology*, vol. 66, no. 11, pp. 2947–2957, 2014.

[10] C. A. Hitchon and H. S. El-Gabalawy, "Oxidation in rheumatoid arthritis," *Arthritis Research and Therapy*, vol. 6, no. 6, pp. 265–278, 2004.

[11] L. W. Moreland and J. R. O'Dell, "Glucocorticoids and rheumatoid arthritis: back to the future?" *Arthritis and Rheumatism*, vol. 46, no. 10, pp. 2553–2563, 2002.

[12] P. Nandi, G. H. Kingsley, and D. L. Scott, "Disease-modifying antirheumatic drugs other than methotrexate in rheumatoid arthritis and seronegative arthritis," *Current Opinion in Rheumatology*, vol. 20, no. 3, pp. 251–256, 2008.

[13] S. Lü, Q. Wang, G. Li, S. Sun, Y. Guo, and H. Kuang, "The treatment of rheumatoid arthritis using Chinese medicinal plants: from pharmacology to potential molecular mechanisms," *Journal of Ethnopharmacology*, vol. 176, pp. 177–206, 2015.

[14] M. Yoshikawa, T. Morikawa, T. Murakami, I. Toguchida, S. Harima, and H. Matsuda, "Medicinal flowers. I. Aldose reductase inhibitors and three new eudesmane-type sesquiterpenes, kikkanols A, B, and C, from the flowers of *Chrysanthemum indicum* L.," *Chemical and Pharmaceutical Bulletin*, vol. 47, no. 3, pp. 340–345, 1999.

[15] X.-L. Wu, X.-X. Feng, C.-W. Li et al., "The protective effects of the supercritical-carbon dioxide fluid extract of chrysanthemum indicum against lipopolysaccharide-induced acute lung injury in mice via modulating toll-like receptor 4 signaling pathway," *Mediators of Inflammation*, vol. 2014, Article ID 246407, 2014.

[16] G. Liu, W. Ren, D. Su et al., "Dietary L-arginine supplementation improves the immune responses in mouse model infected porcine circovirus types 2," *Journal of Animal and Veterinary Advances*, vol. 11, no. 16, pp. 2980–2985, 2012.

[17] G. Liu, G. Yang, G. Guan et al., "Effect of dietary selenium yeast supplementation on porcine circovirus type 2 (PCV2) infections in mice," *PLoS ONE*, vol. 10, no. 2, Article ID e0115833, 2015.

[18] W. Cheng, J. Li, T. You, and C. Hu, "Anti-inflammatory and immunomodulatory activities of the extracts from the inflorescence of *Chrysanthemum indicum* Linné," *Journal of Ethnopharmacology*, vol. 101, no. 1–3, pp. 334–337, 2005.

[19] G. Liu, S. Chen, J. Zhong, K. Teng, and Y. Yin, "Crosstalk between tryptophan metabolism and cardiovascular disease, mechanisms, and therapeutic implications," *Oxidative Medicine and Cellular Longevity*, vol. 2017, Article ID 1602074, 5 pages, 2017.

[20] D. Y. Lee, G. Choi, T. Yoon, M. S. Cheon, B. K. Choo, and H. K. Kim, "Anti-inflammatory activity of Chrysanthemum indicum extract in acute and chronic cutaneous inflammation," *Journal of Ethnopharmacology*, vol. 123, no. 1, pp. 149–154, 2009.

[21] M. Dong, D. Yu, V. Duraipandiyan, and N. Abdullah Al-Dhabi, "The protective effect of *Chrysanthemum indicum* extract against ankylosing spondylitis in mouse models," *BioMed Research International*, vol. 2017, Article ID 8206281, 7 pages, 2017.

[22] B. H. Waksman, "Immune regulation in adjuvant disease and other arthritis models: relevance to pathogenesis of chronic arthritis," *Scandinavian Journal of Immunology*, vol. 56, no. 1, pp. 12–34, 2002.

[23] A. Kamanli, M. Naziroglu, N. Aydilek, and C. Hacievliyagil, "Plasma lipid peroxidation and antioxidant levels in patients with rheumatoid arthritis," *Cell Biochemistry and Function*, vol. 22, no. 1, pp. 53–57, 2004.

[24] A. Seven, S. Güzel, M. Aslan, and V. Hamuryudan, "Lipid, protein, DNA oxidation and antioxidant status in rheumatoid arthritis," *Clinical Biochemistry*, vol. 41, no. 7-8, pp. 538–543, 2008.

[25] Y.-F. Xian, Q.-Q. Mao, S.-P. Ip, Z.-X. Lin, and C.-T. Che, "Comparison on the anti-inflammatory effect of Cortex Phellodendri Chinensis and Cortex Phellodendri Amurensis in 12-O-tetradecanoyl-phorbol-13-acetate-induced ear edema in mice," *Journal of Ethnopharmacology*, vol. 137, no. 3, pp. 1425–1430, 2011.

[26] J. F. Comar, A. Babeto de Sá-Nakanishi, A. L. de Oliveira et al., "Oxidative state of the liver of rats with adjuvant-induced arthritis," *Free Radical Biology and Medicine*, vol. 58, pp. 144–153, 2013.

[27] J. S. Duncan, J. P. Turowec, K. E. Duncan et al., "A peptide-based target screen implicates the protein kinase CK2 in the global regulation of caspase signaling," *Science Signaling*, vol. 4, no. 172, article ra30, 2011.

[28] P. Jia, G. Chen, W.-Y. Qin, Y. Zhong, J. Yang, and X.-F. Rong, "Xitong Wan attenuates inflammation development through inhibiting the activation of nuclear factor-κB in rats with adjuvant-induced arthritis," *Journal of Ethnopharmacology*, vol. 193, pp. 266–271, 2016.

[29] K.-C. Choi, Y.-H. Lee, M. G. Jung et al., "Gallic acid suppresses lipopolysaccharide-induced nuclear factor-κB signaling by preventing RelA acetylation in A549 lung cancer cells," *Molecular Cancer Research*, vol. 7, no. 12, pp. 2011–2021, 2009.

[30] I. Andújar, J. L. Ríos, R. M. Giner, J. Miguel Cerdá, and M. D. C. Recio, "Beneficial effect of shikonin on experimental colitis induced by dextran sulfate sodium in Balb/C mice," *Evidence-based Complementary and Alternative Medicine*, vol. 2012, Article ID 271606, 2012.

Hindawi
Evidence-Based Complementary and Alternative Medicine
Volume 2017, Article ID 2675631, 8 pages
https://doi.org/10.1155/2017/2675631

Research Article

In Vitro Screening for Cytotoxic Activity of Herbal Extracts

Valter R. M. Lombardi, Iván Carrera, and Ramón Cacabelos

Health Biotechnology Department, EBIOTEC, Bergondo, La Coruña, Spain

Correspondence should be addressed to Iván Carrera; biotecnologiasalud@ebiotec.com

Received 4 January 2017; Revised 16 February 2017; Accepted 6 March 2017; Published 13 March 2017

Academic Editor: Valeria Sulsen

Experimental studies have shown that a variety of chemopreventive plant components affect tumor initiation, promotion, and progression and the main difference, between botanical medicines and synthetic drugs, resides in the presence of complex metabolite mixtures shown by botanical medicine which in turn exert their action on different levels and via different mechanisms. In the present study, we performed an in vitro screening of ethanol extracts from commercial plants in order to investigate potential antitumor activity against human tumor cell lines. Experimental results obtained through a variety of methods and techniques indicated that extracts of *I. verum*, *G. glabra*, *R. Frangula*, and *L. usitatissimum* present significant reduction in *in vitro* tumor cell proliferation, suggesting these extracts as possible chemotherapeutical adjuvants for different cancer treatments.

1. Introduction

The plant kingdom contains a great source of new bioactive compounds which, due to their intrinsic biological properties, may be used in medicine as well as in other human health promoting areas. Phytopharmaceuticals play an important role in general medical practice for the treatment of diseases of the cardiac and vascular system [1], nervous system [2], and immune system [3], and a large number of herbal drugs have a suggested prophylactic effect besides their use for therapy of diseases [4, 5]. It has been estimated that 7 to 10 years and a cost over $5,000,000 are required to develop new anticancer drugs. This includes costs for the initial collection of specimens, evaluation of crude extracts, purification, identification and synthesis of the active substance, and preclinical and clinical studies. Many commercially sold medicinal plants might contain chemical substances with potential mutagenic and/or carcinogenic properties [6, 7] as well as with antitumor properties [8, 9], and the active extracts detected by screening methods should be subjected to accurate bioassays to determine their specific pharmacological activity.

The increase in interest in apoptosis, or programmed cell death (PCD), has had a major impact on many fields within the biological sciences, including oncology [10, 11]. The delineation of discrete apoptotic pathways has affected not only our basic concepts of the development of cancer, but also our approaches toward the prevention and therapy of the disease. It is now evident that the balance between cellular proliferation and death plays a vital role in the maintenance of normal tissue homeostasis, and the derangements of either of these processes can lead to the dysregulated clonal expansion that is characteristic of all neoplastic diseases [12–15]. The recognition of apoptosis as a major mechanism of action of many standard cytotoxic agents has led to novel experimental approaches aimed at stimulating apoptotic pathways in order to improve therapeutic response. The essential role of natural compounds in regulating cellular proliferation and differentiation has been known for over 50 years, yet their importance as physiological and pharmacological regulators of cell death has only recently been appreciated. The recognition of natural products as prominent mediators of the critical pathways involved in the development and progression of cancer has renewed interest in their potential as chemopreventive and chemotherapeutic anticancer agents [16, 17].

In the present study, we report comparative data regarding the in vitro cytotoxic effect of different plant extracts on a panel of human tumor cell lines. Our results indicate that the *Illicium verum, Glycyrrhiza glabra, Rhamnus Frangula,*

and *Linum usitatissimum* extracts induce downregulation of antiapoptosis genes at the same time that leads to a strong cytotoxic effect against the majority of tested tumor cells.

2. Methods

2.1. Materials. The human liposarcoma cell line (SW872), the human synovial sarcoma cell line (SW982), the human bone osteosarcoma cell line (HS 39.T), the human connective tissue leiomyosarcoma cell line (HS 5.T), the human acute promyelocytic leukemia cell line (HL-60), the human melanoma cell line (M14WM), the human breast adenocarcinoma cell line (MCF-7), and the human colon carcinoma (HT29) cell lines were purchased from American Type Culture Collection (Rockville, MD). Dulbecco's modified Eagle's medium (DMEM), Leibovitz's L-15 (L-15), penicillin, streptomycin, gentamicin, and L-glutamine were from GIBCO BRL; HEPES was from United States Biochemical; fetal bovine serum was from HyClone; the apoptosis inducers, well characterized and effective, for example, in disrupting mitochondrial transmembrane potential and activating caspases as well as inducing phosphatidyl-serine (PS) exposure, DNA fragmentation, and other apoptotic characteristics, were from PromoKine.

2.2. Plant Material. All plants used in the study *(Salvia officinalis, Malva sylvestris, Illicium verum, Glycyrrhiza glabra, Mentha piperita, Chamaemelum nobile, Melissa officinalis, Rhamnus Frangula, Thymus vulgaris, Plantago lanceolata, Calendula officinalis, Tilia europaea, Aloysia citrodora, Linum usitatissimum, Syzygium aromaticum, Coriandrum sativum, Cinnamomum verum, Papaver rhoeas, Aframomum, Helianthus annuus, Cuminum cyminum L., Sesamum indicum, Coffea arabica, Curcuma longa, Equisetum arvense, Hypericum perforatum, Origanum vulgare, Rosmarinus officinalis, Camellia sinensis,* and *Vaccinium myrtillus)* were purchased from a local herbalist in La Coruña and belonged to the pharmaceutical company Soria Natural, Soria, Spain. 50 grams of seeds, roots, or leaves was mechanically powered and extracted with 70% ethanol for 48 h at room temperature in a percolator. After this incubation extracts were filtered and evaporated with rotary evaporator to render the extracts alcohol free. All the extracts were weighted, collected in amber vials, and kept in refrigerator until being used.

2.3. Cell Culture. All cell lines were grown as a monolayer culture (except HL-60 which grows in suspension in RPMI 1640 medium) in DMEM (HS 5.T, HS 39T, MCF-7, and HT29), L15 (SW872, SW982), and MEM (M14WM) supplemented with 1% nonessential amino acids, 1% L-glutamine, 100 IU per mL penicillin, 100 IU per mL streptomycin, 20 mg/mL glutamine, and 10% fetal bovine serum (20% for HL-60 cell line) at 37°C in a 5% CO_2 humidified atmosphere and 95% air in a CO_2 incubator. Cells were passed twice/week under sterile conditions.

2.4. Cell Viability and Cell Morphology. Log phase cell suspension of all cell lines at a concentration of 10^5/mL in culture medium (with 10% FBS) was used for the experiments in 96-well microtitre sterile plate. To each well 100 μL of cell suspension was placed. The test extract was added at different concentrations (5, 25, and 50 μg/mL) and the viable count was done by Trypan blue exclusion method after 24 h of treatment. To identify morphological changes induced by extract treatment, cells were examined using a phase contrast microscope. Cells displaying apoptotic changes were identified using previously defined morphological criteria including chromatin condensation, nuclear fragmentation, and blebbing of cytoplasmic membrane.

2.5. Antiproliferative Assay. Cell lines at exponential growth phase were washed, trypsinized, and resuspended in fresh medium. Cells were kept at a concentration of 10^5 cells/well in 96-microtitre plate. The cells were treated with different concentration of test extract (5, 25, and 50 μg/mL) against the apoptosis inducers as a positive controls (actinomycin D, dexamethasone, and etoposide, at a concentration of 1 μg/mL/each) and the negative controls which contained only the medium and incubated for 24 h at 37°C. MTT [3-(4,5-dimethylthiazole-2-yl)-2,5-diphenyltetrazolium bromide] solution was added to each well to obtain the final concentration of 400 μg/mL and further incubated at 37°C in a CO_2 incubator for 3 h. The reaction resulted in the reduction of MTT by the mitochondrial dehydrogenase of viable cells to a purple formazan product. The MTT-formazan product was dissolved in DMSO and estimated by measuring the absorbance at 570 nm in an ELISA plate reader.

2.6. Apoptosis Quantification by ELISA. Apoptosis was determined by using a commercial cellular DNA fragmentation ELISA, a photometric enzyme-linked immunosorbent assay for the detection of BrdU-labeled DNA fragments in culture supernatants and cell lysates. Cells proliferating in vitro were incubated at 37°C in a humidified atmosphere (5% CO_2) for 6 h with the nonradioactive thymidine analogue BrdU, which is incorporated into the genomic DNA. Plates were centrifuged 10 min at 250 ×g. Supernatants were removed and 100 μL of lysing solution was added to wells and incubated for 30 min at room temperature. Plates were centrifuged and BrdU-labeled DNA fragments released from the cells into the cell cytoplasm during apoptosis were detected immunologically by using an anti-DNA antibody bound to the microtitre plate to capture the DNA fragments. After an incubation of 90 min at room temperature with anti-BrdU-antibody peroxidase-conjugate, plates were washed, 100 μL of substrate solution was added to each well, and plates were read in an ELISA reader at 450 nm.

2.7. Reverse Transcriptase Polymerase Chain Reaction (RT-PCR). Total RNAs were isolated from SW872, SW982, HS 39.T, HS 5.T, HL-60, M14WM, MCF-7, and HT29 cell lines treated with *Illicium verum, Glycyrrhiza glabra, Rhamnus Frangula, and Linum usitatissimum* extracts. Total RNAs were isolated according to the acid guanidium thiocyanate-phenol-chloroform extraction method [18]. RNA was precipitated in absolute cold alcohol, washed twice in 70% ethanol, dried, and resuspended in sterile water. Total RNA was

quantified by NanoDrop™ Lite Spectrophotometer (Thermo Scientific, Waltham, MA, USA). One microgram of RNA was reverse-transcribed into cDNA by using a synthesis kit and oligo-dT (Clontech Labs, Palo Alto, CA). The resulting cDNA was amplified by PCR with the following set of primers: p53 [exon 7 (sense: TCT CCT AGG TTG GCT CTG ACT G; antisense: GCA AGT GGC TCC TGA CCT GGA)]; β-globin (sense: CTT CAT CCA CGT TCA CC; antisense: ACA CCT GTG TTC ACT AGC); Bcl-2 (sense: AGA TGT CCA GCC AGC TGC CAC CTG AC; antisense: TCG AAC GAG TGG GAC CAC GGA TAG A); Bcl-x (sense: CGG GCA TTC AGT GAC CTG AAC; antisense: GAA GTT GGC GAC CAA GGA CT); Bax (sense: ATG GAC GGG TCC GGG GAG CAG C; antisense: TTG TAC ATT TGG TAC ATC ACT CCA). Real time PCR reactions were performed using SybrGreen master mix in a 7500 real time PCR system (Applied Biosystems, Walthman, MA, USA). 35 cycles were carried out, each consisting of denaturation at 95°C for 30 sec, annealing for 30 sec at 60°C, and extension at 72°C for 30 sec. Extension during the final cycle continued at 72°C for 10 min. The resulting amplified fragments were identified on 1.5% agarose gel electrophoresis by ethidium bromide staining and the intensity of bands was quantified by densitometry. To calculate the changes in mRNA expression, we first normalized mRNA expression of target gene to the β-globin mRNA expression in a given sample; the mRNA expression for each gene in the experimental treatment was compared with the level of mRNA expression in the nontreated cells.

2.8. Statistical Analysis. Data were analyzed using SPSS 12.0 software for Windows. The experimental data were expressed as mean ± SD, the significance of difference among the various treated groups and positive and negative control groups was analyzed by means of one-way ANOVA, and the level of significance was set at $p < 0.05$.

3. Results

To demonstrate the potential biological activity of alcoholic extracts, we carried out a screening of the extracts by measuring their in vitro antiproliferative properties against several common human cancer cell lines. Some plant extracts exhibited antiproliferative activity toward all the cancer cell lines. The cellular growth inhibition percentages for the positive extracts are reported in Figure 1. The alcoholic extracts exhibiting the strongest antiproliferative activities in vitro at 50 μg/mL concentration were *Illicium verum, Glycyrrhiza glabra, Rhamnus Frangula,* and *Linum usitatissimum*. Their levels of growth inhibition occurred at very similar values with regard to all the different cell lines. A weaker activity was observed for the *Linum usitatissimum*, which showed only a 25% of inhibition toward the SW872 cell line. The lowest in vitro inhibitory activity was observed for the *Mentha piperita, Chamaemelum nobile, Melissa officinalis, Thymus vulgaris, Plantago lanceolata, Calendula officinalis, Tilia europaea, Aloysia citrodora, Syzygium aromaticum, Coriandrum sativum, Cinnamomum verum, Papaver rhoeas, Aframomum, Helianthus annuus, Cuminum cyminum L., Sesamum indicum, Coffea arabica, Curcuma longa, Equisetum arvense, Hypericum perforatum, Origanum vulgare, Rosmarinus officinalis, Camellia sinensis,* and *Vaccinium myrtillus* plant extracts, all being inactive as antiproliferative agent toward the human cell lines (Table 1). The four alcoholic extracts exhibiting the most significant antiproliferative activities at 50 μg/mL *(Illicium verum, Glycyrrhiza glabra, Rhamnus Frangula,* and *Linum usitatissimum)* were tested at lower concentration, 10 and 25 μg/mL, respectively. Data are reported in Tables 2 and 3. Although the cellular growth inhibition percentages were reduced, they still show significant antiproliferative effects with respect to the untreated controls. The *Linum usitatissimum* exhibited, at 10 μg/mL, high levels of cell growth inhibition toward almost all cell lines. Both *Illicium verum* and *Glycyrrhiza glabra* showed low levels of activity toward the SW872, SW982, HS 5.T, and HL-60 cell lines.

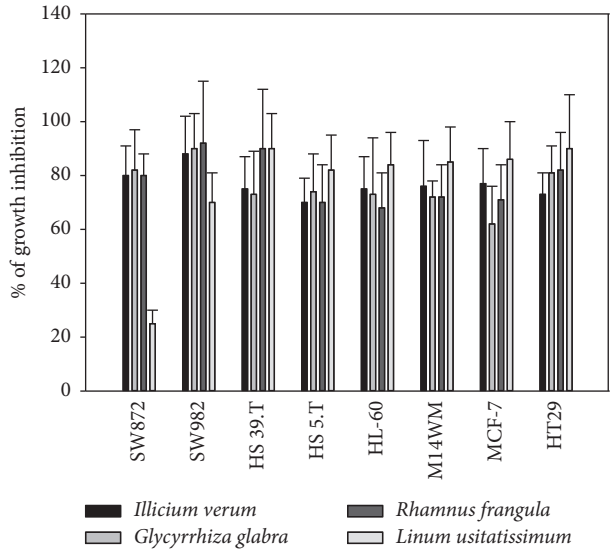

Figure 1: Effects of *Illicium verum* and *Linum usitatissimum* seed extracts, *Glycyrrhiza glabra* root extracts, and *Rhamnus Frangula* leave extracts on the growth of different tumor cell lines.

Drastic morphological changes, suggesting induction of apoptosis, were observed after treatment with *Illicium verum, Glycyrrhiza glabra, Rhamnus Frangula,* and *Linum usitatissimum* at a concentration of 25 μg/mL. Representative results are shown in Figure 2. The untreated SW872 cells show only round and uniform cells growing in a monolayer shape. The positive SW872 cells treated with the apoptosis inducers show the characteristics features of apoptosis of small irregular nuclei, nuclear fragments, and red staining cytoplasm. In a similar way, SW872 cells treated with *Illicium verum* show signs of apoptosis (membrane blebbing, fragmented nuclei).

A significant level of apoptosis was observed in SW872, SW982, HS 39.T, HS 5.T, HL-60, M14WM, MCF-7, and HT29 cell lines treated with *Illicium verum, Glycyrrhiza glabra, Rhamnus Frangula,* and *Linum usitatissimum* at a concentration of 10, 25, and 50 μg/mL, as compared to negative controls (Table 4). The highest apoptosis level was found in

Table 1: Growth inhibition percentages recorded at screening concentration of 50 μg/mL.

	SW872	SW982	HS 39.T	HS 5.T	HL-60	M14WM	MCF-7	HT29
Salvia officinalis	8	11	10	11	9	8	9	9
Malva sylvestris	7	10	11	9	8	7	3	10
Mentha piperita	8	11	9	11	9	8	6	9
Chamaemelum nobile	9	10	9	8	9	7	8	5
Melissa officinalis	10	11	10	11	9	7	9	6
Thymus vulgaris	11	11	12	11	12	13	12	9
Plantago lanceolata	9	9	11	13	14	11	9	6
Calendula officinalis	8	11	12	11	14	11	10	8
Tilia europaea	5	9	11	12	11	10	8	5
Aloysia citrodora	7	11	11	10	14	11	5	6
Syzygium aromaticum	8	11	11	15	14	11	7	9
Coriandrum sativum	10	11	10	12	13	10	11	9
Cinnamomum verum	11	10	9	7	6	8	11	10
Papaver rhoeas	15	11	12	11	10	11	10	5
Aframomum	10	10	11	12	11	15	11	6
Helianthus annuus	11	11	12	11	9	8	6	4
Cuminum cyminum L.	9	6	7	7	4	9	11	10
Sesamum indicum	8	11	12	11	15	11	13	11
Coffea arabica	8	12	13	11	11	10	11	12
Curcuma longa	9	9	9	7	7	8	10	10
Equisetum arvense	7	11	12	11	13	11	10	10
Hypericum perforatum	7	9	9	8	9	7	7	12
Origanum vulgare	10	11	12	13	11	10	9	9
Rosmarinus officinalis	9	11	10	11	11	13	15	15
Camellia sinensis	4	11	10	14	15	15	15	11
Vaccinium myrtillus	8	12	11	14	9	9	11	9

Values are the mean of at least three independent determinations; coefficient of variation was less than 15%; not significant (below 15% inhibition).

Table 2: Growth inhibition percentages recorded at screening concentration of 25 μg/mL.

	SW872	SW982	HS 39.T	HS 5.T	HL-60	M14WM	MCF-7	HT29
Illicium verum	65 ± 9	70 ± 15	70 ± 14	65 ± 13	60 ± 12	66 ± 13	61 ± 19	58 ± 16
Glycyrrhiza glabra	70 ± 22	75 ± 14	70 ± 18	68 ± 13	65 ± 15	65 ± 21	55 ± 16	58 ± 18
Rhamnus frangula	65 ± 13	71 ± 23	72 ± 12	60 ± 16	61 ± 15	66 ± 16	60 ± 17	60 ± 18
Linum usitatissimum	20 ± 6	58 ± 18	65 ± 10	66 ± 17	60 ± 14	55 ± 19	58 ± 16	65 ± 13

Values are the mean of at least three independent determinations; coefficient of variation was less than 15%; not significant (below 15% inhibition).

Table 3: Growth inhibition percentages recorded at screening concentration of 10 μg/mL.

	SW872	SW982	HS 39.T	HS 5.T	HL-60	M14WM	MCF-7	HT29
Illicium verum	13 ± 8	14 ± 3	12 ± 4	11 ± 4	14 ± 9	28 ± 11	31 ± 11	25 ± 8
Glycyrrhiza glabra	11 ± 8	11 ± 7	21 ± 8	13 ± 7	12 ± 5	27 ± 9	11 ± 4	28 ± 4
Rhamnus frangula	11 ± 6	14 ± 3	26 ± 9	11 ± 6	32 ± 12	25 ± 5	12 ± 4	12 ± 8
Linum usitatissimum	19 ± 6	25 ± 11	25 ± 6	31 ± 7	26 ± 7	28 ± 8	26 ± 4	23 ± 7

Values are the mean of at least three independent determinations; coefficient of variation was less than 15%; not significant (below 15% inhibition).

SW872, SW982, HS 39.T, HS 5.T, HL-60, M14WM, MCF-7, and HT29 cell lines treated with *Rhamnus Frangula* and no difference between extract's concentrations was observed, suggesting the presence of factors with a strongly apoptosis inducer activity at very low concentrations.

The major biochemical hallmark of apoptotic cell death is the cleavage of chromosomal DNA at internucleosomal sites into fragments or multiple of about 200 bp. DNA isolated from SW872, SW982, HS 39.T, HS 5.T, HL-60, M14WM, MCF-7, and HT29 cell lines treated with *Illicium verum*,

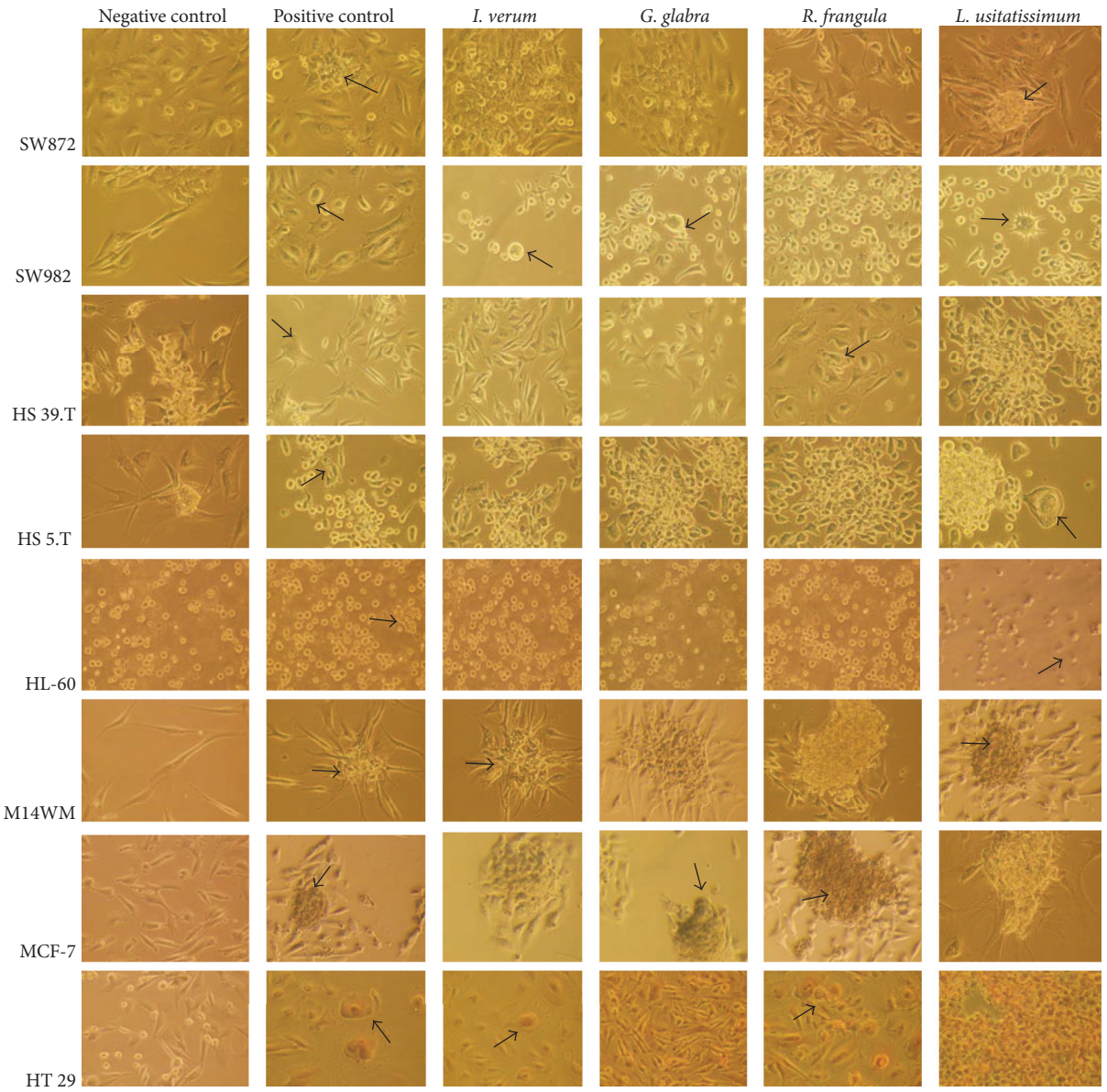

Figure 2: Phase contrast micrograph fields of untreated and treated cell lines used in the study. Black arrows show clear signs of apoptotic morphology (condensed/fragmented nuclei).

Glycyrrhiza glabra, Rhamnus Frangula, and *Linum usitatissimum* at a concentration of 25 μg/mL for two days showed DNA fragmentation patterns (data not shown).

RT-PCR analysis detected Bax and p53 mRNAs in almost all cell lines treated with 10 μg/mL of *Illicium verum, Glycyrrhiza glabra, Rhamnus Frangula,* and *Linum usitatissimum*. The percentage of positive mRNA expression was variable for different cell lines, being the highest positive cell lines observed in the group treated with *Glycyrrhiza glabra* and *Rhamnus Frangula*. Conversely, the expression of both Bcl-2 and Bcl-XL was almost negative in all cell lines treated with *Illicium verum, Glycyrrhiza glabra, Rhamnus Frangula,* and *Linum usitatissimum* extracts (Figure 3). Since RT-PCR is a very sensitive method to detect minimal levels of RNA, it is reasonable to think that both Bcl-2 and Bcl-XL are completely switched off in treated cell lines.

4. Discussion

Shikimic acid extracted from the pods (which wraps the seeds) of Chinese star anise *(Illicium verum)* is the starting material of Tamiflu® (Roche Laboratories), an antiviral drug which has gained popularity with the recent spread of the bird flu (H5N1). In addition anise extract typically contains 1% to 3% volatile anise oil. The primary constituent of anise oil is anethole (80% to 90%). Other components include alpha-pinene, linalool, anisaldehyde, and methyl chavicol. The composition of anise oil from *Illicium verum* resembles that of anise oil obtained from *Pimpinella anisum* but also contains trace quantities of safrole and myristicin [19].

Glycyrrhiza glabra (licorice) has a long history of medicinal use in Europe and Asia. At high doses, it shows potentially

Table 4: Induction of apoptosis by 10, 25, and 50 μg/mL of *Illicium verum, Glycyrrhiza glabra, Rhamnus Frangula,* and *Linum usitatissimum* alcoholic extracts in SW872, SW982, HS 39.T, HS 5.T, HL-60, M14WM, MCF-7, and HT29 cell lines measured by ELISA.

	SW872	SW982	HS 39.T	HS 5.T	HL-60	M14WM	MCF-7	HT29
Illicium verum, 10 μg/mL	45 ± 4	55 ± 11	54 ± 11	26 ± 5	33 ± 8	32 ± 10	17 ± 10	22 ± 7
Illicium verum, 25 μg/mL	66 ± 5	57 ± 10	45 ± 13	33 ± 9	36 ± 6	34 ± 12	26 ± 18	28 ± 9
Illicium verum, 50 μg/mL	70 ± 5	67 ± 12	58 ± 14	45 ± 9	44 ± 8	45 ± 16	38 ± 13	25 ± 10
Glycyrrhiza glabra, 10 μg/mL	55 ± 11	44 ± 9	55 ± 10	26 ± 11	46 ± 10	43 ± 8	44 ± 9	28 ± 7
Glycyrrhiza glabra, 25 μg/mL	67 ± 12	45 ± 7	58 ± 11	32 ± 12	47 ± 11	44 ± 11	57 ± 9	28 ± 9
Glycyrrhiza glabra, 50 μg/mL	65 ± 11	66 ± 11	77 ± 12	35 ± 11	44 ± 9	44 ± 15	88 ± 23	33 ± 9
Rhamnus frangula, 10 μg/mL	66 ± 9	77 ± 11	65 ± 14	75 ± 12	65 ± 12	88 ± 9	78 ± 9	74 ± 11
Rhamnus frangula, 25 μg/mL	70 ± 11	74 ± 12	64 ± 11	78 ± 21	68 ± 15	62 ± 12	68 ± 11	75 ± 21
Rhamnus frangula, 50 μg/mL	78 ± 9	88 ± 11	79 ± 13	89 ± 22	98 ± 17	96 ± 10	95 ± 12	86 ± 24
Linum usitatissimum, 10 μg/mL	43 ± 10	54 ± 10	34 ± 12	34 ± 11	32 ± 11	19 ± 6	44 ± 13	18 ± 6
Linum usitatissimum, 25 μg/mL	56 ± 12	77 ± 14	44 ± 16	45 ± 9	46 ± 10	25 ± 11	58 ± 14	34 ± 9
Linum usitatissimum, 50 μg/mL	50 ± 14	86 ± 18	54 ± 18	55 ± 9	66 ± 13	28 ± 11	98 ± 28	66 ± 16

The data represent mean ± SD of at least three independent experiments; coefficient of variation was less than 15%; data are expressed as the mean percentage of apoptotic cells.

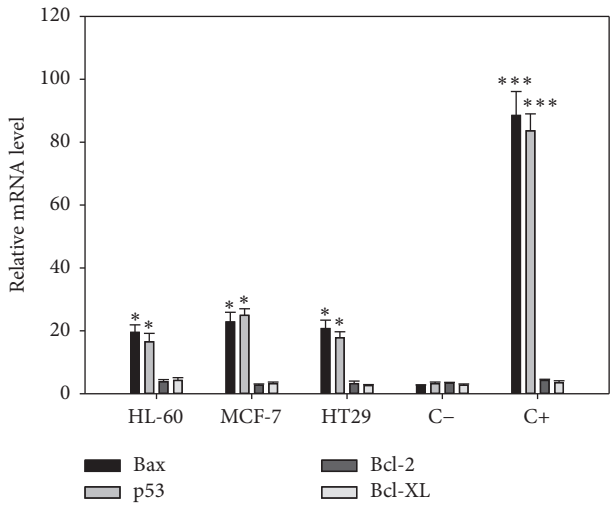

Figure 3: mRNA expression profile of Bax, p53, Bcl-2, and Bcl-XL in HL-60, MCF-7, and HT29 cell lines. A total of 1×10^6 cells were treated with 10 μg/mL of alcoholic extracts for 24 h. Total RNA was isolated and treated with DNase; 1 μg of RNA was reverse-transcribed into cDNA with a synthesis kit, using oligo-dT and a random hexamer. mRNA levels were compared by RT-qPCR. Results were normalized to the β-globin gene and expressed as the mean ± SD relative to the negative control (C−, untreated cells). As positive control (C+) cells were treated with 7 μM of staurosporine. Experiments were done in triplicate. $^*p < 0.05$ versus C−; $^{***}p < 0.001$ versus C−.

severe side effects, including hypertension (high blood pressure), hypokalemia (low blood potassium levels), and fluid retention. Most adverse effects have been attributed to triterpene saponins (glycyrrhiza, or glycyrrhizic, constitutes the major chemical components of licorice). The other compounds vary from species to species and depend on the provenance of the plant. Several flavonoids, as well as other phenolic constituents, are found in licorice; amines, amino acids, sterols, sugars, and starch are also present [20] and ethanolic extract of *G. glabra* has shown considerable antioxidant activity and protective effect against the human lipoprotein oxidative system.

A systematic fractionation of an ethanol-water (1 : 1) extract of the seeds of *Rhamnus Frangula*, guided by assays for tumor-inhibitory activity, led to the isolation of aloe emodin [21]. This compound was found to show significant antileukemic activity against the P-388 lymphocytic leukemia in mice [22].

Linum usitatissimum is a rich source of the essential fatty acid alpha-linolenic acid, which is a biologic precursor to omega-3 fatty acids such as eicosapentaenoic acid. Although omega-3 fatty acids have been associated with improved cardiovascular outcomes, evidence from human trials is mixed regarding the efficacy of flaxseed products for coronary artery disease or hyperlipidemia. The lignan constituents of flaxseed (not flaxseed oil) possess in vitro antioxidant and possible estrogen receptor agonist/antagonist properties, prompting theories of efficacy for the treatment of breast cancer.

The results obtained in this study suggest that alcoholic extracts from *Illicium verum, Glycyrrhiza glabra*, *Rhamnus Frangula,* and *Linum usitatissimum* are able to induce growth inhibition and apoptosis and modulate the expression of both Bax and p53 proapoptotic genes and the extent of gene expression was obtained at only 10 μg/mL cell culture treatment. Although with some differences, all tumor cell lines showed similar results, being the highest regulation in gene expression observed in SW 982 and SW 872 cell lines with low differences between the four alcoholic extracts.

These results are in line with previous reports that suggested a possible use for the management of metastatic malignant tumors [23]. In a recent study RT-PCR results showed downregulation of HSP90 gene expression which implied an ability of *Glycyrrhiza glabra* to induce apoptosis in HT-29 cells and confirmed its anticancer property [24]. In addition, the extract of *Linum usitatissimum* containing mainly sterols and triterpenes (21.4%), free fatty acids (17.8%), lignin dimers

(12.2%), and lipids (7.7%) showed significant cell lethality and suppression of cell vitality and proliferation of tumor cell lines [25].

Many advances in the management of cancer have been achieved since those early times when cancer chemotherapy started to take shape with the discovery of antitumor activity of alkylating agents [26] and certain hormones [27] and the advent of antimetabolites of DNA building blocks. In the Sixties and later, clinical studies of combination therapy brought about major advances leading to the demonstration that complete remission of certain neoplasia could be induced with available anticancer drugs. At the same time, new agents such as anthracycline antibiotics [28], the Vinca alkaloids [29], the Platinum complexes [30], and hormone antagonists provided additional powerful tools [31].

The advances in cancer chemotherapy were also greatly aided by progress made in diagnostic procedures, by the advent of combined modalities of treatment, and, last but not least, by the development of improved criteria for regimen design and result assessment [32]. As a consequence of these advances, it is now possible to induce complete tumor regression in patients with different types of neoplasia and to obtain disease-free survival lusting many years in a significant percentage of them.

Despite this progress, major difficulties remain to be overcome before cancer therapeutics can become generally successful in the curative management of cancer. This is particularly so in the case of the common so-called solid tumors. These difficulties can be attributed for the most part to the lack of agents acting uniquely and specifically on tumors, or at least having sufficiently marked selectivity of antitumor action, and to the phenomenon of resistance.

These two limitations combined are the main reasons for ultimate failure: in fact, even a minor level of cellular resistance may be sufficient to impart clinical resistance because one cannot overcome it by increasing adequately drug dose intensity without incurring nonacceptable toxicity. During the past two decades new vistas have been opening up in cancer therapeutics consequent to progress made in the understanding of the molecular biology of the cancer cell, of the interaction between tumor and host regulatory mechanisms, and of the mechanisms responsible for different forms of resistance.

The main purpose of this study was to evaluate the induction of apoptosis in human cell lines treated with alcoholic herbal extracts. Apoptosis is a selective physiologic deletion of cells that are no longer required. The concept of apoptosis could be of great importance for cancer treatment since the internal cellular program of cells to commit suicide can be initiated by cell damaging agents like antineoplastic drugs as well as by natural derived compounds. Some researchers have postulated that the effect of some antineoplastic compounds is caused by apoptosis-induction. It has been found by several authors that inhibition of apoptosis induces resistance to chemotherapeutic drugs [33]. Bax and p53 are the most well-known proapoptotic genes, and both are important in multicellular organisms, where they regulate the cell cycle and thus function as a tumor suppressor that is involved in preventing tumor development. Current studies about the interrelationship between drug resistance and apoptosis were mainly determined by Bax and p53 and therefore for the intrinsic power to inhibit apoptosis [34].

Although much remains to be learned in each of antitumor research areas that no doubt will have an impact on the management of cancer, it is already possible to identify new directions in cancer therapeutics aimed at exploiting the knowledge acquired so far. The approaches that are being pursued at present are essentially as follows: (1) the development of specific or highly selective antitumor agents affecting newly discovered cellular sites of potential intervention; (2) the increase of antitumor effectiveness of available drugs through the design of improved treatments, including combination treatments based on the knowledge of the mechanisms of antitumor and toxic drug action; (3) the modification or prevention of resistance to individual or multiple drugs, whether natural or acquired, through the alteration of relevant gene expression and/or the modification of biochemical mechanisms involved; (4) the induction of therapeutically profitable alterations of biological responses to tumor through the administration of soluble or cellular effectors, or their blockage and/or modulation; (5) the development of combined treatment modalities maximizing antitumor action and taking advantage of differences in the limiting toxicities of the treatments combined; and (6) the development of treatments tailored to individual patients based on improved assessments of potential tumor responsiveness and of the limitations related to the heterogeneity of tumor cell populations.

In summary, extracts of *Illicium verum, Glycyrrhiza glabra, Rhamnus Frangula,* and *Linum usitatissimum* have shown significant reduction in in vitro tumor cell proliferation. Additional studies are needed to identify how these natural extracts could be used as a complementary approach to currently used chemotherapies for different cancers. Also, more studies designed to investigate the molecular mechanisms underlying anticancer activity are needed. Altogether, natural extract use holds promise as an adjuvant treatment to prevent tumor cell growth.

Conflicts of Interest

The authors declare that they have no conflicts of interest.

References

[1] B. Baharvand-Ahmadi, M. Bahmani, P. Tajeddini, M. Rafieian-Kopaei, and N. Naghdi, "An ethnobotanical study of medicinal plants administered for the treatment of hypertension," *Journal of Renal Injury Prevention*, vol. 9, pp. 123–128, 2016.

[2] P. Srivastava and R. S. Yadav, "Efficacy of natural compounds in neurodegenerative disorders," *Advances in Neurobiology*, vol. 12, pp. 107–123, 2016.

[3] C. T. Ford, S. Richardson, F. McArdle et al., "Identification of (poly)phenol treatments that modulate the release of pro-inflammatory cytokines by human lymphocytes," *British Journal of Nutrition*, vol. 115, no. 10, pp. 1699–1710, 2016.

[4] Y. S. Kim, H. J. Park, T. K. Kim, D. E. Moon, and H. J. Lee, "The effects of ginkgo biloba extract EGB 761 on mechanical and cold allodynia in a rat model of neuropathic pain," *Anesthesia & Analgesia*, vol. 108, no. 6, pp. 1958–1963, 2009.

[5] Z. Amirghofran, M. Bahmani, A. Azadmehr, K. Javidnia, and R. Miri, "Immunomodulatory activities of various medicinal plant extracts: effects on human lymphocytes apoptosis," *Immunological Investigations*, vol. 38, no. 2, pp. 181–192, 2009.

[6] P. Yao, F. Song, K. Li et al., "Ginkgo biloba extract prevents ethanol induced dyslipidemia," *The American Journal of Chinese Medicine*, vol. 35, no. 4, pp. 643–652, 2007.

[7] P. Rattanachaikunsopon and P. Phumkhachorn, "Prophylactic effect of *Andrographis paniculata* extracts against *Streptococcus agalactiae* infection in Nile tilapia (*Oreochromis niloticus*)," *Journal of Bioscience and Bioengineering*, vol. 107, no. 5, pp. 579–582, 2009.

[8] Y. Wang, J. Wang, H. Wang, and W. Ye, "Novel taxane derivatives from *Taxus wallichiana* with high anticancer potency on tumor cells," *Chemical Biology & Drug Design*, vol. 88, no. 4, pp. 556–561, 2016.

[9] G. C. Orfali, A. C. Duarte, V. Bonadio et al., "Review of anticancer mechanisms of isoquercitin," *World Journal of Clinical Oncology*, vol. 7, no. 2, pp. 189–199, 2016.

[10] D. W. Felsher, "Tumor dormancy and oncogene addiction," *APMIS*, vol. 116, no. 7-8, pp. 629–637, 2008.

[11] C. M. Shachaf and D. W. Felsher, "Rehabilitation of cancer through oncogene inactivation," *Trends in Molecular Medicine*, vol. 11, no. 7, pp. 316–321, 2005.

[12] G. C. Bagby, "Discovering early molecular determinants of leukemogenesis," *The Journal of Clinical Investigation*, vol. 118, no. 3, pp. 847–850, 2008.

[13] C. B. Rountree, S. Senadheera, J. M. Mato, G. M. Crooks, and S. C. Lu, "Expansion of liver cancer stem cells during aging in methionine adenosyltransferase 1A-deficient mice," *Hepatology*, vol. 47, no. 4, pp. 1288–1297, 2008.

[14] K. D. Siegmund, P. Marjoram, Y.-J. Woo, S. Tavaré, and D. Shibata, "Inferring clonal expansion and cancer stem cell dynamics from DNA methylation patterns in colorectal cancers," *Proceedings of the National Academy of Sciences of the United States of America*, vol. 106, no. 12, pp. 4828–4833, 2009.

[15] S. J. Leedham and N. A. Wright, "Expansion of a mutated clone: from stem cell to tumour," *Journal of Clinical Pathology*, vol. 61, no. 2, pp. 164–171, 2008.

[16] S. Safe and R. Kasiappan, "Natural products as mechanism-based anticancer agents: sp transcription factors as targets," *Phytotherapy Research*, vol. 30, no. 11, pp. 1723–1732, 2016.

[17] P. Chanvorachote, S. Chamni, C. Ninsontia, and P. P. Phiboonchaiyanan, "Potential anti-metastasis natural compounds for lung cancer," *Anticancer Research*, vol. 36, no. 11, pp. 5707–5717, 2016.

[18] P. Chomczynski and N. Sacchi, "Single-step method of RNA isolation by acid guanidinium thiocyanate-phenol-chloroform extraction," *Analytical Biochemistry*, vol. 162, no. 1, pp. 156–159, 1987.

[19] F. Bakkali, S. Averbeck, D. Averbeck, and M. Idaomar, "Biological effects of essential oils—a review," *Food and Chemical Toxicology*, vol. 46, no. 2, pp. 446–475, 2008.

[20] N. P. Visavadiya, B. Soni, and N. Dalwadi, "Evaluation of antioxidant and anti-atherogenic properties of *Glycyrrhiza glabra* root using *in vitro* models," *International Journal of Food Sciences and Nutrition*, vol. 60, supplement 2, pp. 135–149, 2009.

[21] H. I. Abd-Alla, M. Shaaban, K. A. Shaaban, N. S. Abu-Gabal, N. M. M. Shalaby, and H. Laatsch, "New bioactive compounds from *Aloe hijazensis*," *Natural Product Research*, vol. 23, no. 11, pp. 1035–1049, 2009.

[22] S. E. Kintzios, "Terrestrial plant-derived anticancer agents and plant species used in anticancer research," *Critical Reviews in Plant Sciences*, vol. 25, no. 2, pp. 79–113, 2006.

[23] A. Kim, M. Im, and J. Y. Ma, "Anisi stellati fructus extract attenuates the in vitro and in vivo metastatic and angiogenic potential of malignant cancer cells by downregulating proteolytic activity and pro-angiogenic factors," *International Journal of Oncology*, vol. 45, no. 5, pp. 1937–1948, 2014.

[24] S. M. Nourazarian, A. Nourazarian, M. Majidinia, and E. Roshaniasl, "Effect of root extracts of medicinal herb *Glycyrrhiza glabra* on HSP90 gene expression and apoptosis in the HT-29 colon cancer cell line," *Asian Pacific Journal of Cancer Prevention*, vol. 16, no. 18, pp. 8563–8566, 2016.

[25] C. Theil, V. Briese, D.-U. Richter, U. Jeschke, and K. Friese, "An ethanolic extract of *Linum usitatissimum* caused cell lethality and inhibition of cell vitality/—proliferation of MCF-7 and BT20 mamma carcinoma cells in vitro," *Archives of Gynecology and Obstetrics*, vol. 288, no. 1, pp. 149–153, 2013.

[26] W. Sun, A. L. Kalen, B. J. Smith, J. J. Cullen, and L. W. Oberley, "Enhancing the antitumor activity of adriamycin and ionizing radiation," *Cancer Research*, vol. 69, no. 10, pp. 4294–4300, 2009.

[27] G. Mezo, M. Manea, I. Szabó, B. Vincze, and M. Kovács, "New derivatives of GnRH as potential anticancer therapeutic agents," *Current Medicinal Chemistry*, vol. 15, no. 23, pp. 2366–2379, 2008.

[28] P. Mukhopadhyay, M. Rajesh, S. Bátkai et al., "Role of superoxide, nitric oxide, and peroxynitrite in doxorubicin-induced cell death in vivo and in vitro," *American Journal of Physiology—Heart and Circulatory Physiology*, vol. 296, no. 5, pp. H1466–H1483, 2009.

[29] C. Gourmelon, H. Bourien, P. Augereau, A. Patsouris, J. S. Frenel, and M. Campone, "Vinflunine for the treatment of breast cancer," *Expert Opinion on Pharmacotherapy*, vol. 17, no. 13, pp. 1817–1823, 2016.

[30] C. Gabbiani, A. Pratesi, L. Marchetti et al., "Potent in vitro antiproliferative properties for a triplatinum cluster toward triple negative breast cancer cells," *Journal of Inorganic Biochemistry*, vol. 163, pp. 318–322, 2016.

[31] I. Talon, V. Lindner, C. Sourbier et al., "Antitumor effect of parathyroid hormone-related protein neutralizing antibody in human renal cell carcinoma in vitro and in vivo," *Carcinogenesis*, vol. 27, no. 1, pp. 73–83, 2006.

[32] J. S. D. Mieog and C. J. H. van de Velde, "Neoadjuvant chemotherapy for early breast cancer," *Expert Opinion on Pharmacotherapy*, vol. 10, no. 9, pp. 1423–1434, 2009.

[33] A. Ganju, M. M. Yallapu, S. Khan, S. W. Behrman, S. C. Chauhan, and M. Jaggi, "Nanoways to overcome docetaxel resistance in prostate cancer," *Drug Resistance Updates*, vol. 17, no. 1-2, pp. 13–23, 2014.

[34] S. Del Mare, H. Husanie, O. Iancu et al., "WWOX and p53 dysregulation synergize to drive the development of osteosarcoma," *Cancer Research*, vol. 76, no. 20, pp. 6107–6117, 2016.